OPERATIONS REPORT

Issue 1/2023 rev. 2

Reporting period: January – June 2023

EUMETSAT
AC SAF

REFERENCE:	**SAF/AC/FMI/OPS/RP/001**
ISSUE:	1/2023 rev. 2
DATE:	22/01/2024
PAGES:	142

Authors	
Prepared by	
NAME	**INSTITUTE**
Jari Hovila	FMI
Contributions	
NAME	**INSTITUTE**
Jari Hovila, Jukka Kujanpää, Kaisa Lakkala	FMI
Axel Schmidt, Matthias Hofmann, Pieter Valks	DLR
Olaf Tuinder, Robert van Versendaal	KNMI
Helge Jønch-Sørensen	DMI
Katerina Garane, MariLiza Koukouli, Konstantinos Michailidis	AUTH
Jeroen van Gent, José Granville, François Hendrick, Jean-Christopher Lambert, Bavo Langerock, Gaia Pinardi, Tijl Verhoelst	BIRA-IASB
Andy Delcloo	KMI
Peggy Tesche-Achtert	DWD
Anne Boynard, Cathy Clerbaux, Maya George, Camille Viatte	LATMOS
Rosa Astoreca, Pierre-François Coheur, Daniel Hurtmans, Catherine Wespes	ULB
Carlos Vicente	EUMETSAT
Approved by	

AC SAF Technical Manager	Jari Hovila / FMI	22/01/2024	*Signature*

Document change log		
Revision	Date	Description of change
1	27/10/2023	Initial revision
2	22/01/2024	List of abbreviations: updated Section 1.5: Updates in Table 1.2: product acronyms removed, optimal accuracy values added. Online monitoring added as means of quality assurance for NTR IASI CO. Section 3.1.2: In Tables 3.3 and 3.4 the timeliness values for tropical tropospheric ozone couldn't be determined for the whole reporting period, footnote added. Section 3.2: Typo corrected in Table 3.7 Section 5.1.2: Maximum timeliness value for April corrected and marked with red color Section 7.1.1.1: Sentence clarifying the use of M-124 instruments in validation analysis added Section 7.1.1.2: Paragraph explaining why temperature corrected reference data is not used added Section 7.3: Modified paragraph below Table 7.11. Updated/added the two last paragraphs about GOME-2B and GOME-2C SO2 algorithm fitting windows. Section 7.3.1: "System developments" bullets updated, NO2 and HCHO images updated. Added sentence to clarify why difference between GOME-2B and GOME-2C SO2 hasn't been solved yet. Section 7.4: FTIR added to the list of upper stratosphere reference data instruments. Paragraph added to clarify that "validation" refers to both NRT and offline products. Section 7.5: The first paragraph of "AUTH results" and Table 7.16 updated Section 7.7: Modified the title of Table 7.20. "Benchmark validation" changed to "online quality monitoring" throughout the chapter. Link to NRT IASI CO online monitoring website added. Paragraph clarifying the difference between individual pixels in native and BUFR format added above Table 7.22. Reference to Rodgers *et al.*, 2003, added.

List of abbreviations

AC SAF	Satellite Application Facility on Atmospheric Composition Monitoring
ARP	Absorbing Aerosol Index from PMDs data product
ARP-A	Absorbing Aerosol Index from PMDs data product from Metop-A
ARP-B	Absorbing Aerosol Index from PMDs data product from Metop-B
ARP-C	Absorbing Aerosol Index from PMDs data product from Metop-C
ARS	Absorbing Aerosol Height data product
ARS-A	Absorbing Aerosol Height data product from Metop-A
ARS-B	Absorbing Aerosol Height data product from Metop-B
ARS-C	Absorbing Aerosol Height data product from Metop-C
ATMOS	Atmospheric Parameters Measured by in-Orbit Spectroscopy (DLR data service)
ATO	Assimilated Total Ozone
AUTH	Aristotle University of Thessaloniki
BIRA-IASB	Belgian Institute for Space Aeronomy
BrO	Bromine Oxide
CDOP	Continuous Development and Operations phase
CO	Carbon Monoxide
DLR	German Aerospace Center
DMI	Danish Meteorological Institute
DWD	German Weather Service
ECMWF	European Centre for Medium-Range Weather Forecasts
EDC	EUMETSAT Data Centre
EDD	Erythemal Daily Dose
EOWEB	Earth Observation on the WEB
EPS	European Polar System
EUMETCast	EUMETSAT's primary dissemination mechanism for the near real-time delivery of satellite data and products
EUMETSAT	European Organisation for the Exploitation of Meteorological Satellites
FMI	Finnish Meteorological Institute
GOME	Global Ozone Monitoring Experiment
H2O	Water Vapour
HCHO	Formaldehyde
HR	High resolution
KMI	Royal Meteorological Institute of Belgium
KNMI	Royal Netherlands Meteorological Institute
L1b	Level 1b data product
L1c	Level 1c data product
L2	Level 2 data product
L3	Level 3 data product

LATMOS	Laboratoire Atmosphères, Milieux, Observations Spatiales
LER	Lambertian-equivalent reflectivity data record
NHP	Near Real-time High-resolution Ozone Profile data product
NO2	Nitrogen Dioxide
NRT	Near Real-time
NTO	Near Real-time Total Column data product
NUV	Near Real-time UV index data product
O3	Ozone
O3M SAF	Satellite Application Facility on Ozone and Atmospheric Chemistry Monitoring
OHP	Offline High-resolution Ozone Profile data product
OHP-A	Offline High-resolution Ozone Profile data product from Metop-A
OHP-B	Offline High-resolution Ozone Profile data product from Metop-B
OHP-C	Offline High-resolution Ozone Profile data product from Metop-C
OEM	Optimal Estimation Method
OOP	Coarse resolution Offline Ozone Profile product
OPERA	Ozone Profile Retrieval Algorithm
OTO	Offline Total Column data product
OUV	Offline Surface UV data product
OUV-A	Offline Surface UV data product from Metop-A
OUV-AB	Offline Surface UV data product from Metop-A and Metop-B
OUV-B	Offline Surface UV data product from Metop-B
OUV-BC	Offline Surface UV data product from Metop-B and Metop-C
PDU	Product Dissemination Unit
PGE	Product Generation Element
PMD	Polarisation Measurement Device
RD	Reference Document
RMS	Root Mean Square
RMSE	Root Mean Square Error
SACS	Support to Aviation Control Service
SO2	Sulphur Dioxide
TOC	Total Ozone Column data product
TrOC	Global Tropospheric Ozone Column data product
TTrOC	Tropical Tropospheric Ozone Column data product
ULB	Université libre de Bruxelles
UTC	Coordinated Universal Time

TABLE OF CONTENTS

1. Introduction

1.1. Scope

The scope of this document is to summarise the operational activities concerning the products in operation and the associated services during the reporting period to see that the general requirements applicable to these services and products of the AC SAF [RD1, RD2, RD3] are fulfilled. Intended readers of this document are the members of AC SAF project team, Review Board of the annual Operations Review, AC SAF Steering Group and EUMETSAT OPS/WG as well as the users of the AC SAF products.

Operations Reports include information about product availability/timeliness, quality assurance, website usage, and delivery statistics. Main events, major anomalies and software/hardware updates are reported also. AC SAF Operations Report is published twice a year.

1.2. Reporting period

This Operations Report covers the period January – June 2023.

1.2.1. Highlights

New products

- 21 April: Offline GOME-2 daily/monthly L3 trace gas column products declared operational

1.3. Reference documents

Table 1.1. Operations Report reference documents

Reference	Title	Issued	Reporting period
RD1	Product Requirements Document (SAF/AC/FMI/RQ/PRD/001)	01/12/2022	N/A
RD2	Service Specification (SAF/AC/FMI/RQ/SESP/001)	22/06/2022	N/A
RD3	EUMETSAT Operational Services Specification (EUM/OPS/SPE/20/109969)	16/02/2023	N/A
RD4	EPS End User Requirements Document (EPS/MIS/REQ/93001)		N/A
RD5	O3M SAF Validation Report for NRT, offline and reprocessed total ozone columns	11/12/2015	January 2007 – December 2014
RD6	AC SAF Validation Report for NRT, offline, reprocessed and level 3 total/tropospheric NO2 columns	10/11/2017	Metop-A: January 2007 – July 2015 Metop-B: January 2013 – July 2015

Reference	Title	Issued	Reporting period
RD7	O3M SAF Validation Report for Metop-A NRT and offline coarse/high-resolution ozone profiles	20/02/2012	January 2007 – May 2011
RD8	O3M SAF Validation Report for Metop-B NRT and offline coarse/high-resolution ozone profiles	30/06/2013	December 2012 – April 2013
RD9	O3M SAF Validation Report for Metop-B NRT UV indexes	27/05/2013	May 2013
RD10	O3M SAF Validation Report for NRT, offline and reprocessed total SO2 columns	09/12/2015	January 2007 – December 2014
RD11	O3M SAF Validation Report for offline and reprocessed total BrO columns	09/12/2015	January 2007 – December 2014
RD12	O3M SAF Validation Report for NRT, offline and reprocessed total HCHO columns	30/10/2015	January 2007 – July 2015
RD13	O3M SAF Validation Report for offline and reprocessed total H2O columns	30/10/2015	January 2007 – August 2015
RD14	O3M SAF Validation Report for NRT and offline aerosol products	25/06/2013	January 2007 – May 2013
RD15	O3M SAF Validation Report for Metop-B offline UV products	03/02/2015	June 2012 – May 2013
RD16	O3M SAF Validation Report for Metop-A reprocessed total ozone columns	19/02/2010	January 2007 – June 2009
RD17	AC SAF Validation Report for GOME-2 surface LER product	27/03/2019	MSC: February 2007 – June 2018 PMD: April 2008 – June 2018
RD18	O3M SAF Validation Report for offline tropospheric ozone columns (cloud slicing)	03/07/2015	January 2007 – December 2014
RD19	O3M SAF Validation Report for NRT and offline tropospheric ozone columns (ozone profiles)	09/09/2015	January 2007 – December 2014
RD20	O3M SAF Validation Report for NRT IASI CO	17/11/2015	September 2015 – November 2015
RD21	AC SAF Validation Report for OClO data record	29/05/2017	January 2007 – September 2016

Reference	Title	Issued	Reporting period
RD22	AC SAF Validation Report for NRT IASI SO2	17/11/2017	Metop-A: January 2007 – December 2013 June 2017 – October 2017 Metop-B: June 2017 – December 2017
RD23	AC SAF Validation Report for level-3 total H2O data record	06/11/2017	Metop-A: January 2007 – December 2014 Metop-B: January 2013 – December 2014
RD24	AC SAF Validation Report for Metop-C offline tropical tropospheric ozone columns	05/06/2020	February – December 2019
RD25	AC SAF Validation Report for Metop-C NRT and offline global tropospheric ozone columns	05/06/2020	February – December 2019
RD26	AC SAF Validation Report for Metop-C NRT and offline high-resolution ozone profiles	05/06/2020	February – December 2019
RD27	AC SAF Validation Report for Metop-C NRT and offline total ozone columns	25/05/2020	February – July 2019
RD28	AC SAF Validation Report for Metop-C NRT and offline total/tropospheric nitrogen dioxide columns	25/11/2019	February – July 2019
RD29	AC SAF Validation Report for Metop-C NRT and offline total formaldehyde columns	19/05/2020	February – July 2019
RD30	AC SAF Validation Report for Metop-C offline total bromine monoxide columns	19/05/2020	February – July 2019
RD31	AC SAF Validation Report for Metop-C offline total water vapour columns	30/03/2020	February – July 2019
RD32	AC SAF Validation Report for NRT, offline and reprocessed absorbing aerosol height products	03/07/2020	2007-2019
RD33	AC SAF Validation Report for Metop-C NRT and offline absorbing aerosol index from PMDs products	09/10/2019	January – October 2019

Reference	Title	Issued	Reporting period
RD34	AC SAF Validation Report for Metop-C NRT and offline total sulphur dioxide products	21/01/2021	February – July 2019
RD35	AC SAF Validation Report for NRT IASI total O3 and O3 profiles	28/02/2022	December 2019 – November 2020
RD36	AC SAF Validation Report for NRT IASI HNO3	26/04/2022	December 2019 – December 2021

Online documents:

Service Specification, Validation Reports

1.4. Definition of terms

Availability is based on the definition in the EUMETSAT Operational Services Specification [RD3].

Product-specific clarifications:

- For NRT products, the monthly availability limit is 97.5 %. The availability is calculated as a "worst case scenario":

$$\frac{\text{in time processed and disseminated L2 PDUs}}{\text{received L1b PDUs} + \text{missed L1b PDUs marked as "reception confirmed" in the EUMETCast sendlist}}$$

- For offline products, the monthly availability limit is 95.5 %. The availability is defined by the ratio of the number of in time processed, archived and quality-approved L2 products to the number of orbits for which L1b PDUs have been received per month.
- NUV and OUV are daily L3 products, and availability is defined as the fraction of days in a month with products fulfilling the timeliness requirements.

Timeliness defines whether the product is near real time (NRT) product which is disseminated or ready for download in three hours from sensing at the latest or offline product which is available for download in two weeks after sensing at the latest, during system availability. System unavailability will in most cases not lead to loss of data but to delays with respect to the specified timeliness. In practice, timeliness of a product is determined by calculating the time from sensing to EUMETCast or archive upload. In the Operations Reports, the timeliness is presented as monthly average, minimum and maximum values.

Accuracy is defined as in the EPS End User Requirements Document [RD4]: the values of accuracy "represent RMS values" taking as reference the 'true value' measured by ground based instruments.

1.5. Accuracy requirements of AC SAF products

The following table lists all operational AC SAF products and their accuracy requirements as defined in [RD2].

Table 1.2. Accuracy requirements of AC SAF products

Product identifier	Product name	Threshold accuracy	Target accuracy	Optimal accuracy	Means of quality assurance
O3M-41.1	NRT total O3	20 %	4 % (SZA < 80°) 6 % (SZA > 80°)	1.5 %	Online monitoring Validation report
O3M-300					
O3M-50.1	NRT total NO2	20 % of annual mean	8-15 % of annual mean	4 – 8 % of annual mean	Online monitoring Validation report
O3M-338					
O3M-52.1	NRT tropospheric NO2	50 %	30 %	20 %	Online monitoring Validation report
O3M-341					
O3M-55.1	NRT total SO2	100 %	50 % (SZA < 70°)	30 %	Online monitoring Validation report
O3M-374					
O3M-177	NRT total HCHO	100 %	50 % (polluted)	30 %	Online monitoring Validation report
O3M-344					

Product identifier	Product name	Threshold accuracy	Target accuracy	Optimal accuracy	Means of quality assurance
O3M-47.1 O3M-311	NRT high-resolution ozone profile	30 % in stratosphere 70 % in troposphere	15 % in stratosphere 30 % in troposphere	10 % in stratosphere 25 % in troposphere	Online monitoring Validation report
O3M-78 O3M-364	NRT absorbing aerorol height	3 km (layer height < 10 km) 4 km (layer height > 10 km)	1 km (layer height < 10 km) 2 km (layer height > 10 km)	1 km (layer height < 10 km) 2 km (layer height > 10 km)	Online monitoring Validation report
O3M-72.1 O3M-362	NRT absorbing aerosol index from PMDs	1.0 index points	0.5 index points	0.2 index points	Online monitoring Validation report
O3M-409	NRT UV index, clear-sky	20 %	10 %	5 %	Online monitoring Validation report
O3M-410	NRT UV index, cloud-corrected				
O3M-80 O3M-352	NRT IASI CO	25 % (normal conditions) 50 % (high pollution or low signal)	12 % (normal conditions) 20 % (high pollution or low signal)	5 % (normal conditions) 10 % (high pollution or low signal)	Online monitoring Validation report
O3M-57 O3M-377	NRT IASI SO2	200 % (below 10 km) 100 % (above 10 km)	100 % (below 10 km) 35 % (above 10 km)	50 % (below 10 km) 20 % (above 10 km)	Validation report
O3M-81 O3M-336	NRT IASI HNO3	50 %	35 %	10 %	Validation report
O3M-44 O3M-306	NRT IASI total ozone	10 %	5 %	1 %	Validation report
O3M-49 O3M-315	NRT IASI ozone profile	30 % in stratosphere 50 % in troposphere	15 % in stratosphere 30 % in troposphere	5 % in stratosphere 10 % in troposphere	Validation report
O3M-06.1 O3M-42.1 O3M-301	Offline total O3	20 %	4 % (SZA < 80°) 6 % (SZA > 80°)	1.5 %	Validation report Online monitoring Validation report
O3M-07.1 O3M-51.1 O3M-339	Offline total NO2	20 % of annual mean	8-15 % of annual mean	4 – 8 % of annual mean	Online monitoring Validation report
O3M-37.1 O3M-53.1 O3M-342	Offline tropospheric NO2	50 %	30 %	20 %	Online monitoring Validation report
O3M-09.1 O3M-56.1 O3M-375	Offline total SO2	100 %	50 % (SZA < 70°)	30 %	Online monitoring Validation report

Product identifier	Product name	Threshold accuracy	Target accuracy	Optimal accuracy	Means of quality assurance
O3M-08.1	Offline total BrO	50 %	30 %	15 %	Online monitoring Validation report
O3M-82.1					
O3M-317					
O3M-10.1	Offline total HCHO	100 %	50 % (polluted cond.)	30 %	Online monitoring Validation report
O3M-58.1					
O3M-345					
O3M-12.1	Offline total H2O	25 %	10 %	5 %	Validation report
O3M-86.1					
O3M-386					
O3M-35	Offline tropical tropospheric ozone	50 %	25 %	15 %	Validation report
O3M-43					
O3M-302					
O3M-303	Offline L3 daily averaged total O3	20 %	4 % (SZA < 80°) 6 % (SZA > 80°)	1.5 %	Online monitoring Validation report
O3M-388	Offline L3 monthly averaged total O3				
O3M-340	Offline L3 daily averaged total NO2	20 %	8 %	5 %	Online monitoring Validation report
O3M-389	Offline L3 monthly averaged total NO2				
O3M-343	Offline L3 daily averaged tropospheric NO2	50 %	30 %	20 %	Online monitoring Validation report
O3M-390	Offline L3 monthly averaged tropospheric NO2				
O3M-376	Offline L3 daily averaged total SO2	100 %	50 % (SZA < 70˚)	30 %	Online monitoring Validation report
O3M-397	Offline L3 monthly averaged total SO2				
O3M-318	Offline L3 daily averaged total BrO	50 %	30 %	15 %	Online monitoring Validation report
O3M-391	Offline L3 monthly averaged total BrO				
O3M-387	Offline L3 daily averaged total H2O	25 %	10 %	5 %	Online monitoring Validation report
O3M-393	Offline L3 monthly averaged total H2O				
O3M-346	Offline L3 daily averaged total HCHO	100 % (polluted cond.)	50 % (polluted cond.)	30 % (polluted cond.)	Online monitoring Validation report
O3M-394	Offline L3 monthly averaged total HCHO				

Product identifier	Product name	Threshold accuracy	Target accuracy	Optimal accuracy	Means of quality assurance
O3M-39.1 O3M-48.1 O3M-312	Offline high-resolution ozone profile	30 % in stratosphere 70 % in troposphere	15 % in stratosphere 30 % in troposphere	10 % in stratosphere 25 % in troposphere	Online monitoring Validation report
O3M-172 O3M-174 O3M-304	NRT global tropospheric ozone	50 %	20 %	15 %	Validation report
O3M-173 O3M-175 O3M-305	Offline global tropospheric ozone	50 %	20 %	15 %	Validation report
O3M-69 O3M-79 O3M-365	Offline absorbing aerosol height	3 km (layer height < 10 km) 4 km (layer height > 10 km)	1 km (layer height < 10 km) 2 km (layer height > 10 km)	1 km (layer height < 10 km) 2 km (layer height > 10 km)	Online monitoring Validation report
O3M-63.1 O3M-73.1 O3M-363	Offline absorbing aerosol index from PMDs	1.0 index points	0.5 index points	0.2 index points	Online monitoring Validation report
O3M-450 – O3M-464	Offline surface UV	50 %	20 %	10 %	Online monitoring Validation report

Latest validation reports for all pre-operational and operational AC SAF products are listed in Section 1.3.

Online monitoring, when applicable, can be used to replace the regular validation reporting. Online monitoring results are found from dedicated sections "Online quality monitoring", if the processing centre in question has such functionality.

2. Processing centre: FMI

2.1. Offline surface UV

Offline surface UV (OUV) product is a multi-mission (Metop-B+C) product consisting of 15 sub-products which are listed in Table 2.1. Since they are all archived in the same file, single entries in the tables in the following sections represent them all.

Table 2.1. OUV sub-products

Product Identifier	Product Name	Product Acronym
O3M-450	Offline UV daily dose, erythemal (CIE) weighting	MM-O-UV_DD_CIE
O3M-451	Offline UV daily dose, plant response weighting	MM-O- UV_DD_PLANT
O3M-452	Offline UV daily dose, DNA damage weighting	MM-O-UV_DD_DNA
O3M-453	Offline UV daily dose, UVA range (315-400 nm)	MM-O-UV_DD_UVA
O3M-454	Offline UV daily dose, UVB range (280-315 nm)	MM-O-UV_DD_UVB
O3M-455	Offline UV daily maximum dose rate, erythemal (CIE) weighting	MM-O-UV_MDSR_CIE
O3M-456	Offline UV daily maximum dose rate, plant response weighting	MM-O-UV_MDSR_PLANT
O3M-457	Offline UV daily maximum dose rate, DNA damage weighting	MM-O-UV_MDSR_DNA
O3M-458	Offline UV daily maximum dose rate, UVA range (315-400 nm)	MM-O-UV_MDSR_UVA
O3M-459	Offline UV daily maximum dose rate, UVB range (280-315 nm)	MM-O-UV_MDSR_UVB
O3M-460	Offline UV solar noon UV index	MM-O-UV_NOON_UVI
O3M-461	Offline UV daily maximum ozone photolysis rate	MM-O-UV_MPHR_O3
O3M-462	Offline daily maximum nitrogen dioxide photolysis rate	M-O-UV_MPHR_NO2
O3M-463	Offline UV daily dose, vitamin D weighting	MM-O-UV_DD_VITD
O3M-464	Offline UV daily maximum dose rate, vitamin D weighting	MM-O-UV_MDSR_VITD

2.1.1. Availability

Availability requirement for OUV has been defined in Section 1.4. The availability statistics of FMI products are presented in Table 2.2. If the availability requirement has been violated, those values are marked with red colour, identified by numbers and reported in Table 2.7.

Table 2.2. Availability of OUV product during the reporting period

1/2023	2/2023	3/2023	4/2023	5/2023	6/2023
100 %	100 %	100 %	100 %	100 %	100 %

2.1.2. Timeliness

Timeliness indicates the elapsed time between sensing and product dissemination. Timeliness requirement is 15 days for offline products. If the requirement has been violated, those values are

marked with red colour. In addition, the violations are identified by numbers and reported in Table 2.7 if they have caused the availability values to drop below the allowed limits.

Note: timeliness violations are not listed as anomalies if the availability is above the limit.

The values in Table 2.3 indicate the elapsed times (days, hours and minutes in the format [ddT]hh:mm) from sensing to archive upload. In each cell, the values from top to bottom represent observed monthly average, minimum and maximum times.

Table 2.3. Timeliness of OUV product during the reporting period

1/2023	2/2023	3/2023	4/2023	5/2023	6/2023
avg: 03T01:30 min: 03T00:07 max: 03T19:12	avg: 03T00:58 min: 03T00:47 max: 03T01:02	avg: 03T06:38 min: 03T00:57 max: 05T06:22	avg: 03T18:49 min: 03T01:02 max: 04T01:52	avg: 04T01:20 min: 04T00:32 max: 04T01:42	avg: 04T01:13 min: 04T00:42 max: 04T01:52

2.2. Services, main events and anomalies

Table 2.4. FMI service statistics related to product archiving, ordering and AC SAF Helpdesk

Description of service / event	1/2023	2/2023	3/2023	4/2023	5/2023	6/2023
Product ordering [1]						
Number of users (cumulative)	613	615	619	628	635	600[*]
Number of orders	23	12	7	21	10	38
Number of ordered products	OHP: 104 ARS: 1722 OUV time-series: 90857	ARS: 2598 ARP: 2289 OUV subset: 22804	ARS: 795 ARP: 91 OUV subset: 12220	OHP: 2176 ARP: 170 OUV time-series: 74978	OOP: 414 OHP: 1274 ARP: 167 OUV subset: 1 OUV time-series: 5768	OHP: 28771 ARS: 2589 ARP: 238 OUV subset: 6515 OUV time-series: 5709
Ordered data volume	OHP: 26.0 GB ARS: 1.77 GB OUV time-series: 9.14 MB	ARS: 2.67 GB ARP: 16.4 GB OUV subset: 1.88 GB	ARS: 817 MB ARP: 653 MB OUV subset: 25.7 GB	OHP: 546 GB ARP: 1.06 GB OUV time-series: 8.76 MB	OOP: 20.0 GB OHP: 230 GB ARP: 1.19 GB OUV subset: 17.5 MB OUV time-series: 601 kB	OHP: 7.17 TB ARS: 2.68 GB ARP: 1.73 GB OUV subset: 7.76 GB OUV time-series: 594 kB
Number of bulk orders	0	0	0	0	0	0
Number of failed orders [2]	0	0	0	0	0	5
Archive statistics [3]						
Number of archived products (Metop-B)	OHP: 439 ARS: 439 ARP: 439	OHP: 397 ARS: 397 ARP: 397	OHP: 437 ARS: 437 ARP: 437	OHP: 424 ARS: 424 ARP:424	OHP: 439 ARS: 439 ARP:439	OHP: 425 ARS: 425 ARP:425
Size of archived products (Metop-B)	OHP: 110 GB ARS: 450 MB ARP: 3.13 GB	OHP: 100 GB ARS: 407 MB ARP: 2.84 GB	OHP: 109 GB ARS: 449 MB ARP: 3.13 GB	OHP: 106 GB ARS: 438 MB ARP: 3.02 GB	OHP: 110 GB ARS: 455 MB ARP: 3.13 GB	OHP: 107 GB ARS: 442 MB ARP: 3.07 GB
Number of archived products (Metop-C)	OHP: 437 ARS: 437 ARP: 437	OHP: 398 ARS: 398 ARP: 398	OHP: 438 ARS: 438 ARP: 438	OHP: 425 ARS: 425 ARP:425	OHP: 439 ARS: 439 ARP:439	OHP: 425 ARS: 425 ARP:425

Size of archived products (Metop-C)	OHP: 109 GB ARS: 450 MB ARP: 3.13 GB	OHP: 100 GB ARS: 410 MB ARP: 2.86 GB	OHP: 110 GB ARS: 451 MB ARP: 3.15 GB	OHP: 106 GB ARS: 440 MB ARP: 3.04 GB	OHP: 110 GB ARS: 457 MB ARP: 3.15 GB	OHP: 106 GB ARS: 443 MB ARP: 3.08 GB
Number of archived multi-mission products	OUV: 31	OUV: 28	OUV: 31	OUV: 30	OUV: 31	OUV: 30
Size of archived multi-mission products	OUV: 484 MB	OUV: 526 MB	OUV: 569 MB	OUV: 527 MB	OUV: 538 MB	OUV: 502 MB
GOME-2 L1b PDU rolling archive statistics [4]						
PDUs archived / PDUs "reception confirmed" (Metop-B)	13291/14878 89.3 %	12459/13435 92.7 %	13615/14858 91.6 %	13340/14394 92.7 %	13765/14872 92.6 %	13380/14381 93.0 %
PDUs archived / PDUs "reception confirmed" (Metop-C)	13300/14874 89.4 %	12433/13433 92.6 %	13628/14872 91.6 %	12997/14389 90.3 %	13908/14877 93.5 %	13721/14350 95.6 %
Helpdesk statistics						
Number of emails	0	0	0	0	0	0
Number of email threads	0	-	-	-	-	-
Average response time ([ddT]hh:mm)	-	-	-	-	-	-

[1] More detailed information about the orders is available in Appendix 1
[2] Failed orders are detailed in Appendix 2
[3] Based on sensing start time
[4] For Level 1b products, the availability is defined as the number of archived L1b PDUs divided by the number of L1b PDUs with status "reception confirmed" in the EUMETCast sendlist
[*] AC SAF Helpdesk received multiple notifications for invalid email addresses when AC SAF news bulletin was sent to the users in June. Owners of those addresses were removed from the list of AC SAF users.

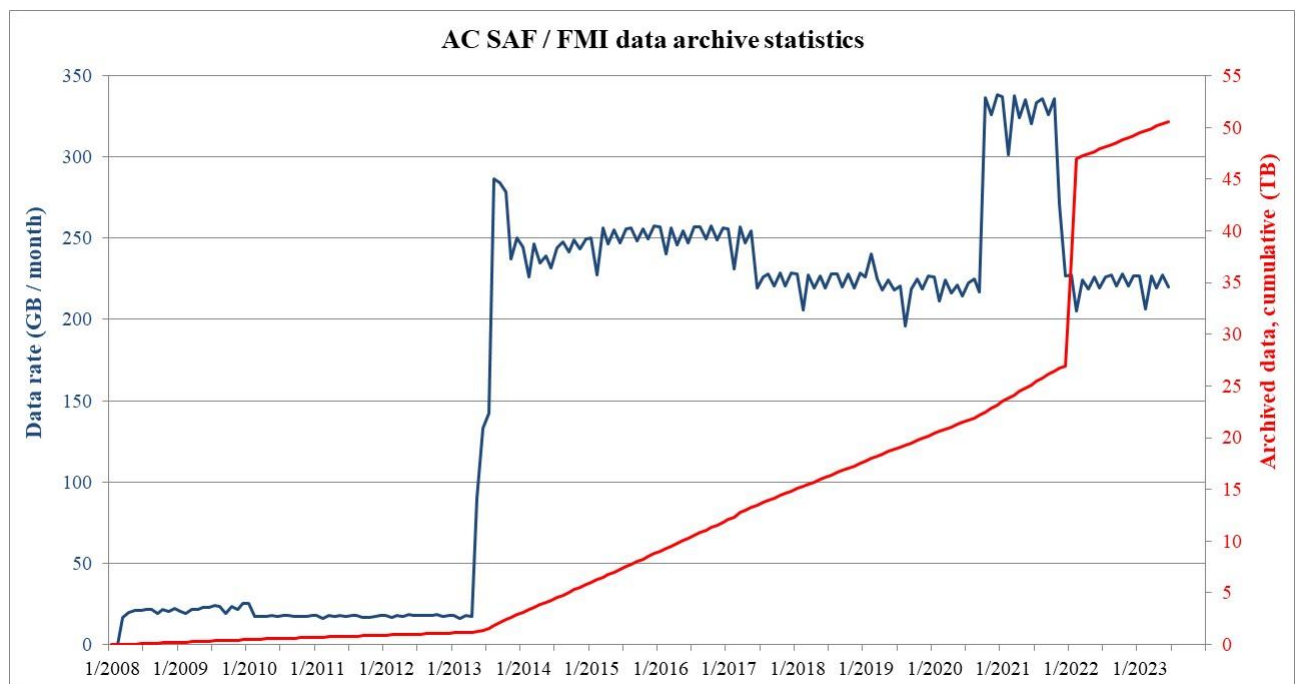Data archive statistics since 2008 are illustrated in Figure 2.1.

Figure 2.1. FMI data archive statistics: data rate and cumulative amount of data

Sudden increase in the cumulative amount of archived data in January – February 2022 is due to archiving of Metop-A/B high-resolution ozone profile data record R1.

Events affecting the data rate are presented in Table 2.5.

Table 2.5. Events affecting the FMI archive data rate

Date	Event	Data rate (GB/month)
03/2008	Archiving of OOP-A started	19.1 – 22.2
06/2009	Archiving of OUV-A started	19.2 – 23.8
11/2009	Archiving of ARS-A started	25.3
02/2010	Compression of OOP-A started	16.2 – 18.3
05/2013	Archiving of OHP-A started	133 – 142
08/2013	Archiving of OOP-B, OHP-B and ARS-B started	279 – 284
11/2013	Archiving of ARP-A and ARP-B started. KNMI implements shuffling algorithm in the hdf5 compression	226 – 250
03/2014	Archiving of OUV-A discontinued, archiving of OUV-B started	227 – 250
02/2015	OPERA algorithm update, tropospheric integrated profiles added	247 – 257
06/2017	Archiving of OOP-A and OOP-B discontinued	206 – 229
10/2020	Archiving of ARS-C, ARP-C and OHP-C started	302 – 338
11/2021	Archiving of OHP-A, ARS-A and ARP-A discontinued	206 – 228
01/2023	Archiving of IASI-B/C L3 CO started	206 – 227

Table 2.6 lists the main events (product/service/hardware/software updates etc.) at FMI during the reporting period.

Table 2.6. Main events at FMI during the reporting period

Date	Description
13 April	Offline surface UV processing delay increased to four days

Table 2.7 lists the main local and external anomalies during the reporting period. Corrective and preventive actions should be provided also when applicable.

Table 2.7. Main local and external anomalies affecting FMI systems and performance during the reporting period

ID	Time period	Description
		Nothing to report.

3. Processing centre: DLR

3.1. NRT and offline total/tropospheric trace gas columns, tropical tropospheric ozone

This section reports availability and timeliness of the operational NRT and offline L2 products processed for GOME-2 on Metop-B and Metop-C.

3.1.1. Availability

For Level 1b products, the availability is defined as the number of L1b PDUs with status "reception confirmed", i.e. EUMETSAT received these L1b PDUs through its EUMETCast reference receiving station, divided by the total number of L1b PDUs listed in the EUMETCast sendlist.

Availability for offline L2 products has been defined in Section 1.4. The availability statistics of DLR products are presented in Table 3.1 and Table 3.2. If the availability requirements have been violated, those values are marked with red colour, identified by numbers and reported in Table 3.7.

Table 3.1. Availability of Metop-B total and tropospheric trace gas column products during the reporting period

Product Identifier	Product Name	1/2023	2/2023	3/2023	4/2023	5/2023	6/2023
L1b	PDUs received / PDUs "reception confirmed"	14877/14877 100 %	13297/12954 102.6 % (1)	14856/14858 99.9 %	14392/14394 99.9 %	14871/14872 99.9 %	14380/14381 99.9 %
O3M-41.1	NRT total O3	100 %	102.6 % (1)	99.9 %	99.9 %	99.9 %	99.8 %
O3M-50.1	NRT total NO2						
O3M-52.1	NRT tropospheric NO2						
O3M-55.1	NRT total SO2						
O3M-177.0	NRT total HCHO						
O3M-42.1	Offline total O3	100 %	100 %	100 %	100 %	100 %	100 %
O3M-51.1	Offline total NO2						
O3M-53.1	Offline tropospheric NO2						
O3M-56.1	Offline total SO2						
O3M-58.1	Offline total HCHO						
O3M-82.1	Offline total BrO						
O3M-86.1	Offline total H2O						
O3M-43	Offline tropical tropospheric ozone	100 %	100 %	100 %	100 %	100 %	100 %

Table 3.2. Availability of Metop-C total and tropospheric trace gas column products during the reporting period

Product Identifier	Product Name	1/2023	2/2023	3/2023	4/2023	5/2023	6/2023
L1b	PDUs received / PDUs "reception confirmed"	14873/14873 100 %	13302/12953 102.6 % (1)	14869/14872 99.9 %	14388/14389 99.9 %	14859/14877 99.8 %	14348/14350 99.9 %
O3M-300	NRT total O3	99.9 %	102.6 % (1)	99.9 %	99.9 %	999.9 %	99.8 %
O3M-338	NRT total NO2						
O3M-341	NRT tropospheric NO2						
O3M-374	NRT total SO2						
O3M-344	NRT total HCHO						
O3M-301	Offline total O3	100 %	100 %	100 %	100 %	100 %	100 %
O3M-339	Offline total NO2						
O3M-342	Offline tropospheric NO2						
O3M-375	Offline total SO2						
O3M-345	Offline total HCHO						
O3M-317	Offline total BrO						
O3M-386	Offline total H2O						
O3M-302	Offline tropical tropospheric ozone	100 %	100 %	100 %	100 %	100 %	100 %

3.1.2. Timeliness

Timeliness indicates the elapsed time between sensing and product dissemination. Timeliness requirements are 3 hours for NRT products and 15 days for offline products. If the requirements have been violated, those values are marked with red colour. In addition, the violations are identified by numbers and reported in Table 3.7 if they have caused the availability values to drop below the allowed limits.

Note: timeliness violations are not listed as anomalies if the availability is above the limit.

The values for NRT products in Table 3.3 and Table 3.4 indicate the elapsed times (days, hours and minutes in the format [ddT]hh:mm) from sensing to EUMETCast (NRT) upload. In each cell, the values from top to bottom represent observed monthly average, minimum and maximum times for NRT products.

Offline products (excluding the tropospheric product) are monthly aggregates and the reported value is the absolute time of archive upload to the EOWEB catalogue.

Table 3.3. Timeliness of Metop-B total and tropospheric trace gas column products during the reporting period

Product Identifier	Product Name	1/2023	2/2023	3/2023	4/2023	5/2023	6/2023
O3M-41.1	NRT total O3	avg: 00:51 min: 00:29 max: 01:46	avg: 00:51 min: 00:30 max: 01:52	avg: 00:52 min: 00:29 max: 06:24	avg: 00:50 min: 00:29 max: 01:48	avg: 00:56 min: 00:31 max: 01:50	avg: 00:58 min: 00:31 max: 02:01
O3M-50.1	NRT total NO2						
O3M-52.1	NRT tropospheric NO2						
O3M-55.1	NRT total SO2						
O3M-177.0	NRT total HCHO						
O3M-42.1	Offline total O3	2023-02-13T13:25:04	2023-03-13T13:19:25	2023-04-13T10:26:45	2023-05-13T09:48:06	2023-06-13T10:26:31	2023-07-13T10:21:51
O3M-51.1	Offline total NO2						
O3M-53.1	Offline tropospheric NO2						
O3M-56.1	Offline total SO2						
O3M-58.1	Offline total HCHO						
O3M-82.1	Offline total BrO						
O3M-86.1	Offline total H2O						
O3M-43	Offline tropical tropospheric ozone	Unknown [1]	Unknown [1]	2023-04-04	2023-05-15	2023-06-13	2023-07-10

[1] There was an issue with the archiving of this product on the FTP site in February 2023. It was solved, but earlier products from 2023 were re-uploaded and the original timeliness values couldn't be determined anymore.

Table 3.4. Timeliness of Metop-C total and tropospheric trace gas column products during the reporting period

Product Identifier	Product Name	1/2023	2/2023	3/2023	4/2023	5/2023	6/2023
O3M-300	NRT total O3	avg: 01:41 min: 01:10 max: 02:12	avg: 01.41 min: 00:36 max: 02:15	avg: 01:44 min: 00:34 max: 02:32	avg: 01:43 min: 00:34 max: 02:17	avg: 01:35 min: 00:35 max: 02:17	avg: 01:35 min: 00:37 max: 02:43
O3M-338	NRT total NO2						
O3M-341	NRT tropospheric NO2						
O3M-374	NRT total SO2						
O3M-344	NRT total HCHO						
O3M-301	Offline total O3	2023-02-13T12:48:55	2023-03-13T12:46:10	2023-04-13T09:50:08	2023-05-13T10:23:46	2023-06-13T09:49:40	2023-07-13T09:46:45
O3M-339	Offline total NO2						
O3M-342	Offline tropospheric NO2						
O3M-375	Offline total SO2						
O3M-345	Offline total HCHO						
O3M-317	Offline total BrO						
O3M-386	Offline total H2O						
O3M-302	Offline tropical tropospheric ozone	Unknown [1]	Unknown [1]	2023-04-04	2023-05-15	2023-06-13	2023-07-10

[1] There was an issue with the archiving of this product on the FTP site in February 2023. It was solved, but earlier products from 2023 were re-uploaded and the original timeliness values couldn't be determined anymore.

3.2. Services, main events and anomalies

Table 3.5. DLR service statistics related to product archiving and ordering

Description of service / event	1/2023	2/2023	3/2023	4/2023	5/2023	6/2023
Archive statistics [2]						
Number of archived products (cumulative) – according to product insertion time	536403	537192	538053	538904	539784	540636
Size of archived products (TB, cumulative)	16.76	16.78	16.83	16.89	16.94	17.00
Number of missing orbit products – according to sensing time	1	0	18	0	0	0
Number of archived products with good/poor/error[3] quality assessed per month – according to product insertion time	875/0/13	782/1/6	855/0/6	846/2/4	874/0/5	845/1/6
Online Access [1]						
Number of searches in the GOME.TC collection	144	183	148	160	128	70
Number of FTP (ATMOS/VELA) subscribers	551	556	561	566	574	542[*]
Number of FTP (ATMOS/VELA) downloads	215493	289006	165703	180244	130007	105463
Downloaded data volume (GB)	1131.5	3202.2	1210.8	1459.0	699.78	327.34
Product ordering						
Number of EOWEB orders	11	2	4	6	0	2
Delivered data volume (GB)	23.92	36.30	119.6	16.89	0	23.42

[1] NTO product and OTO product is stored at the DLR for external search and download

[2] O3MOTO product (collection GOME.TC, Metop missions) is archived and available to non-NRT users

[3] good: max. 2 PDUs missing, poor/error: more than 2 PDUs missing

[*] AC SAF Helpdesk received multiple notifications for invalid email addresses when AC SAF news bulletin was sent to the users in June. Owners of those addresses were removed from the list of AC SAF users.

Table 3.6 lists the main events (product/service/hardware/software updates etc.) at DLR during the reporting period.

Table 3.6. Main events at DLR during the reporting period

Date	Event
April	27 March the updated version of the GOME-2 L3 processor was deployed in the operational processing environment. The following L3 daily and monthly products are being processed: O3, NO2, SO2, HCHO, BrO and H2O. In addition, and as a requirement to successfully run the processor, the processing instance has been updated. Since April 2023 the offline L3 GOME2 trace gas columns are publicly available.

Table 3.7 lists the main and external local anomalies at DLR during the reporting period. Corrective and preventive actions should be provided also when applicable.

Table 3.7. Main local and external anomalies affecting DLR systems and performance during the reporting period

ID	Time period	Description
1	February	More L1b PDUs seem to have been received than there were PDUs with status "reception confirmed". This offset is due to the non-availability of the sendlist file 24 February at DLR.
		Corrective action: N/A
		Preventive action: Planned implementation of an automated monitoring, which checks sendlist file completeness. In case of missing sendlist files a notification will be send to AC SAF operations, triggering the re-retrieval of the missing file(s).

4. Processing centre: KNMI

4.1. NRT and offline ozone profiles, absorbing aerosol height and index, global tropospheric ozone

4.1.1. Availability

For Level 1b products, the availability is defined as the number of unique L1b PDUs received either via EUMETCast Satellite or EUMETCast Terrestrial (demonstrational dissemination service), divided by the number of L1b PDUs not marked as "not sent" in the EUMETCast Satellite sendlist. This approximation presumes that all PDUs marked as "sent not confirmed" are still available via EUMETCast Terrestrial.

Availability for offline L2 products has been defined in Section 1.4. The availability statistics of KNMI products are presented in Table 4.1 and Table 4.2. If the availability requirements have been violated, those values are marked with red colour, identified by numbers and reported in Table 4.9.

Tropospheric ozone products are included in the ozone profile products and have the same statistics. The same applies to scattering aerosol index products which are included in the absorbing aerosol index products.

Table 4.1. Availability of Metop-B L1b PDUs, ozone profile products and aerosol products during the reporting period

Product Identifier	Product Name	1/2023	2/2023	3/2023	4/2023	5/2023	6/2023
EUMETCast							
L1b	PDUs received / sent	14877/14877 100 %	13435/13435 100 %	14858/14858 100 %	14394/14394 100 %	14874/14874 100 %	14392/14392 100 %
O3M-47.1	NRT high-resolution ozone profile	100 %	99.0 %	99.6 %	100 %	100 %	100 %
O3M-78	NRT absorbing aerosol height	100 %	98.9 %	99.1 %	100 %	100 %	100 %
O3M-72.1	NRT absorbing aerosol index from PMDs	100 %	98.9 %	99.1 %	100 %	100 %	100 %
WMO/GTS							
O3M-47.1	NRT high-resolution ozone profile	100 %	99.0 %	99.6 %	100 %	100 %	100 %
FMI archive							
O3M-48.1	Offline high-resolution ozone profile	100 %	100 %	100 %	100 %	100 %	100 %
O3M-79	Offline absorbing aerosol height	100 %	100 %	100 %	100 %	100 %	100 %
O3M-73.1	Offline absorbing aerosol index from PMDs	100 %	100 %	100 %	100 %	100 %	100 %

Table 4.2. Availability of Metop-C L1b PDUs, ozone profile products and aerosol products during the reporting period

Product Identifier	Product Name	1/2023	2/2023	3/2023	4/2023	5/2023	6/2023
EUMETCast							
L1b	PDUs received / sent	14873/14873 100 %	13433/13433 100 %	14872/14872 100 %	14389/14389 100 %	14876/14877 100 %	14362/14363 100 %
O3M-311	NRT high-resolution ozone profile	100 %	98.8 %	98.6 %	100 %	100 %	100 %
O3M-364	NRT absorbing aerosol height	100 %	99.1 %	99.1 %	100 %	100 %	100 %
O3M-362	NRT absorbing aerosol index from PMDs	100 %	99.1 %	99.1 %	100 %	100 %	100 %
WMO/GTS							
O3M-311	NRT high-resolution ozone profile	100 %	98.9 %	98.6 %	100 %	100 %	100 %
FMI archive							
O3M-312	Offline high-resolution ozone profile	100 %	100 %	100 %	100 %	100 %	100 %
O3M-365	Offline absorbing aerosol height	100 %	100 %	100 %	100 %	100 %	100 %
O3M-363	Offline absorbing aerosol index from PMDs	100 %	100 %	100 %	100 %	100 %	100 %

4.1.2. Timeliness

Timeliness indicates the elapsed time between sensing and product dissemination. Timeliness requirements are 3 hours for NRT products and 15 days for offline products. If the requirements have been violated, those values are marked with red colour. In addition, the violations are identified by numbers and reported in Table 4.9 if they have caused the availability values to drop below the allowed limits.

Note: timeliness violations are not listed as anomalies if the availability is above the limit.

The values in Table 4.3 and Table 4.4 indicate elapsed times (days, hours and minutes in the format [ddT]hh:mm) from sensing to EUMETCast and WMO/GTS (NRT) or archive upload (offline). In each cell, the values from top to bottom represent observed monthly average, minimum and maximum times.

Tropospheric ozone products are included in the ozone profile products and have the same statistics.

Table 4.3. Timeliness of Metop-B ozone profile and aerosol products during the reporting period

Product Identifier	Product Name	1/2023	2/2023	3/2023	4/2023	5/2023	6/2023
EUMETCast							
O3M-47.1	NRT high-resolution ozone profile	avg: 01:06 min: 00:41 max: 02:00	avg: 01:07 min: 00:30 max: 05:59	avg: 01:06 min: 00:30 max: 05:03	avg: 01:02 min: 00:30 max: 01:58	avg: 01:07 min: 00:32 max: 02:09	avg: 01:09 min: 00:32 max: 02:05
O3M-78	NRT absorbing aerosol height	avg: 00:51 min: 00:28 max: 01:46	avg: 00:53 min: 00:29 max: 05:40	avg: 00:53 min: 00:29 max: 05:58	avg: 00:49 min: 00:29 max: 01:47	avg: 00:54 min: 00:30 max: 01:48	avg: 00:55 min: 00:30 max: 01:47
O3M-72.1	NRT absorbing aerosol index from PMDs	avg: 00:51 min: 00:28 max: 01:46	avg: 00:53 min: 00:30 max: 05:40	avg: 00:53 min: 00:29 max: 05:58	avg: 00:49 min: 00:29 max: 01:47	avg: 00:54 min: 00:30 max: 01:48	avg: 00:55 min: 00:30 max: 01:47
WMO/GTS							
O3M-47.1	NRT high-resolution ozone profile	avg: 01:07 min: 00:42 max: 02:02	avg: 01:08 min: 00:31 max: 05:55	avg: 01:07 min: 00:31 max: 05:06	avg: 01:03 min: 00:31 max: 02:00	avg: 01:08 min: 00:33 max: 02:11	avg: 01:10 min: 00:33 max: 02:06
FMI archive							
O3M-48.1	Offline high-resolution ozone profile	avg: 01T23:59 min: 06:54 max: 02T03:11	avg: 01T23:32 min: 06:57 max: 02T07:50	avg: 01T23:33 min: 07:00 max: 02T04:12	avg: 01T23:58 min: 06:48 max: 02T03:05	avg: 01T14:28 min: 06:48 max: 02T03:20	avg: 15:21 min: 06:48 max: 02T03:19
O3M-79	Offline absorbing aerosol height	avg: 01T23:59 min: 06:58 max: 02T03:01	avg: 01T23:31 min: 06:58 max: 02T07:45	avg: 01T23:32 min: 07:01 max: 02T04:07	avg: 01T23:57 min: 06:52 max: 02T03:13	avg: 01T14:26 min: 06:43 max: 02T03:20	avg: 15:17 min: 06:43 max: 02T03:04
O3M-73.1	Offline absorbing aerosol index from PMDs	avg: 01T23:56 min: 06:55 max: 02T03:07	avg: 01T23:28 min: 06:58 max: 02T07:10	avg: 01T23:31 min: 07:04 max: 02T04:22	avg: 01T23:53 min: 06:52 max: 02T03:01	avg: 01T14:25 min: 06:43 max: 02T03:13	avg: 15:17 min: 06:46 max: 02T02:55

Table 4.4. Timeliness of Metop-C ozone profile and aerosol products during the reporting period

Product Identifier	Product Name	1/2023	2/2023	3/2023	4/2023	5/2023	6/2023
EUMETCast							
O3M-311	NRT high-resolution ozone profile	avg: 01:53 min: 01:07 max: 02:24	avg: 01:55 min: 00:35 max: 05:59	avg: 01:56 min: 00:35 max: 05:59	avg: 01:51 min: 00:35 max: 02:21	avg: 01:45 min: 00:36 max: 02:15	avg: 01:45 min: 00:39 max: 04:35
O3M-364	NRT absorbing aerosol height	avg: 01:38 min: 01:07 max: 02:04	avg: 01:41 min: 00:35 max: 06:00	avg: 01:43 min: 00:33 max: 05:58	avg: 01:39 min: 00:34 max: 02:05	avg: 01:32 min: 00:34 max: 01:59	avg: 01:31 min: 00:36 max: 04:16
O3M-362	NRT absorbing aerosol index from PMDs	avg: 01:38 min: 01:07 max: 02:04	avg: 01:41 min: 00:35 max: 06:00	avg: 01:43 min: 00:33 max: 05:58	avg: 01:39 min: 00:34 max: 02:05	avg: 01:32 min: 00:34 max: 01:59	avg: 01:31 min: 00:36 max: 04:16

Product Identifier	Product Name	1/2023	2/2023	3/2023	4/2023	5/2023	6/2023
WMO/GTS							
O3M-311	NRT high-resolution ozone profile	avg: 01:54 min: 01:08 max: 02:25	avg: 01:56 min: 00:36 max: 06:00	avg: 01:57 min: 00:36 max: 06:00	avg: 01:52 min: 00:36 max: 02:23	avg: 01:46 min: 00:37 max: 02:16	avg: 01:46 min: 00:40 max: 04:36
FMI archive							
O3M-312	Offline high-resolution ozone profile	avg: 02T00:00 min: 07:15 max: 02T03:30	avg: 02T00:18 min: 07:27 max: 02T07:38	avg: 01T23:57 min: 07:30 max: 02T07:57	avg: 01T23:42 min: 07:30 max: 02T03:41	avg: 01T14:23 min: 07:24 max: 02T03:45	avg: 15:20 min: 07:21 max: 02T03:47
O3M-365	Offline absorbing aerosol height	avg: 02T00:03 min: 07:28 max: 02T03:34	avg: 02T00:16 min: 07:22 max: 02T07:28	avg: 01T23:56 min: 07:34 max: 02T07:52	avg: 01T23:42 min: 07:34 max: 02T03:37	avg: 01T14:22 min: 07:19 max: 02T03:40	avg: 15:18 min: 07:28 max: 02T03:43
O3M-363	Offline absorbing aerosol index from PMDs	avg: 02T00:01 min: 07:19 max: 02T03:28	avg: 02T00:15 min: 07:22 max: 02T07:58	avg: 01T23:52 min: 07:25 max: 02T08:22	avg: 01T23:41 min: 07:34 max: 02T03:40	avg: 01T14:21 min: 07:28 max: 02T03:48	avg: 15:14 min: 07:19 max: 02T03:58

4.2. Services, main events and anomalies

Tropospheric ozone products are included in the ozone profile products and have the same statistics.

Table 4.5. Number of products sent to FMI archive[1]

Product Identifier	Product Name	Metop satellite	1/2023	2/2023	3/2023	4/2023	5/2023	6/2023
O3M-48.1	Offline high-resolution ozone profile	B	439	397	437	424	439	425
O3M-312		C	437	398	438	425	439	425
O3M-79	Offline absorbing aerosol height	B	439	397	437	424	439	425
O3M-365		C	437	398	438	425	439	425
O3M-73.1	Offline absorbing aerosol index from PMDs	B	439	397	437	424	439	425
O3M-363		C	437	398	438	425	439	425

Table 4.6. Number of products stored locally at KNMI[2]

Product Identifier	Product Name	Metop satellite	1/2023	2/2023	3/2023	4/2023	5/2023	6/2023
O3M-47.1	NRT high-resolution ozone profile	B	8380	7575	8325	7976	8294	8303
O3M-311		C	8345	7558	8224	8000	8305	8253
O3M-78	NRT absorbing aerosol height	B	8380	7583	8204	7976	8294	8303
O3M-364		C	8345	7583	8186	8000	8305	8253

Product Identifier	Product Name	Metop satellite	1/2023	2/2023	3/2023	4/2023	5/2023	6/2023
O3M-72.1	NRT absorbing aerosol index from PMDs	B	8380	7583	8204	7976	8294	8303
O3M-362		C	8345	7583	8186	8000	8305	8253
O3M-48.1	Offline high-resolution ozone profile	B	439	397	437	424	439	425
O3M-312		C	437	398	438	425	439	425
O3M-79	Offline absorbing aerosol height	B	439	397	437	424	439	425
O3M-365		C	437	398	438	425	439	425
O3M-73.1	Offline absorbing aerosol index from PMDs	B	439	397	437	424	439	425
O3M-363		C	437	398	438	425	439	425

Table 4.7. EUMETCast and WMO/GTS uploads[3]

Product Identifier	Product Name	Metop satellite	1/2023	2/2023	3/2023	4/2023	5/2023	6/2023
O3M-47.1	NRT high-resolution ozone profile	B	8380/8380	7498/7498	8294/8294	7976/7976	8294/8294	8303/8303
O3M-311		C	8345/8345	7471/7473	8106/8105	8000/8000	8305/8305	8252/8252
O3M-78	NRT absorbing aerosol height	B	8380	7502	8133	7976	8294	8303
O3M-364		C	8345	7516	8114	8000	8305	8252
O3M-72.1	NRT absorbing aerosol index from PMDs	B	8380	7502	8133	7976	8294	8303
O3M-362		C	8345	7516	8114	8000	8305	8252

[1] Products are archived in HDF5 format.
[2] Products are stored for 3 years (in HDF5 and BUFR formats).
[3] NRT high-resolution ozone profile is disseminated via EUMETCast and WMO/GTS in BUFR format. NRT absorbing aerosol index and NRT absorbing aerosol index from PMDs are disseminated only via EUMETCast (in HDF5 and BUFR formats).

Table 4.8 lists the main events (product/service/hardware/software updates etc.) at KNMI during the reporting period.

Table 4.8. Main events at KNMI during the reporting period

Date	Description
17 April	OPERA update to software version 2.20

Table 4.9 lists the main local and external anomalies at KNMI during the reporting period. Corrective and preventive actions should be provided also when applicable.

Table 4.9. Main local and external anomalies affecting KNMI systems and performance during the reporting period

ID	Time period	Description
1		*Nothing to report.*

5. Processing centre: DMI

5.1. NRT clear-sky and cloud-corrected UV index

5.1.1. Availability

NUV product is required to be produced every day, either on the basis of new GOME ATO input or in the case of ATO delivery failure based on back-up total ozone data (ECMWF or climatology).

Availability requirement for NUV has been defined in Section 1.4. The availability statistics of DMI products are presented in Table 5.1. If the requirement is violated, those values are marked with red colour, identified by numbers and reported in Table 5.5.

Table 5.1. Availability of NRT UV products during the reporting period

Product Identifier	Product Name	1/2023	2/2023	3/2023	4/2023	5/2023	6/2023
O3M-409	NRT UV index, clear-sky	100 %	100 %	100 %	94 % (1)	100 %	100 %
O3M-410	NRT UV index, cloud-corrected						

5.1.2. Timeliness

Timeliness requirement for NUV says that the final NUV product is to be delivered to users no later than two hours after receiving the ATO input and not later than 04:00 UTC. Processing is started at 02:45 UTC thus the maximum processing time allowed is 1 hour 15 min. If the timeliness requirement is violated, those values are marked with red colour. In addition, the violations are identified by numbers and reported in Table 5.5 if they have caused the availability values to drop below the allowed limits.

Days where no products are produced or could be delivered to users (as indicated in Table 5.1) are not included in Table 5.2.

Note: timeliness violations are not listed as anomalies if the availability is above the limit.

The values in Table 5.2 indicate elapsed processing times (hours, minutes and seconds in the format [hh:]mm:ss). In each cell, the values from top to bottom represent observed monthly average, minimum and maximum processing times.

Table 5.2. Timeliness of NRT UV products during the reporting period

Product Identifier	Product Name	1/2023	2/2023	3/2023	4/2023	5/2023	6/2023
O3M-409	NRT UV index, clear-sky	avg: 05:57 min: 05:24 max: 09:17	avg: 05:54 min: 05:46 max: 06:06	avg: 05:11 min: 04:20 max: 06:11	avg: 05:09 min: 04:29 max: 10:00	avg: 05:00 min: 04:39 max: 05:14	avg: 04:45 min: 04:25 max: 05:00
O3M-410	NRT UV index, cloud-corrected						

5.2. Services, main events and anomalies

Table 5.3. Number of products stored locally at DMI[1]

Description of service / event	1/2023	2/2023	3/2023	4/2023	5/2023	6/2023
Storage statistics						
Number of stored products (NRT UV index, clear-sky)	31	28	31	30	31	30
Number of stored products (NRT UV index, cloud-corrected)	31	28	31	30	31	30
Total size of stored products (MB)	248	224	248	240	248	240

[1] NUV products are stored at the DMI at least until the end of the Metop programs.

Table 5.4 lists the main events (product/service/hardware/software updates etc.) at DMI during the reporting period.

Table 5.4. Main events at DMI during the reporting period

Date	Event
	During the reporting period DMI started the work on moving the IT systems to a new location.

Table 5.5 lists the main local and external anomalies at DMI during the reporting period. Corrective and preventive actions should be provided also when applicable.

Table 5.5. Main local and external anomalies affecting DMI systems and performance during the reporting period

ID	Time period	Description
1	23-24 April	On April 23 a power failure during the transition of hardware to new DMI location caused a crash of all virtual machines. Nothing was produced April 23, and on April 24 NUV was produced with a 10-hour delay. Corrective action: The product for April 23 was produced when the system was up and running on April 24. Thus, no missing data in Table 5.3. Preventive action: None, as this was a consequence of a special situation in connection with the move.

6. Processing centre: EUMETSAT

6.1. NRT IASI CO, SO2, HNO3 and ozone profile

6.1.1. Availability

For Level 1c products, the availability is defined as the number of available PDUs divided by the number of maximum expected PDUs.

For NRT products, the availability requirement is 97.5 % and it is defined by the ratio of the number of in time processed and disseminated products to the number of maximum expected input products (L1c PDUs) per month.

The availability statistics of EUMETSAT products are presented in Table 6.1 and Table 6.2. If the availability requirements have been violated, those values are marked with red colour, identified by numbers and reported in Table 6.7 and/or Table 6.8.

Note that in the frame of this product processing centre being the EUMETSAT HQ in Darmstadt, the L1c data is directly available to the algorithm, i.e., its availability is not dependable of EUMETCast dissemination. Furthermore, since there is no relay of information from *Satellite* processing centres, the L2 product availability in the following tables concern the end-to-end availability as they were recorded in the EUMETSAT Reference Receiving Stations.

Table 6.1. Availability of Metop-B L1c PDUs and IASI NRT products during the reporting period

Product Identifier	Product Name	1/2023	2/2023	3/2023	4/2023	5/2023	6/2023
L1c	PDUs available / PDUs expected	14783/14880	13377/13440	14816/14880	14362/14400	14756/14880	14373/14400
L1c	Availability	99.4 %	99.5 %	99.6 %	99.7 %	99.2 %	99.8 %
O3M-80	NRT IASI CO	97.7 %	99.0 %	97.7 %	99.7 %	97.9 %	99.1 %
O3M-57	NRT IASI SO2	97.7 %	99.0 %	97.7 %	99.7 %	97.9 %	99.1 %
O3M-81	NRT IASI HNO3	97.7 %	99.0 %	97.7 %	99.7 %	97.9 %	99.1 %
O3M-49	NRT IASI ozone profile	97.7 %	99.0 %	97.7 %	99.7 %	97.9 %	99.1 %

Table 6.2. Availability of Metop-C L1c PDUs and IASI NRT products during the reporting period

Product Identifier	Product Name	1/2023	2/2023	3/2023	4/2023	5/2023	6/2023
L1c	PDUs available / PDUs expected	14765/14880	13394 / 13440	14866/14880	14266/14400	14655/14880	14351/14400
L1c	Availability	99.2 %	99.7 %	99.9 %	99.1 %	98.5 %	99.7 %
O3M-352	NRT IASI CO	98.1 %	98.5 %	98.7 %	99.1 %	97.9 %	98.4 %
O3M-377	NRT IASI SO2	98.1 %	98.5 %	98.7 %	99.0 %	97.9 %	98.4 %
O3M-336	NRT IASI HNO3	98.1 %	98.5 %	98.7 %	99.0 %	97.9 %	98.4 %
O3M-315	NRT IASI ozone profile	98.1 %	98.5 %	98.7 %	99.0 %	97.9 %	98.4 %

6.1.2. Timeliness

Timeliness indicates the elapsed time between sensing and product dissemination. Timeliness requirement is 3 hours for NRT products. If the requirements have been violated, those values are marked with red colour. In addition, the violations are identified by numbers and reported in Table 6.8 if they have caused the availability values to drop below the allowed limits.

Note: timeliness violations are not listed as anomalies if the availability is above the limit.

The values in Table 6.3 and Table 6.4 indicate elapsed times (hours and minutes in the format hh:mm) from sensing to EUMETCast Reference Receiving Station, i.e., end-to-end timeliness. In each cell, the values from top to bottom represent observed monthly average, minimum and maximum times.

Table 6.3. Timeliness of Metop-B IASI NRT products during the reporting period

Product Identifier	Product Name	1/2023	2/2023	3/2023	4/2023	5/2023	6/2023
O3M-80	NRT IASI CO	avg: 01:10 min: 00:42 max: 01:57	avg: 01:08 min: 00:45 max: 01:58	avg: 01:09 min: 00:43 max: 02:32	avg: 01:12 min: 00:58 max: 02:10	avg: 01:15 min: 01:00 max: 02:11	avg: 01:12 min: 00:58 max: 02:11
O3M-57	NRT IASI SO2	avg: 01:10 min: 00:42 max: 01:57	avg: 01:08 min: 00:45 max: 01:58	avg: 01:09 min: 00:43 max: 02:32	avg: 01:12 min: 00:58 max: 02:10	avg: 01:15 min: 01:00 max: 02:11	avg: 01:13 min: 00:59 max: 02:11
O3M-81	NRT IASI HNO3	avg: 01:10 min: 00:42 max: 01:57	avg: 01:08 min: 00:45 max: 01:58	avg: 01:09 min: 00:43 max: 02:29	avg: 01:12 min: 00:58 max: 02:10	avg: 01:15 min: 01:00 max: 02:11	avg: 01:13 min: 00:59 max: 02:11
O3M-49	NRT IASI ozone profile	avg: 01:10 min: 00:42 max: 01:57	avg: 01:08 min: 00:45 max: 01:58	avg: 01:09 min: 00:43 max: 02:32	avg: 01:12 min: 00:58 max: 02:10	avg: 01:15 min: 01:00 max: 02:11	avg: 01:13 min: 00:59 max: 02:11

Table 6.4. Timeliness of Metop-C IASI NRT products during the reporting period

Product Identifier	Product Name	1/2023	2/2023	3/2023	4/2023	5/2023	6/2023
O3M-352	NRT IASI CO	avg: 01:39 min: 01:00 max: 02:27	avg: 01:39 min: 00:48 max: 02:27	avg: 01:42 min: 01:00 max: 02:28	avg: 01:55 min: 01:04 max: 02:29	avg: 01:54 min: 01:05 max: 02:29	avg: 01:55 min: 01:08 max: 02:26
O3M-377	NRT IASI SO2	avg: 01:39 min: 01:00 max: 02:27	avg: 01:39 min: 00:48 max: 02:27	avg: 01:42 min: 01:00 max: 02:31	avg: 01:55 min: 01:04 max: 02:30	avg: 01:54 min: 01:05 max: 02:29	avg: 01:55 min: 01:08 max: 02:26
O3M-336	NRT IASI HNO3	avg: 01:39 min: 01:00 max: 02:27	avg: 01:39 min: 00:48 max: 02:27	avg: 01:42 min: 01:00 max: 02:31	avg: 01:55 min: 01:04 max: 02:30	avg: 01:54 min: 01:05 max: 02:29	avg: 01:55 min: 01:08 max: 02:26
O3M-315	NRT IASI ozone profile	avg: 01:39 min: 01:00 max: 02:27	avg: 01:39 min: 00:48 max: 02:27	avg: 01:42 min: 01:00 max: 02:31	avg: 01:55 min: 01:04 max: 02:30	avg: 01:54 min: 01:05 max: 02:29	avg: 01:55 min: 01:08 max: 02:26

6.2. Services, main events and anomalies

Table 6.5. Number of products stored locally at EUMETSAT[1]

Product Identifier	Product Name	Metop satellite	1/2023	2/2023	3/2023	4/2023	5/2023	6/2023
O3M-80	NRT IASI CO	B	29072	13300	14592	14363	14613	13809
O3M-352		C	29207	13235	14686	14263	14605	14164
O3M-57	NRT IASI SO2	B	29072	13299	14589	14362	14614	13804
O3M-377		C	29207	13219	14686	14262	14605	14166
O3M-81	NRT IASI HNO3	B	29072	13299	14589	14362	14614	13804
O3M-336		C	29207	13219	14686	14262	14605	14166
O3M-49	NRT IASI ozone profile	B	29072	13299	14589	14362	14614	13804
O3M-315		C	29207	13303	14686	14262	14614	14166

[1] PDUs are concatenated back to orbit-based products before being stored

Table 6.6. EUMETCast uploads[1]

Product Identifier	Product Name	Metop satellite	1/2023	2/2023	3/2023	4/2023	5/2023	6/2023
O3M-80	NRT IASI CO	B	29072	13300	14592	14363	14613	14282
O3M-352		C	29207	13235	14686	14263	14605	14164
O3M-57	NRT IASI SO2	B	29072	13299	14589	14362	14614	13804
O3M-377		C	29207	13219	14731	14262	14605	14166
O3M-81	NRT IASI HNO3	B	29072	13299	14589	14362	14614	13804
O3M-336		C	29207	13219	14686	14262	14605	14166
O3M-49	NRT IASI ozone profile	B	29072	13299	14589	14362	14614	13804
O3M-315		C	29207	13303	14731	14262	14614	14166

[1] NRT IASI products are disseminated via EUMETCast (in BUFR format)

Table 6.7 lists the main events (product/service/hardware/software updates etc.) at EUMETSAT during the reporting period.

Table 6.7. Main planned activities at EUMETSAT during the reporting period

ID	Date	Description
1		*Nothing to report.*

Table 6.8 lists the main local and external anomalies at EUMETSAT during the reporting period. Corrective and preventive actions should be provided also when applicable.

Table 6.8. Main local and external anomalies affecting EUMETSAT systems and performance during the reporting period

ID	Time period	Description
		Nothing to report.

7. Validation and quality monitoring

This section describes the validation status and validation/quality monitoring activities of NRT and offline data products during the reporting period. Validation reports for data records are found from https://acsaf.org/valreps.html

Reference documents are listed in Section 1.3 and accuracy requirements in Section 1.5.

7.1. Total ozone column products

Table 7.1. Validation status of total ozone column products

Product Identifier	Product Name	Accuracy	Reference	Validating Institute	Correlative data sources
O3M-41.1	NRT total O3	Fulfils threshold accuracy requirement	RD5	AUTH	World Ozone Mapping Centre
O3M-300			RD27		
O3M-06.1	Offline total O3	Fulfils threshold accuracy requirement	RD5	AUTH	World Ozone and Ultraviolet Radiation Data Center (WOUDC), of the World Meteorological Organization, (WMO), Global Atmosphere Watch, (GAW)
O3M-42.1					
O3M-301			RD27		

Validation results can be found in more detail on the AC SAF validation & quality assessment website at http://acsaf.physics.auth.gr/eumetsat/validation/near_real and http://acsaf.physics.auth.gr/eumetsat/validation/offline

7.1.1. GOME-2B and GOME-2C total ozone column validation

This summary presents the validation activities for total ozone column products (TOCs), reported by the GOME-2/Metop-B and GOME-2/Metop-C instruments (hereafter GOME-2B and GOME-2C, respectively). Members of the Laboratory of Atmospheric Physics of the Aristotle University of Thessaloniki (LAP/AUTH), Thessaloniki, Greece, involved in the validation activities include Professor, Dr. Dimitris Balis, Special Teaching Fellow & Researcher, Dr. Katerina Garane and Research Associate, Dr. MariLiza Koukouli.

During the reporting period, the operational validation of offline total ozone and NRT total ozone products continued as per previous periods.

7.1.1.1 Update of database for reference ground-based data

For the nominal validation, the ground-based TOCs from Brewer, Dobson and M-124 instruments reported to the World Ozone and Ultraviolet Radiation Data Centre (WOUDC), are employed. WOUDC is one of the World Data Centres which are part of the Global Atmosphere Watch (GAW) programme of the World Meteorological Organization (WMO). For the quality of the reference ground-based data used for the validation of the total ozone products, updated information were extracted from recent inter-comparisons and calibration records. This continuously updated selection of ground-based measurements has already been used numerous times in the validation and analysis of global total ozone records such as the inter-comparison between the OMI/Aura TOMS and OMI/Aura DOAS algorithms [Balis *et al.*, 2007a], the validation of ten years of GOME/ERS-2 ozone record [Balis *et al.*, 2007b], the validation of the updated version of the OMI/Aura TOMS algorithm [Antón *et al.*, 2009], the GOME-2/Metop-A validation [Loyola *et al.*,

2011; Koukouli *et al.*, 2012], the GOME-2B validation [Hao et al., 2014] and the evaluation of the European Space Agency's Ozone Climate Change Initiative project [O$_3$-CCI] TOCs [Koukouli *et al.*, 2015, Garane *et al.*, 2018], as well as in TROPOMI/S5P TOCs validation [Garane *et al.*, 2019]. In all the aforementioned works, LAP/AUTH assumes the leading role in the validation efforts. The number of WOUDC ground-based stations used in the full operational periods of the two instruments, alongside the mean difference between ground- and space-based TOC estimates is given in Table 7.2.

The comparisons and validation results with respect to the M-124 instruments are available via the validation website, but not shown herein for reasons of brevity.

7.1.1.2 Validation results for GOME-2B and GOME-2C offline total ozone products

GOME-2B and GOME-2C OTO data for the period December 2012 (or January 2019 for GOME-2C) to June 2023 have been downloaded, quality-assured and pre-processed in order to perform the validation strategies. The GDP-4.8 algorithm is the latest version of the GDP-4.x suite of algorithms that have been used for the operational processing of GOME-2B total ozone columns. GOME-2C is processed with GDP-4.9. The main differences between GDP-4.8 and GDP-4.9 concern the SO$_2$ vertical column retrieval. For ozone only minor updates have been performed, such as the optimization of the slit function, the introduction of a pseudo absorber for possible orbital variations of the resolution etc. Therefore, the ozone columns from GOME-2C can be assumed to be similar to the respective data from GOME-2B, analyzed with the previous version of the algorithm.

This period's satellite-to-ground-based measurements comparisons were performed and were added to the existing time series. The majority of the quality-assured ground-based Brewer and Dobson TOCs are reported to the WOUDC repository between 3 and 6 months after measurement, which accounts for the last couple of months missing from the comparative plots shown below. This is a common reporting feature, quite unavoidable.

In Figure 7.1, left column of figures, the status of GOME-2B and GOME-2C TOCs since the beginning of each individual mission is shown in the form of a monthly mean time-series of the percentage differences between each sensor and ground-based observations. Panel a shows the co-locations with Brewer Northern Hemisphere (NH) stations, panel b with Dobson NH stations and panel c with Dobson Southern Hemisphere (SH) stations. The plots shown in the right column of Figure 7.1, show the common time period of operation of the GOME-2B and GOME-2C sensors, hence since the beginning of 2019 onwards.

The monthly mean percentage differences of the two sensors with respect to the ground network range between:

1) -1 to +3 % for GOME-2B and
2) 0 to +3% for the first year of the GOME-2C operation, which is shifted to +1.5 % to +4 % after March 2020,

depending on the season.

This seasonality in the differences between satellite and ground-based is more pronounced in the Dobson co-locations (panels c – f) and is a well-known feature which appears in most operational and scientific satellite TOC comparisons, see for e.g. the validation of the OMI/Aura products [Balis *et al.*, 2007a], the GOME/ERS-2 product [Balis *et al.*, 2007b] and even the recent GOME/ERS-2, SCIAMACHY/Envisat and GOME-2A ESA products [Koukouli *et al.*, 2015, Garane *et al.*, 2018]. The reasons have to do with the treatment of the variability of the stratospheric temperature and how that affects the ozone absorption coefficients used in the different algorithms

[Fragkos *et al.*, 2013; Serdyuchenko *et al.*, 2014]. Hence, when the stratospheric temperature deviates strongly from what is assumed by the algorithms, which is usually the case during the winter months, the differences between ground and satellite increase. See the work of Koukouli *et al.*, 2016, and discussion therein, on this topic.

The well-known reason for the Dobson total ozone seasonality could be treated following a methodology (see Komhyr *et al.*, 1993 and Koukouli *et al.*, 2016) that is followed by LAP/AUTH to post-correct the Dobson ground-based measurements for their effective temperature dependence, but the correction is always dependent on the temperature dataset that is used for its implementation. Additionally, the official repositories such as WOUDC do not provide temperature corrected data and to keep our validation analysis compatible with other studies and validation reports on various other sensors, it was chosen to use the Dobson ground-based dataset as provided by WOUDC.
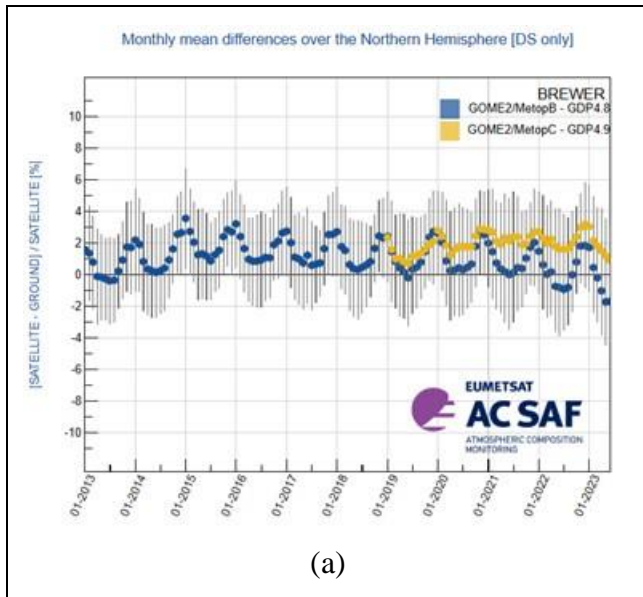
(a)
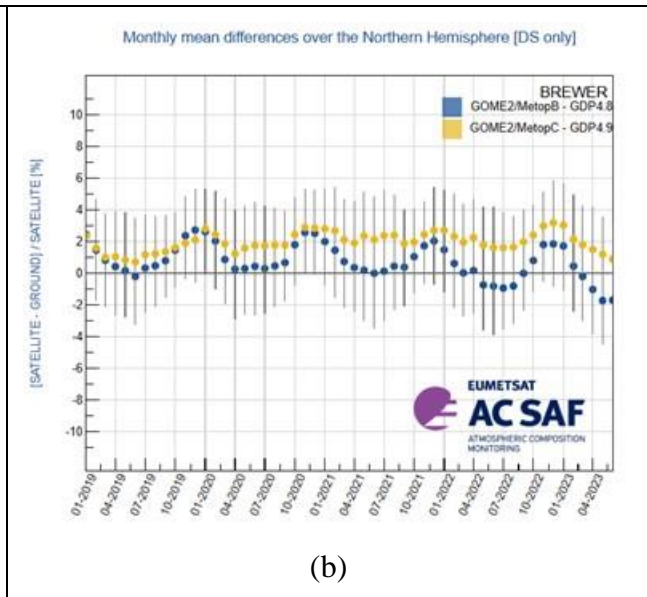
(b)
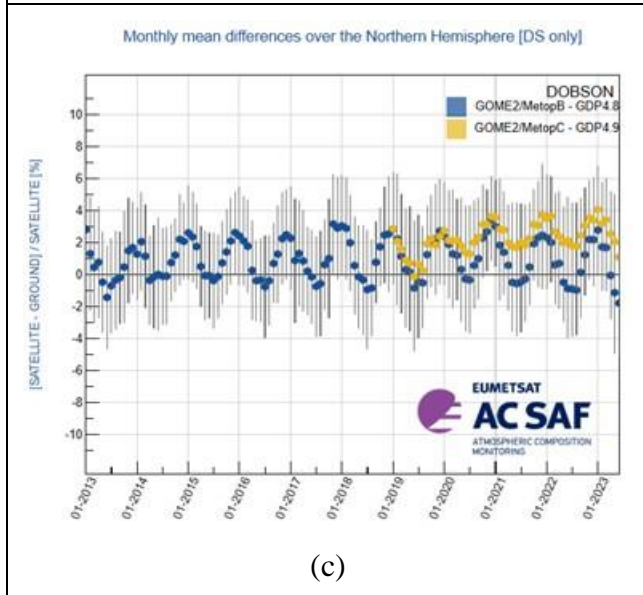
(c)
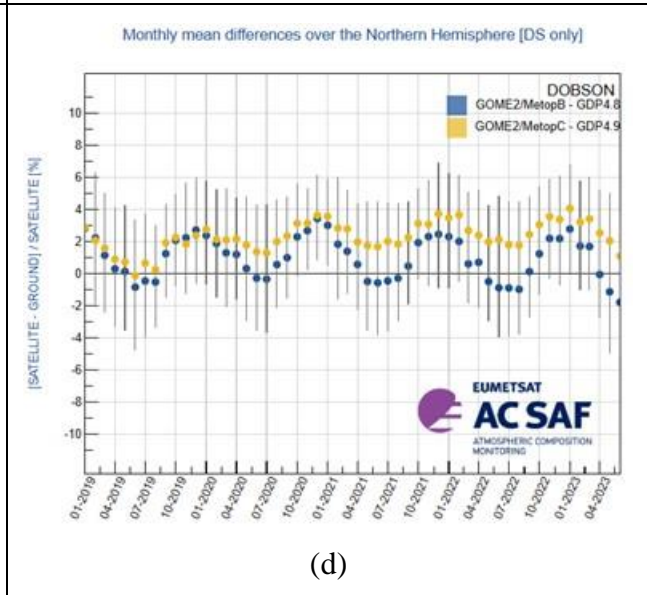
(d)
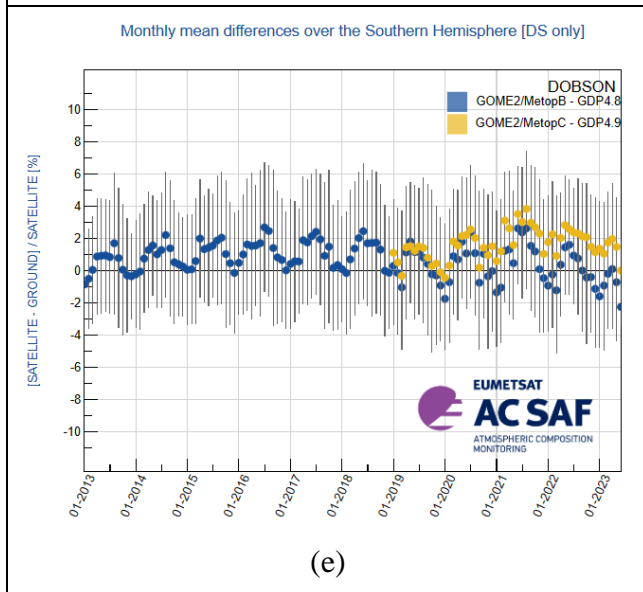
(e)
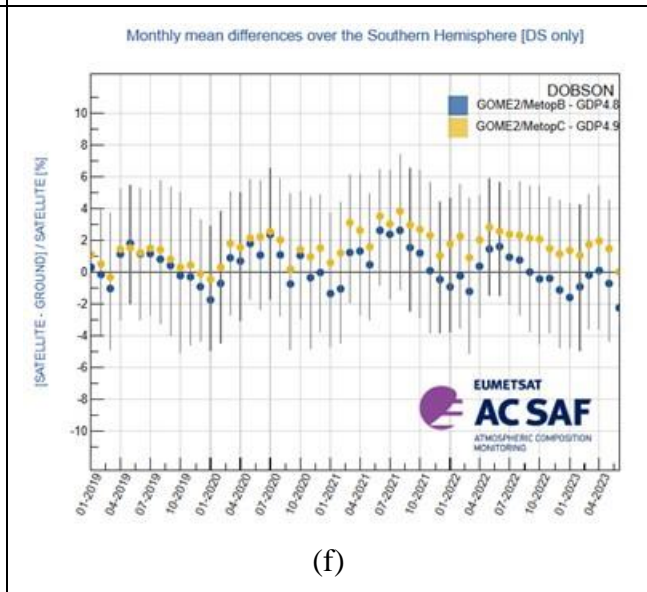
(f)

Figure 7.1. Hemispherical time-series of the monthly mean percentage differences between GOME-2B GDP-4.8 (blue symbols) and GOME-2C GDP-4.9 (orange symbols) total ozone products against ground-based observations. Panels a – d: Northern Hemisphere, panels e and f: Southern Hemisphere. Brewer co-locations are shown in panels a and b (Northern Hemisphere only). Dobson co-locations are shown in panels c – f. The difference between the left and the right column of figures is the time period covered.

As mentioned above, it is noticeable that the agreement between the two sensors in the NH is different before and after spring of 2020:

- Before that point, the deviation of the two sensors was ~ 0 – 1 %, with GOME-2C reporting higher TOCs during summer months by up to ~0.8 % with respect to GOME-2B.

- Since March 2020, their deviation gradually increases up to ~ 3 % (June 2022), with GOME-2B reporting continuously lower TOCs than GOME-2C. The increased difference between the two sensors also has a seasonal dependence, being lower during winter months (~0.5 % for January 2020, ~1 % for January 2021, ~1.2 % for January 2022) and higher during summer months (~1.6 % for June 2020, ~2.3 % for June 2021, ~3.0 % for June 2022).

In the SH (panels c and f) an increased difference, especially pronounced during the spring-summer months, is also seen since March or April 2020, going up to 3 % in January 2023, with GOME-2B reporting continuously lower O_3 values than GOME-2C.

The explanation of GOME-2B continuously decreasing total ozone observations since early 2020 is also confirmed by direct satellite-to-satellite comparisons (not shown here) and is under investigation, but there is already an indication that this is an issue originating from the GOME-2B Level 1b dataset. Hopefully, more information on this feature will be provided in the next reports.

(a)   (b)
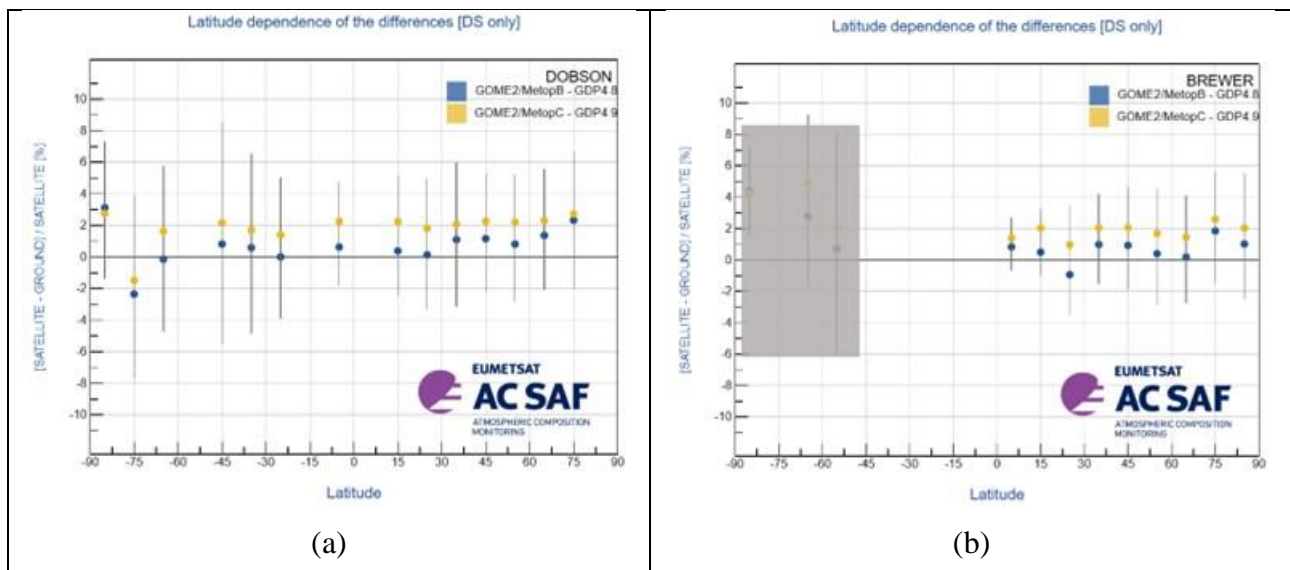
Figure 7.2. The latitudinal dependency of the differences for the Dobson (panel a) and the Brewer network (panel b). The Brewer SH mean biases are greyed-out because the limited number of stations in this part of the earth cannot provide reliable validation results.

In the latitudinal plot (Figure 7.2), it is shown that the overall agreement of both sensors to the ground-based measurements is within 0 – 2 % in the tropics and the mid-latitudes. Additionally, it is noticeable that the comparisons of GOME-2C with respect to ground-based measurements have almost no dependency on latitude, having a very stable relative mean bias of ~2 % for the NH

stations and for co-locations northwards 70°S. The TOC underestimation of GOME-2B with respect to GOME-2C is also shown to be global, but it appears to be more evident for the mid-latitudes and the tropics, where GOME-2B reports lower TOCs by about 1 – 2 % with respect to GOME-2C.

It should be noted that the co-locations used in Figure 7.2 cover the time-period of the two sensors operating in tandem, since January 2019. The respective latitudinal plot made with co-locations covering only 2022 (not shown here), when the divergence between the two sensors is stronger, indicates that these recently increased differences between the GOME-2B and GOME-2C total ozone observations result almost equally from all latitude belts.

7.1.1.3 GOME-2B and GOME-2C TOC validation | Tables of statistics

In Table 7.2, the summary statistics for the GOME-2B and GOME-2C comparisons against co-located total ozone observations from the Dobson and Brewer stations presented in the previous section, are enumerated. The number of individual daily common observations for the Dobsons apply to the entire globe, whereas the Brewer comparisons depict only the NH. As can be noted, the relative differences between GOME-2B and Brewer and Dobson stations is quite stable, with an average mean difference of about +0.7 ± 4.2 %. GOME-2C has a higher mean relative bias with respect to ground-based measurements, of +1.3 to +1.8 ± 4.0 %. Nevertheless, both total ozone products are within the product accuracy requirements (4 % for SZA < 80° and 8 % for SZA>80°).

Table 7.2. Summary statistics for the respective time period of operation of each sensor, based on GOME-2B and GOME-2C OTO data compared to WOUDC Brewer & Dobson observations

		Brewer	**Dobson**
GOME-2B **01/2013 – 06/2023**	# stations:	66	64
	# obs:	163 268	110 943
	Mean Rel. Bias (%):	**0.62 ± 4.00**	**0.68 ± 4.53**
GOME-2C **01/2019 – 06/2023**	# stations:	50	48
	# obs:	60 630	35 969
	Mean Rel. Bias (%):	**1.31 ± 3.58**	**1.82 ± 4.27**

7.1.1.4 Validation results for GOME-2B and GOME-2C NRT total ozone products

The GOME-2B and GOME-2C NRT total ozone products are continuously validated against Brewer and Dobson Total Ozone Columns routinely deposited in the World Meteorological Organisation (WMO) Ozone Mapping Centre, also hosted by the Laboratory of Atmospheric Physics, AUTH. The comparative datasets that cover the last two years of observations, are updated weekly and they are operationally available by the online quality monitoring tool operated by AUTH. Some indicative plots are shown in Figure 7.3.
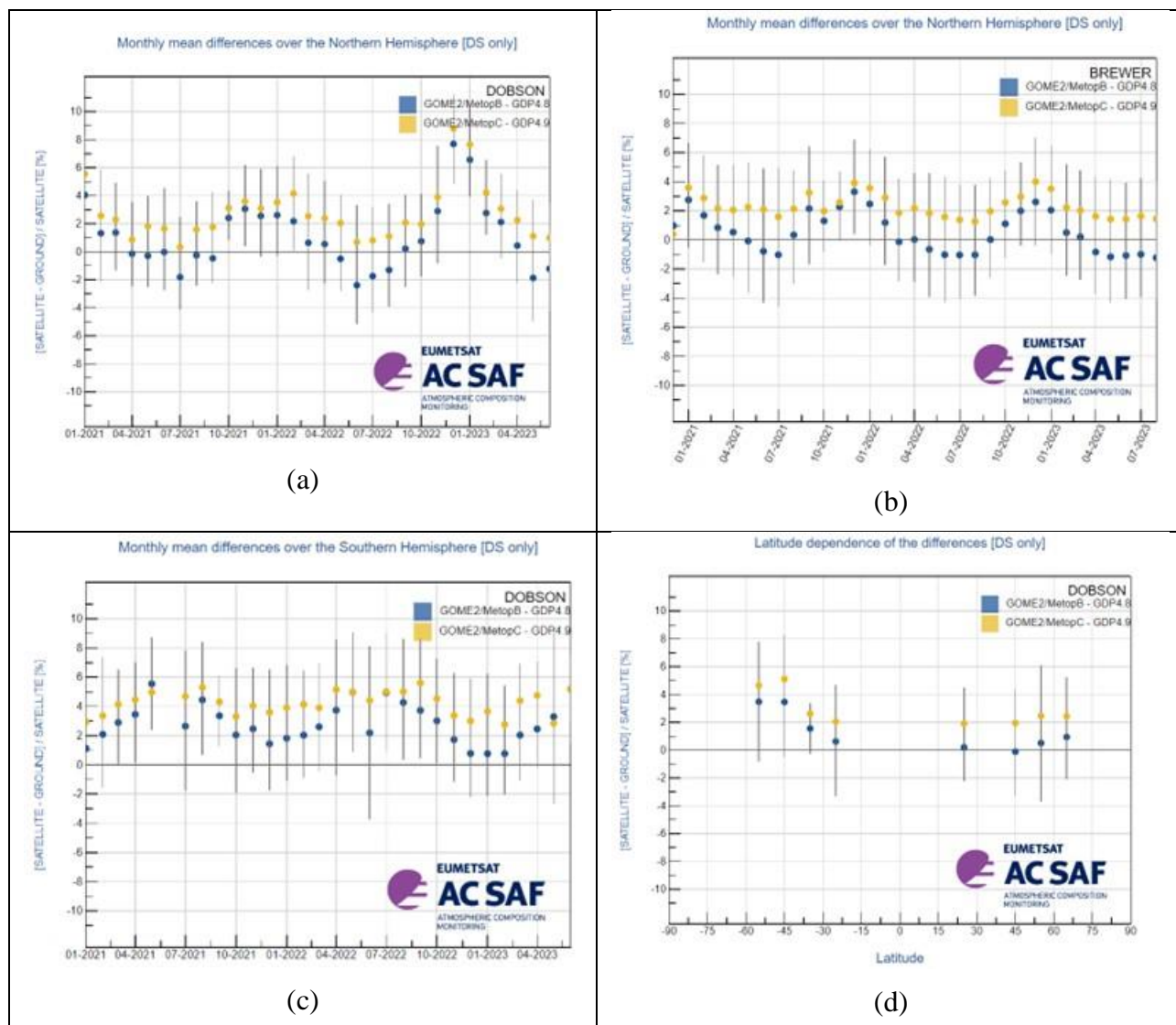
Figure 7.3. The percentage differences of the GOME-2B (orange) and GOME-2C (blue) NRT total ozone observations against the Dobson (panels a, c and d) and Brewer (panel b) ground-based co-located measurements. Panels a and c show the Dobson NH (panel a) and SH (panel c) monthly mean timeseries. Panel b shows the Brewer NH monthly mean timeseries. The Dobson latitudinal dependency plot is shown in panel d, made with co-locations since January 2021.

7.1.2. Validation website

The AC SAF Ozone Validation & Quality Assessment was launched on the initiation of the project's CDOP 2 phase in 2013. The validation webpages host the validation results of GOME-2A GDP-4.8, GOME-2B GDP4.8 and GOME-2C GDP4.9 near real-time and offline total ozone data. Currently, the validation results are available until June 2023.

The website and the processing algorithms that run behind it are routinely inspected and quality controlled. All the necessary actions, needed to keep it at its current good state, are taken by the LAP/AUTH team.

References:

Antón, M., Loyola, D., López, M., Vilaplana, J. M., Bañón, M., Zimmer, W., and Serrano, A.: Comparison of GOME-2/MetOpA total ozone data with Brewer spectroradiometer data over the Iberian Peninsula, Annales Geophysicae, 27, 1377-1386, 2009.
https://doi.org/10.5194/angeo-27-1377-2009

Balis, D., Kroon M., Koukouli, M.E., Brinksma, E. J., Labow, G., Veefkind, J. P., and McPeters, R. D.: Validation of Ozone Monitoring Instrument total ozone column measurements using Brewer and Dobson spectrophotometer ground-based observations, J. Geophys. Res., 112, D24S46, 2007a.
https://doi.org/10.1029/2007JD008796

Balis, D., Lambert, J-C., Van Roozendael, M., Spurr, R., Loyola, D., Livschitz, Y., Valks, P., Amiridis, V., Gerard, P., Granville, J., and Zehner, C.: Ten years of GOME/ERS-2 total ozone data – The new GOME data processor (GDP) version 4: 2. Ground-based validation and comparisons with TOMS V7/V8, J. Geophys. Res., vol. 112, D07307, 2007b.
https://doi.org/10.1029/2005JD006376

Fragkos, K., Bais, A. F., Balis, D., Meleti, C., and Koukouli, M. E.: The effect of three different absorption cross-sections and their temperature dependence on total ozone measured by a mid-latitude Brewer spectrophotometer, Atmos. Ocean, 53, 2015.
https://doi.org/10.1080/07055900.2013.847816

Hao, N., Koukouli, M. E., Inness, A., Valks, P., Loyola, D. G., Zimmer, W., Balis, D. S., Zyrichidou, I., Van Roozendael, M., Lerot, C., and Spurr, R. J. D.: GOME-2 total ozone columns from MetOp-A/MetOp-B and assimilation in the MACC system, Atmos. Meas. Tech., 7, 2937-2951, 2014.
https://doi.org/10.5194/amt-7-2937-2014

Komhyr, W. D., Mateer, C. L., and Hudson, R. D.: Effective Bass-Paur 1985 ozone absorption coefficients for use with Dobson ozone spectrophotometers, J. Geophys. Res., 98(D11), 20451-20465, 1993.
https://doi.org/10.1029/93JD00602

Koukouli, M. E., Balis, D. S., Loyola, D., Valks, P., Zimmer, W., Hao, N., Lambert, J.-C., Van Roozendael, M., Lerot, C., and Spurr, R. J. D.: Geophysical validation and long-term consistency between GOME-2/MetOp-A total ozone column and measurements from the sensors GOME/ERS-2, SCIAMACHY/ENVISAT and OMI/Aura, Atmos. Meas. Tech., 5, 2169-2181, 2012.
https://doi.org/10.5194/amt-5-2169-2012

Koukouli, M. E., Lerot, C., Granville, J., Goutail, F., Lambert, J.-C., Pommereau, J.-P., Balis, D., Zyrichidou, I., Van Roozendael, M., Coldewey-Egbers, M., Loyola, D., Labow, G., Frith, S., Spurr, S., and Zehner, C.: Evaluating a new homogeneous total ozone climate data record from GOME/ERS-2, SCIAMACHY/Envisat and GOME-2/MetOp-A, J. Geophys. Res. Atmos., 120, 12296-12312, 2015.
https://doi.org/10.1002/2015JD023699

Koukouli, M. E., Zara, M., Lerot, C., Fragkos, K., Balis, D., van Roozendael, M., Allart, M. A. F., and van der A, R. J.: The impact of the ozone effective temperature on satellite validation using the Dobson spectrophotometer network, Atmos. Meas. Tech., 9, 2055-2065, 2016.
https://doi.org/10.5194/amt-9-2055-2016

Loyola, D. G., Koukouli, M. E., Valks, P., Balis, D. S., Hao, N., Van Roozendael, M., Spurr, R. J. D., Zimmer, W., Kiemle, S., Lerot, C., and Lambert, J.-C.: The GOME-2 total column ozone product: Retrieval algorithm and ground-based validation, J. Geophys. Res., 116, 2011.
https://doi.org/10.1029/2010JD014675

Serdyuchenko, A., Gorshelev, V., Weber, M., Chehade, W., and Burrows, J. P.: High spectral resolution ozone absorption cross-sections – Part 2: Temperature dependence, Atmos. Meas. Tech.,7, 625-636, 2014.
https://doi.org/10.5194/amt-7-625-2014

Garane, K., Lerot, C., Coldewey-Egbers, M., Verhoelst, T., Koukouli, M. E., Zyrichidou, I., Balis, D. S., Danckaert, T., Goutail, F., Granville, J., Hubert, D., Keppens, A., Lambert, J.-C., Loyola, D., Pommereau, J.-P., Van Roozendael, M., and Zehner, C.: Quality assessment of the Ozone_cci Climate Research Data Package (release 2017) – Part 1: Ground-based validation of total ozone column data products, Atmos. Meas. Tech., 11, 1385-1402, 2018.
https://doi.org/10.5194/amt-11-1385-2018

Garane, K., Koukouli, M.-E., Verhoelst, T., Lerot, C., Heue, K.-P., Fioletov, V., Balis, D., Bais, A., Bazureau, A., Dehn, A., Goutail, F., Granville, J., Griffin, D., Hubert, D., Keppens, A., Lambert, J.-C., Loyola, D., McLinden, C., Pazmino, A., Pommereau, J.-P., Redondas, A., Romahn, F., Valks, P., Van Roozendael, M., Xu, J., Zehner, C., Zerefos, C., and Zimmer, W.: TROPOMI/S5P total ozone column data: global ground-based validation and consistency with other satellite missions, Atmos. Meas. Tech., 12, 5263-5287, 2019.
https://doi.org/10.5194/amt-12-5263-2019

7.1.3. Online quality monitoring

The online quality monitoring tool is operational and consists of the continuous generation of plots showing the slant column density (SCD) distribution, the vertical column density (VCD) distribution as well as the root mean square (RMS) as histograms per sensing day as well as time series per sensing month. These plots are generated for three different geographic regions, the Pacific ocean (25-15S, 210-250E), the Sahara desert (20-30N, 0-30E) and global, in order to represent typical extremes of ground reflectivity and atmospheric conditions as well as the global mean. The plots are generated per sensing instrument (GOME-2B, GOME-2C) and per product (O3, NO2, BrO, HCHO, SO2, H2O).

The online quality monitoring plots are published in PDF format on the DLR AC SAF FTP server (acsaf.eoc.dlr.de) using the following directory schemes:

/oq/GOME-2[BC]/[O3 NO2 BrO HCHO SO2 H2O]/daily/YYYY/MM/DD/[global sahara pacific]/*.[vcd scd rms]_hist.pdf
/oq/GOME-2[BC]/[O3 NO2 BrO HCHO SO2 H2O]/monthly/YYYY/MM/[global sahara pacific]/ *.[vcd scd rms]_series.pdf

More information about quality monitoring of the operational GOME-2 total ozone columns by other AC SAF and external partners is available at the following websites:
https://acsaf.org → Validation & QA → QM websites
http://acsaf.physics.auth.gr/eumetsat/validation/near_real
http://acsaf.physics.auth.gr/eumetsat/validation/offline
https://www.temis.nl/acsaf/vod.php
https://www.ecmwf.int/en/forecasts/charts/obstat/?facets=Parameter,Ozone;Instrument,GOME2

7.2. Tropospheric ozone products

Table 7.3. Validation status of tropospheric ozone products

Product Identifier	Product Name	Accuracy	Reference	Validating Institute	Correlative data sources
O3M-35	Offline tropical tropospheric ozone	Fulfils target accuracy requirement	RD18	KMI	Ozonesonde data from SHADOZ, NDACC, NILU and WOUDC
O3M-43					
O3M-302			RD24		
O3M-174	NRT global tropospheric ozone	Fulfils target accuracy requirement	RD19	KMI	Ozonesonde data from SHADOZ, NDACC, NILU and WOUDC
O3M-304			RD25		
O3M-173	Offline global tropospheric ozone	Fulfils target accuracy requirement	RD19	KMI	Ozonesonde data from SHADOZ, NDACC, NILU and WOUDC
O3M-175					
O3M-305			RD25		

Validation activities summary for global tropospheric ozone:

This summary contains validation results of the GOME-2B and GOME-2C high resolution (HR) global tropospheric ozone column (TrOC) products, retrieved by the Ozone Profile Retrieval Algorithm (OPERA) at KNMI. It covers the time period July 2022 – June 2023. Validation results are shown from two TrOC products, i.e. the tropopause related product and a fixed altitude TrOC product. The TrOC products are derived from the daily operational ozone profile product.

Since these TrOC products are derived from the OPERA ozone profile product, OPERA averaging kernel smoothing has been applied to the ground-based reference profiles before calculating comparison statistics. This AVK smoothing is expected to reduce the vertical smoothing difference error between satellite and ground-based measurements. The outcome is summarized at the end of this section.

The global tropospheric ozone column (TrOC) product has the following user requirements:

- Threshold accuracy: within 50 %
- Target accuracy: within 20 %
- Optimal accuracy: within 15 %

This summary was made available by Dr. Andy Delcloo from KMI. More information on how these values are extracted is available in the validation report. The collocation data used are the same as for the ozone profiles (Figure 7.19).

The statistics on the accuracy of the GOME-2B and GOME-2C HR tropospheric ozone column products (tropopause related) for different latitude belts, validated against $X_{AVK-sonde}$, are shown in Table 7.4 and Table 7.5.

Table 7.4. Relative differences (RD) and standard deviation (STDEV) are shown (in percent) together with the absolute difference (DU) on the accuracy of the GOME-2B HR tropospheric ozone column products (tropopause related) for five different latitude belts, validated against $X_{AVK\text{-}sonde}$

July 2022 – June 2023	GOME-2B HR			
	RD (%)	STDEV (%)	AD (DU)	STDEV (DU)
Northern Polar Region	-4.99	18.1	-1.35	4.92
Northern Mid-Latitudes	-5.43	21.3	-1.52	6.12
Tropical region	-0.63	25.1	-0.31	6.70
Southern Mid-Latitudes	-0.48	21.4	-0.09	3.94
Southern Polar Region	-20.3	36.5	-2.60	5.06

Table 7.5. Relative differences (RD) and standard deviation (STDEV) are shown (in percent) together with the absolute difference (DU) on the accuracy of the GOME-2C HR tropospheric ozone column products (tropopause related) for five different latitude belts, validated against $X_{AVK\text{-}sonde}$

July 2022 – June 2023	GOME-2C HR			
	RD (%)	STDEV (%)	AD (DU)	STDEV (DU)
Northern Polar Region	-2.69	12.9	-0.69	3.42
Northern Mid-Latitudes	8.37	19.4	2.4	5.46
Tropical region	45.8	32.3	11.1	7.24
Southern Mid-Latitudes	10.8	25.5	2.10	4.58
Southern Polar Region	-7.52	36.8	-0.91	5.72

The statistics on the accuracy of the GOME-2A, GOME-2B and GOME-2C HR tropospheric ozone column products (fixed altitude) for different latitude belts, validated against $X_{AVK\text{-}sonde}$, are shown in Table 7.6 and Table 7.7.

Table 7.6. Relative differences (RD) and standard deviation (STDEV) are shown (in percent) together with the absolute difference (DU) on the accuracy of the GOME-2B HR tropospheric ozone column products (fixed altitude) for five different latitude belts, validated against $X_{AVK\text{-}sonde}$

July 2022 – June 2023	GOME-2B HR			
	RD (%)	STDEV (%)	AD (DU)	STDEV (DU)
Northern Polar Region	-2.28	8.57	-0.37	1.48
Northern Mid-Latitudes	-4.06	11.8	-0.64	2.01
Tropical region	-5.45	27.3	-0.77	3.38
Southern Mid-Latitudes	-1.56	11.0	-0.17	1.38
Southern Polar Region	-14.9	11.0	-0.47	0.20

Table 7.7. Relative differences (RD) and standard deviation (STDEV) are shown (in percent) together with the absolute difference (DU) on the accuracy of the GOME-2C HR tropospheric ozone column products (fixed altitude) for five different latitude belts, validated against X_AVK-sonde

July 2022 – June 2023	GOME-2C HR			
	RD (%)	STDEV (%)	AD (DU)	STDEV (DU)
Northern Polar Region	-1.25	6.55	-0.21	1.14
Northern Mid-Latitudes	3.48	9.59	0.58	1.57
Tropical region	41.2	32.3	4.98	3.48
Southern Mid-Latitudes	4.92	11.2	0.56	1.34
Southern Polar Region	-7.26	6.48	-0.26	0.33

For the GOME-2B and GOME-2C TrOC products, most of these products comply with the target accuracy requirement. Only for the tropical region (GOME-2C), this is obviously not the case. Between all sensors, there is a clear offset visible in the results. Also here, a degradation correction will be necessary to correct for this offset.

Validation activities summary for tropical tropospheric ozone:

At the time of writing this report, there was no updated TTrOC reference data available. Therefore, all the results are as in AC SAF Operations Report 2/2022.

This summary contains validation results of the GOME-2B and GOME-2C tropical tropospheric ozone column (TTrOC) products, using the cloud slicing method. The tropospheric ozone retrieval is based on the GOME-2 ozone columns as derived by the GOME Data Processor (GDP, version 4.8) and covers the tropical latitude belt (20S – 20N). This product is available on a monthly basis and has a resolution of 1.25° latitude x 2.5° longitude.

The tropical tropospheric ozone column product has the following user requirements:

- Threshold accuracy: within 50 %
- Target accuracy: within 25 %
- Optimal accuracy: within 15 %

This summary was made available by Dr. Andy Delcloo from KMI. More information on how these values are extracted is available in the validation report. The collocation data used are the same as for the ozone profiles (Figure 7.19).

The time period covered is January 2021 – December 2022 for the GOME-2B and GOME-2C offline TTrOC products.

In Table 7.8 and Table 7.9, the statistics on the accuracy of the GOME-2B/C tropical tropospheric ozone column products for different stations under consideration are shown, showing some general statistics for both datasets. It is shown that most of the stations are within the target accuracy (25 %). The correlation varies between 0.4 and 0.8 with a rmse between 2.8 and 5.5 DU. There is also an offset present between GOME-2B/GOME-2C as described in the validation report. These TTrOC products still fulfil the user requirements.

Table 7.8. Relative Differences (RD), standard deviation (STDEV), correlation, bias and RMSE are shown on the accuracy of the GOME-2B TtrOC product for the time period January 2021 – December 2022

Station	RD (%)	STDEV (%)	Correlation	Bias (DU)	RMSE (DU)
Paramaribo	3.61	28.2	0.43	0.59	5.32
Alajuela	20.8	24.3	0.48	2.98	4.27
Samoa	20.1	28.8	0.56	2.82	5.18
Ascension Island	4.04	13.0	0.83	1.10	3.44
Kuala Lumpur	-6.62	12.1	0.73	-1.47	2.98
Natal	6.44	21.5	0.80	1.93	5.47

Table 7.9. Relative Differences (RD), standard deviation (STDEV), correlation, bias and RMSE are shown on the accuracy of the GOME-2C TtrOC product for the time period January 2021 – December 2022

Station	RD (%)	STDEV (%)	Correlation	Bias (DU)	RMSE (DU)
Paramaribo	12.5	23.9	0.50	2.21	4.85
Alajuela	27.9	20.1	0.78	4.31	5.11
Samoa	18.3	23.7	0.81	2.86	5.03
Ascension Island	6.26	16.9	0.70	1.59	4.53
Kuala Lumpur	0.93	17.7	0.62	-0.18	2.80
Natal	12.1	24.4	0.78	2.86	5.30

7.3. Trace gas products

Table 7.10. Validation status of trace gas products

Product Identifier	Product Name	Accuracy	Reference	Validating Institute	Correlative data sources
O3M-50.1	NRT total NO2	Fulfils threshold accuracy requirement	RD6	BIRA-IASB	NDACC zenithSky measurements
O3M-338			RD28		
O3M-52.1	NRT tropospheric NO2	Fulfils threshold accuracy requirement	RD6	BIRA-IASB	BIRA-IASB and other MAXDOAS stations
O3M-341			RD28		
O3M-55.1	NRT total SO2	Fulfils threshold accuracy requirement	RD10	BIRA-IASB	BIRA-IASB Xianghe MAXDOAS station
O3M-374			RD34		
O3M-177	NRT total HCHO	Fulfils threshold accuracy requirement	RD12	BIRA-IASB	BIRA-IASB and other MAXDOAS stations
O3M-344			RD29		

Product Identifier	Product Name	Accuracy	Reference	Validating Institute	Correlative data sources
O3M-51.1	Offline total NO2	Fulfils threshold accuracy requirement	RD6	BIRA-IASB	NDACC zenithSky measurements
O3M-339			RD28		
O3M-37.1	Offline tropospheric NO2	Fulfils threshold accuracy requirement	RD6	BIRA-IASB	BIRA-IASB and other MAXDOAS stations
O3M-53.1					
O3M-342			RD28		
O3M-09.1	Offline total SO2	Fulfils threshold accuracy requirement	RD10	BIRA-IASB AUTH	BIRA-IASB Xianghe MAXDOAS station
O3M-56.1					
O3M-375			RD34		
O3M-08.1	Offline total BrO	Fulfils threshold accuracy requirement	RD11	BIRA-IASB	BIRA-IASB Harestua zenithSky station
O3M-82.1					
O3M-317			RD30		
O3M-10.1	Offline total HCHO	Fulfils target accuracy requirement	RD12	BIRA-IASB	BIRA-IASB and other MAXDOAS stations
O3M-58.1					
O3M-345			RD29		
O3M-12.1	Offline total H2O	Fulfils threshold accuracy requirement	RD13	FMI, DLR	IGRA, COSMIC-SuomiNet, SSM/I
O3M-86.1					
O3M-386			RD31		Comparison against GOME-2B water vapour data

Validation activities summary:

This summary presents validation activities for offline total and tropospheric NO_2, total HCHO, total BrO and SO_2 data products of GOME-2B/C as performed at BIRA-IASB.

The authors of this summary are Gaia Pinardi (for tropospheric NO_2, HCHO and SO_2 validation), Jean-Christopher Lambert, José Granville and Tijl Verhoelst (for total/stratospheric NO_2 validation), François Hendrick (for BrO validation) and Jeroen van Gent and MariLiza Koukouli (for quality assessment).

Validation exercises are performed following the protocols described in the original Metop-A, Metop-B and Metop-C validation reports and updated in Pinardi *et al*. (AMT 2020) and Verhoelst *et al*. (AMT 2021), and the results presented in this report are based on updates of the correlative datasets with the last available – and sometimes improved – versions. While illustrations at a few stations are included in this report, all the updated figures are reported on the BIRA-IASB trace gases validation server.

Update of database for reference data

For this report, the validation database was updated with ground-based NDACC UVVIS ZenithSky NO_2 data (as usual) and MAXDOAS NO_2 and HCHO data from KNMI and IUPB (as collected for the NIDFORVAL S5p validation project and already used in Pinardi *et al*. (AMT 2020), Verhoelst *et al*. (AMT 2021) and De Smedt et al. (ACP 2021), in order to cover as much as possible the

period until end-2022, as only the Xianghe NO_2 data could be updated compared to the usual BIRA-IASB sites (and only up to August 2022). BIRA-IASB ZenithSky BrO data at Harestua could not be updated for this report, due to BIRA-IASB responsible personnel absence.

ZenithSky NO_2 total columns are collected from the NDACC Data Host Facility (to where the data have to be uploaded by instrument Pis within 1 year after data acquisition) and from the SAOZ rapid delivery operational facility operated by LATMOS. The SAOZ at Bauru (Brazil) is unfortunately no longer operational. The ground-based data are then quality assessed and post-processed at BIRA-IASB in preparation for the data comparisons. This preparation includes calculation of the effective ground-based airmasses with which GOME-2 data co-locations will be sought.

Ground-based BrO columns are derived at Harestua from vertical profiles retrieved by applying an OEM (Optimal Estimation Method)-based profiling technique to zenith-sky measurements at sunrise (Hendrick *et al.*, 2007).

The BIRA-IASB MAXDOAS ground-based dataset are automatically retrieved with an improved version of the bePRO profiling algorithm (Clémer *et al.*, 2010; Hendrick *et al.*, 2014, Vlemmix *et al.*, 2015) developed within the EU FP7 NORS and QA4ECV projects (aiming at rapid delivery of improved NO_2 and HCHO profiles), and is progressively shifting to the FRM4DOAS analysis chain. The FRM4DOAS (Fiducial Reference Measurements for Ground-Based DOAS Air-Quality Observations) is an ESA activity aiming at the development of the first centralised NRT processing system for MAX-DOAS instruments operated within the international Network for the Detection of Atmospheric Composition Change (NDACC). It includes the launch of the NDACC MAX-DOAS Processing Service in a demonstration mode, focusing on tropospheric and stratospheric NO2 vertical profiles, total O3 columns, and tropospheric HCHO profiles as target MAX-DOAS products for the first phase of the project (July 2016 – August 2021), see https://frm4doas.aeronomie.be/. The lower tropospheric profiles and vertical columns processing chain rely on parallel runs of optimal-estimation based MMF (Friedrich *et al.*, 2019) and parametrized approach MAPA (Beirle *et al.*, 2019) algorithms and testings of their results coherence. The service is running in a best-effort mode at the time of writing for a limited number of stations belonging to the project partners.

IUPB and KNMI sites are retrieved respectively with the QA4ECV database approach (https://uv-vis.aeronomie.be/groundbased/QA4ECV_MAXDOAS/index.php), as discussed and used in Pinardi *et al.* (AMT 2020) and Verhoelst *et al.* (AMT 2021) for NO_2 and De Smedt *et al.* (ACP 2021) for HCHO. This approach only provides VCD columns, and profiles are not retrieved. These datasets are also used for the online validation of S5p (https://mpc-vdaf-server.tropomi.eu/no2/no2-offl-maxdoas and https://mpc-vdaf-server.tropomi.eu/hcho/hcho-offl-maxdoas).

The NO_2 and HCHO datasets include the following ground-based stations:

- OHP (from June 2007 to July 2014 with the geometrical approximation, and since August 2014 to March 2017 with the bePRO profiling tool)
- Uccle (from April 2011 to March 2016 with a miniMAXDOAS instrument (Uccle-miniDOAS) and from end of January 2017 to February 2020 with a scientific grade MAXDOAS: Uccle-SG)
- Bujumbura (from November 2013 to July 2017; since then the instrument had a power failure and only limited operations and data transfer was possible)
- LePort, on Reunion Island (from April 2016 to 10 January 2018). The instrument has been reinstalled in June 2018 on the Maido site, and data analysis from the FRM4DOAS analysis

chain was tested, but it is not adapted for tropospheric (NO_2, HCHO) gases validation at this mountaneous site and is not used for this report.

- Xianghe (from March 2010 to July 2018 and from October 2019 to August 2022). Since November 2021 the retrievals in the UV are of bad quality and the UV channel broke down early 2022. SO_2 MAXDOAS profiles were also analysed for the whole time-series (2010 to Oct. 2021), although the SO_2 levels are very low now in China nowadays.
- IUPB Bremen and Athens and KNMI Cabauw and De Bilt data used here covers the periods from April/May 2018 to July 2023 for NO_2 and the KNMI also for HCHO.

Status of GOME-2B and GOME-2C tropospheric NO_2

Comparisons with ground-based MAXDOAS instruments is performed similarly as in previous validation report. In Pinardi *et al*. (2020) it is shown that best results are achieved by filtering out the largest pixels and selecting only pixels covering the stations. For GOME-2, the selection includes keeping only pixels with a size of less than 100 km, while selecting pixels over the station, only slightly changes the results, as generally pixels with their center within 50 km, are covering the station. This improvement of the biases comes at the expenses of a strongly reduced number of pixels (see AC SAF Operations Report 1/2020).

Similarly as last report, no BIRA MAXDOAS stations can be used over the first period of 2023, and we thus used some available MAXDOAS data from KNMI and IUPB, as presented above.

Figure 7.4 shows example of results for GOME-2B and GOME-2C for De Bilt. Monthly mean differences are calculated for every year and for the whole time-series in order to see the evolution in time of the bias. Table 7.11 reports the median differences and the spread (half the percentile 68) at the stations, with and without the smoothing, and the figures for all the stations can be found on the BIRA-IASB validation web server.
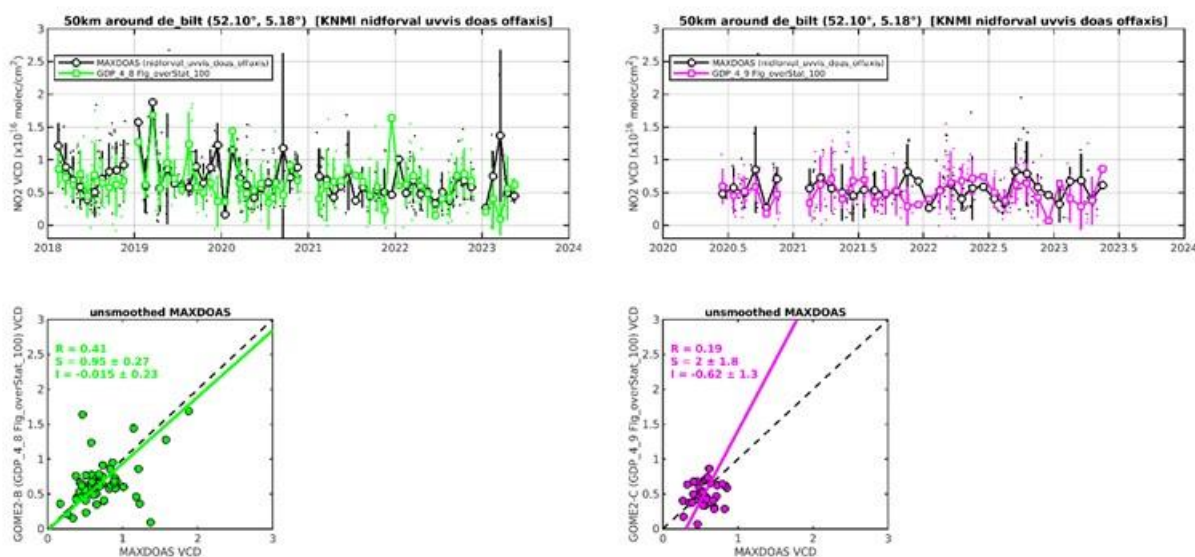
Figure 7.4. Illustration for the De Bilt MAXDOAS versus GOME-2B GDP-4.8 (left) and GOME-2C GDP-4.9 (right) tropospheric NO_2 comparisons.

Table 7.11. Median Absolute Differences (AD=SAT-GB, in 10^{15} molec/cm²), Relative Differences (RD, in %) and spread (0.5*IP68) on the accuracy of GOME-2B and GOME-2C tropospheric NO₂ products when comparing to MAXDOAS data (NOT cloud filtered). Values for the last 12 months are given, and the values for the whole time-series are reported in brackets for comparison. Results for both the original comparisons (pixels over the station, for pixels smaller than 100 km side) and for the smoothed comparisons are reported. <u>Only the first four rows are stations with recent data, the others are given as examples of past results.</u>

	GOME-2B			GOME-2C		
	AD ($\times 10^{15}$)	RD (%)	SPREAD (%)	AD ($\times 10^{15}$)	RD (%)	SPREAD (%)
Bremen (IUPB) Last 12 months: 08/2022 – 07/2023 [whole period: since 04/2018]	-2.6 [-2.2]	-45 [-40]	62 [59]	-1.9 [-2.1]	-46 [-46]	45 [44]
Athens (IUPB) Last 12 months: 07/2022 – 07/2023 [whole period: since 05/2018]	-2.3 [-1.6]	-37 [-38]	47 [38]	-1.4 [-1.8]	-36 [-39	36 [43]
Cabauw (KNMI) Last 12 months: 07/2022 – 06/2023 [whole period: since 04/2018]	0.8 [0.25]	15 [3.8]	25 [33]	0.3 [-0.3]	6.5 [-3.8]	40 [28]
De Bilt (KNMI) Last 12 months: 05/2022 – 04/2023 [whole period: since 04/2018]	0.2 [-0.1]	3.2 [-1.3]	39 [36]	-0.8 [-0.1]	-11 [-2]	46 [37]
Uccle SG last 12 months: 03/2019 – 02/2020 [whole period: 02/2017 – 02/2020]	-1.2 [-1.4]	-16 [-20]	33 [36]	-	-	-
Uccle SG smoothed	-2.5 [-2.7]	-26 [-29]	38 [36]	-	-	-
Reunion Maido (last 12 months: 12/2018 – 11/2019) [whole period: 06/2018 – 11/2019]	-0.02 [-0.02]	-4.2 [-4.3]	76 [93]	-	-	-
Reunion Maido smoothed	-0.03 [-0.01]	-1.4 [-9]	85 [115]	-	-	-
Xianghe (last 12 months: 12/2020 – 07/2022) [whole period: 03/2010 – 07/2022]	0.9 [-0.8]	-4.9 [-4.4]	26 [25]	-0.3 [-0.8]	-1.2 [-9]	23 [21]
Xianghe smoothed	-2.2 [-3.8]	-17 [-18]	28 [36]	-2.1 [-2.4]	-13 [-21]	29 [36]

	GOME-2B			GOME-2C		
Bujumbura **(last 12 months:** **07/2016 – 07/2017)** **[whole period:** **11/2013 – 07/2017]**	-3.4 [-3.2]	-83 [-81]	42 [28]	-	-	-
Bujumbura smoothed	-2 [-1.8]	-70 [-74]	21 [35]	-	-	-
OHP **(last 12months:** **03/2016 – 03/2017)** **[whole period:** **08/2014 – 03/2017]**	-0.7 [-0.6]	-37 [-28]	34 [36]	-	-	-
OHP smoothed	-0.5 [-0.4]	-36 [-24]	41 [39]	-	-	-
Reunion LePort **Last 12 months:** **12/2016 – 12/2017)** **[whole period:** **04/2016 – 12/2017]**	-1.4 [-1.4]	-83 [-84]	25 [25]	-	-	-
Reunion LePort smoothed	-0.41 [-0.42]	-59 [-60]	22 [25]	-	-	-
Uccle minDOAS **(last 12 months:** **03/2015 – 03/2016)** **[whole period:** **04/2011 – 03/2016]**	-2.6 [-3]	-26 [-31]	25 [24]	-	-	-
Uccle minDOAS smoothed	-3.6 [-3.3]	-29 [-33]	20 [30]	-	-	-

From Figure 7.4 it can be seen, that GOME-2C scatter plot is similar to what obtained with GOME-2B in De Bilt (confirming past results from Xianghe), although the statistics are slightly different, probably due to the presence in GOME-2B period of a few larger NO_2 columns (between $1 – 2 \times 10^{15}$ molec/cm²) that strongly influence the regression analysis (Pinardi *et al.*, 2020). There are some differences in the absolute and relative differences for GOME-2B and GOME-2C and for the last 12 months compared to the whole period. These depend from one station to the other (ie. larger bias of 15 % for GOME-2B compared to 6.5 % for GOME-2C in Cabauw and the other way around for De Bilt (3.2 % and -11 % respectively), while for Bremen and Athens the difference is not significant (-45 % and -46 % for Bremen and -37 % and -36 % for Athens). Results in Athens are also particularly coherent between the whole period and over the latest year.

The biases results are usually within or close to the requirements (target accuracy requirement of 30 % in polluted conditions and optimal accuracy of 20 %), as it was the case for the other sensors for Xianghe and Uccle in the past. Cabauw and De Bilt sites are remote sites, with low levels of NO_2 pollution and low biases, while Bremen and Athens are more urban polluted sites, with biases around the -40 % levels, with a spatial comparison mismatch (horizontal dilution component) as highlighted in Pinardi *et al.* (2020) and also seen for other BIRA-IASB sites in the past. Beijing and

OHP report about 50 % biases, while larger values are found for Bujumbura and Reunion, as previously (Pinardi *et al.*, 2014; NO$_2$ Validation Report 2015; Pinardi *et al.*, 2020). As before, smoothing the MAXDOAS profiles with the satellite averaging kernels is not always reducing the mean comparison differences, with an impact of ~10 – 20 % depending on the station (AC SAF Operations Report 1/2018, PT meeting of May 2018). In term of stability most of the stations report differences over time up to 10 % for both GOME-2B and GOME-2C (except the Bremen case), which is also about the level of difference between GOME-2B and GOME-2C (10 to 15 %), and the levels we had in the past between GOME-2A and GOME-2B. These biases could be partly reduced in the future with the improved GDP-4.9 GOME-2 algorithm (Liu *et al.*, 2019).

Status of GOME-2B and GOME-2C total (stratospheric) NO2

Quality monitoring of the GOME-2 NO$_2$ total (stratospheric) column data is regularly carried out using correlative ground-based measurements collected from about 20 Zenith-Scattered-Light DOAS UV-visible (ZSL-DOAS) instruments affiliated with the Network for the Detection of Atmospheric Composition Change (NDACC). The NO$_2$ column validation protocol has already been described in previous AC SAF validation reports with its latest updates published in Verhoelst *et al*. (AMT 2021). This protocol includes the selection of GOME-2/NDACC co-located data pairs based on the air-mass matching technique, a model-based photochemical correction compensating for significant solar local time differences between GOME-2 mid-morning and NDACC twilight observations in polar summer, and a cloud-based filtering of NO$_2$ data over polluted stations aiming at the removal of pollution-affected pixels. At some stations, real-time processing of the ground-based observations still uses NO$_2$ absorption cross-sections at room temperature instead of stratospheric temperature. As a result, the retrieved total NO$_2$ column is affected by a negative systematic bias of 15 – 20 % with a seasonal component. Such data are removed. Thanks to this strict protocol, data comparisons can be carried out within a residual uncertainty of maximum $2 – 3 \times 10^{14}$ molec/cm^2 combining both the ground-based data uncertainty and comparison errors. This uncertainty is indicated by the shaded area on the pole-to-pole graphs.

Figure 7.5 shows the comparison of NO$_2$ column data at the NDACC Antarctic station of Dumont d'Urville, a station located on the polar circle, in a pristine environment without any known source of tropospheric NO$_2$. Comparison results at this station are representative of the validation of purely stratospheric data series, at moderate and large solar zenith angle, and over the full range of NO$_2$ stratospheric column values from winter lows of about 10^{14} molec/cm^2 (wintertime denoxification episodes) up to summer highs of 7×10^{15} molec/cm^2 (complete depletion of N$_2$O$_5$ into NO$_2$ due to polar midnight Sun). On a monthly median basis, and over the 16 years covered by the three satellites, the target bias of $3 – 5 \times 10^{14}$ molec/cm^2 has never been exceeded, except occasionally in October when the station is overpassed frequently by the border of the polar vortex, thus when atmospheric variability contributes significant co-location mismatch noise and bias to the difference in stratospheric NO$_2$. The ground dataset shown in this figure is a composite dataset consisting of the NDACC reprocessed dataset extended through the last year by the near-real-time dataset (latmos_rt).
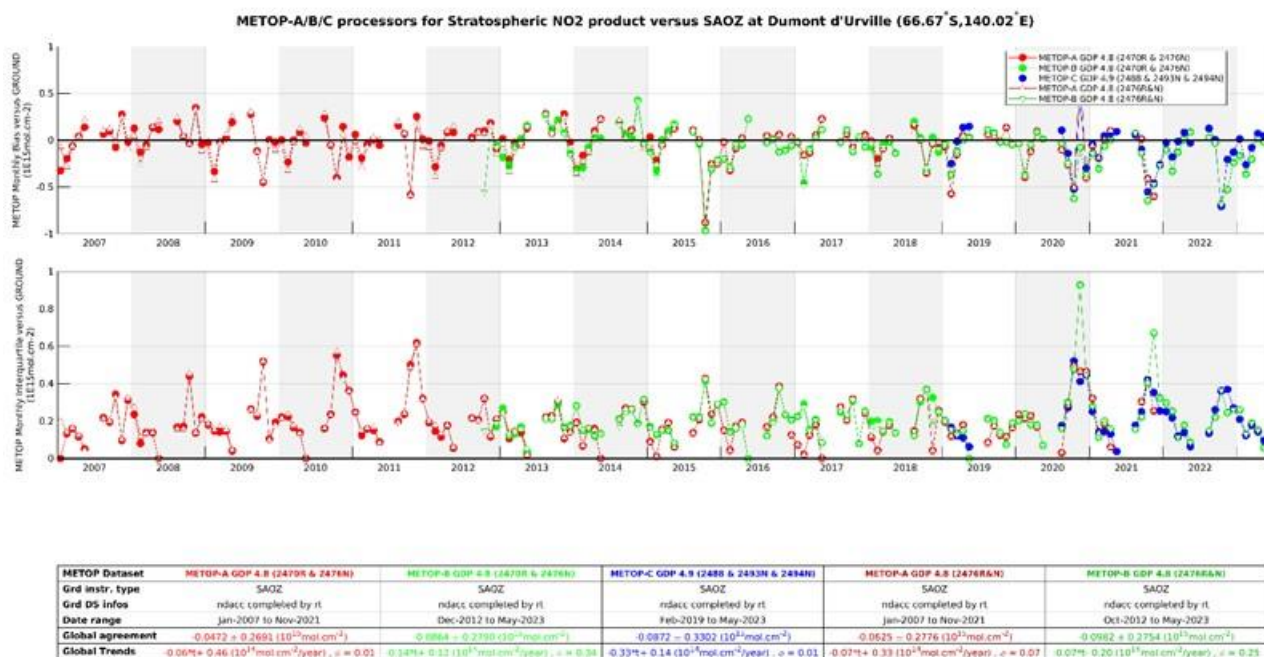
Figure 7.5. Comparison of NO₂ column data measured at the NDACC Antarctic station of Dumont d'Urville by the three GOME-2 instruments) and by the CNRS/LATMOS ZSL-DOAS spectrometer. Top: time-series of the median NO₂ column difference per month; centre: time-series of the dispersion of the NO₂ column difference per month; bottom (table): summary statistics for the different instruments and processors.

Figure 7.6 and Figure 7.7 display similar results obtained at the NDACC Alpine station of Observatoire de Haute Provence in Southern France and the NDACC Southern Tropic station of Saint-Denis de la Réunion, thus in occasional presence of pollution and over a wider range of solar zenith angle. Again, the target bias of $3 - 5 \times 10^{14}$ molec/cm^2 has rarely been exceeded, except in very few cases.
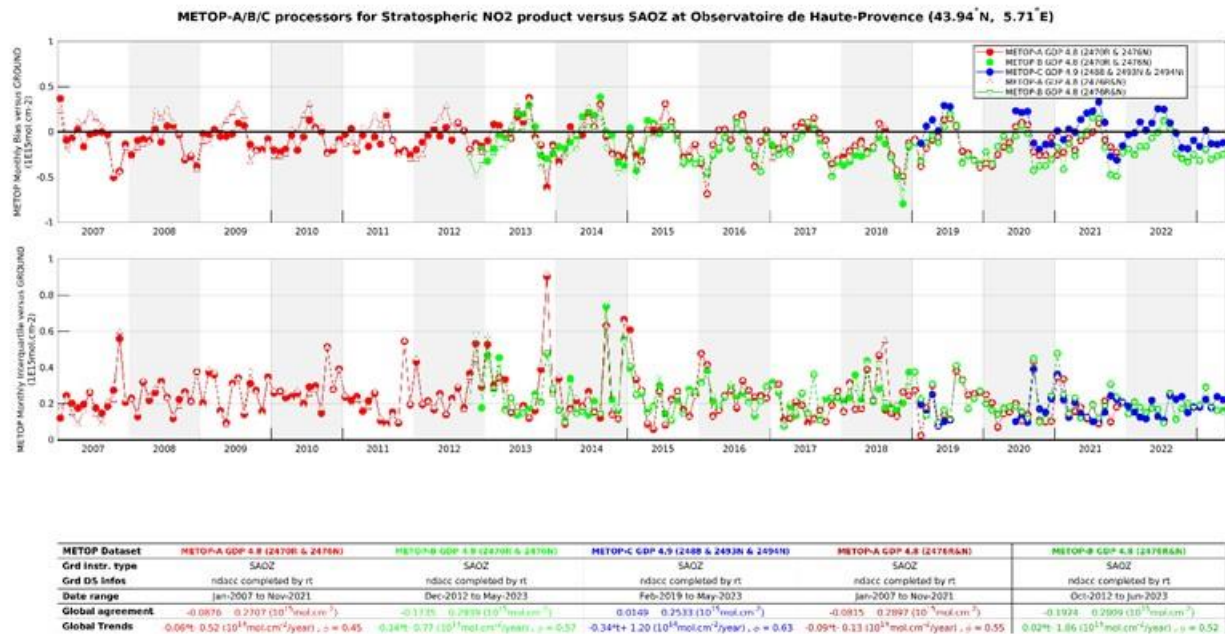
Figure 7.6. Same as Figure 7.5 but at the NDACC Alpine station of Observatoire de Haute Provence.
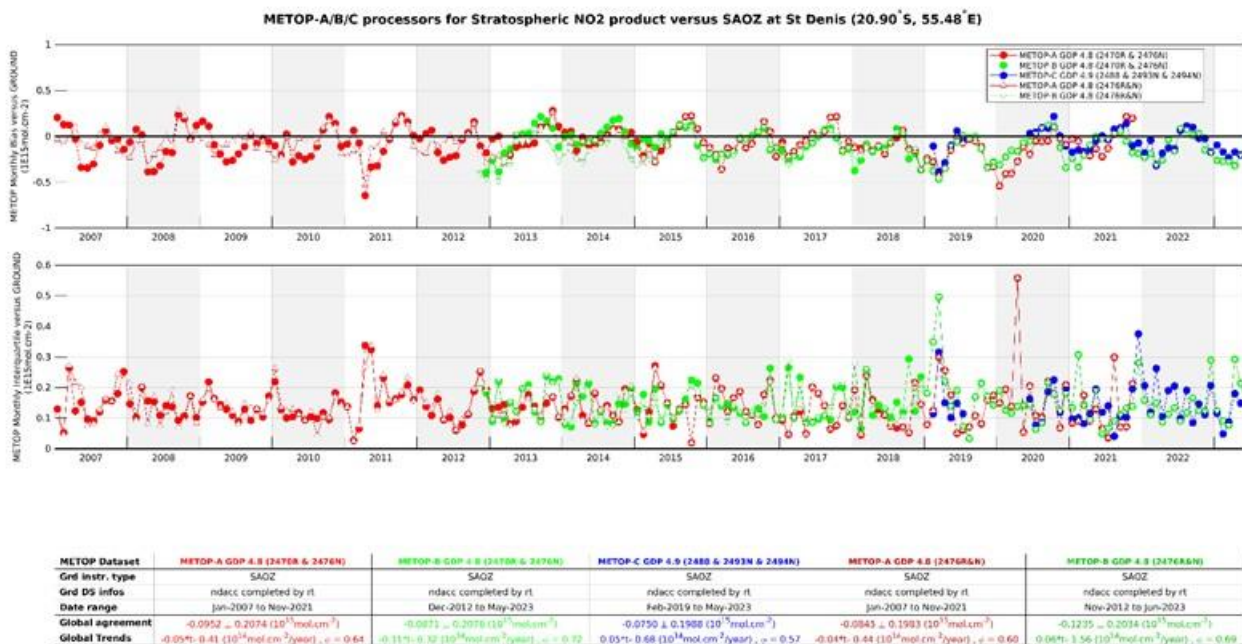
Figure 7.7. Same as Figure 7.5, but at the NDACC Southern Tropical station of Saint-Denis de la Reunion.

Figure 7.8 reports from pole to pole the median value and the dispersion of the differences between GOME-2 and NDACC ZSL-DOAS data, while Figure 7.9 displays, again from pole to pole, the linear drift between GOME-2A/B/C and NDACC data.Those graphs show the good long-term stability of the satellite NO_2 column data with respect to NDACC ZSL-DOAS data at all stations.

They also show that the target bias of $3 - 5 \times 10^{14}$ molec/cm^2 in unpolluted conditions is achieved at virtually all sites for all three satellites. Figure 7.7 also confirms the slight difference already noticed in previous validation reports between the biases observed respectively in the Southern and

Northern hemispheres. Averaging median differences separately over the Northern and Southern Hemispheres concludes to an inter-hemispheric bias of about $2 - 3 \times 10^{14}$ molec/cm^2. GOME-2C NO$_2$ column data present a slightly more positive bias across all latitudes.

Note that for these global statistics visualized in Figure 7.8 and Figure 7.9, only ground instruments yielding co-locations with all 3 satellite instruments (on MetOp-A, B, and C) were used so as to limit selection biases between sounders.
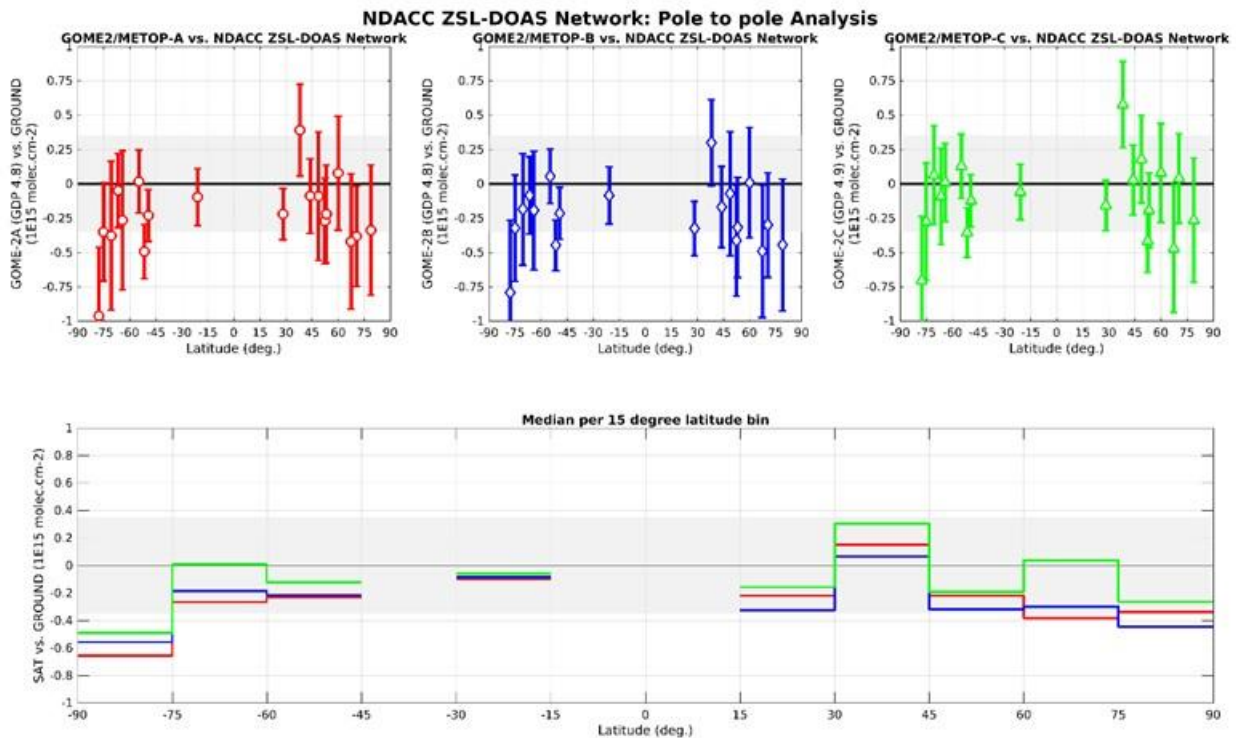
Figure 7.8. From pole to pole, median difference between the NO$_2$ column data reported by GOME-2A/B/C (red/ blue/ green) GDP-4.8 (GDP 4.9 for GOME-2C) and by ground-based ZSL-DOAS spectrometers at about 20 NDACC stations, calculated over 2007 – November 2021 for GOME-2A, 2012 – June 2023 for GOME-2B and 2019 – June 2023 for GOME-2C. Top: median difference at individual stations. Bottom: median difference averaged over 15° latitude bins.
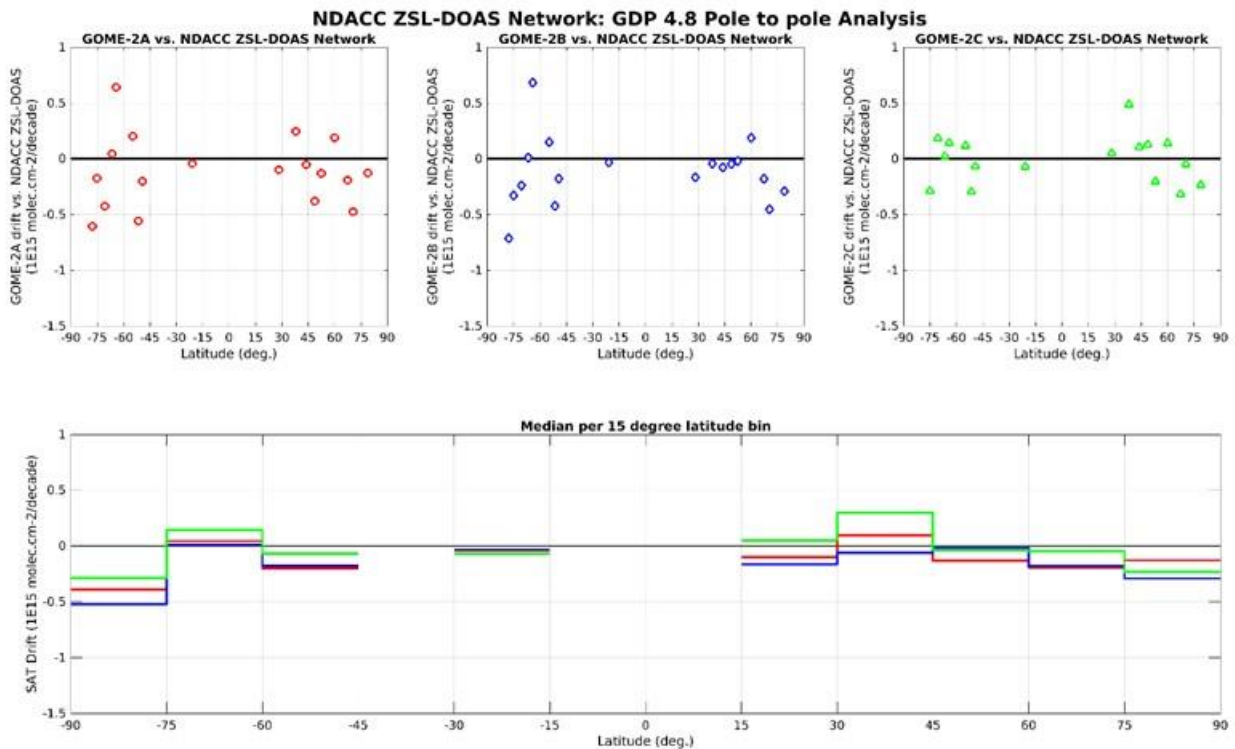
Figure 7.9. From pole to pole, linear drift (in percent by decade) of the difference between the NO₂ column data reported by GOME 2A/B/C (red/ blue/ green) GDP 4.8 (GDP 4.9 for GOME-2C) and by ground-based ZSL-DOAS spectrometers at about 20 NDACC stations, calculated over 2007 – November 2021 for GOME-2A, 2012 – June 2023 for GOME-2B and 2019 – June 2023 for GOME-2C. Top: linear drift estimates at individual stations. Bottom: same linear drift estimates but averaged over 15° latitude bins.

Status of GOME-2B and GOME-2C total HCHO

This validation exercise is an extension of what is presented in the HCHO GDP-4.8 validation report, relying on correlative observations from MAX-DOAS instruments operated by BIRA-IASB at Xianghe, Bujumbura, Uccle (miniDOAS and SG), OHP and Reunion (Le Port and Maido). As discussed above, no updates are possible from BIRA-IASB stations, and KNMI Cabauw and De Bilt sites are added in this report. An illustration of the comparisons for De Bilt are presented in Figure 7.10, past figures can be found on the BIRA validation web server and a summary is presented in Table 7.12.
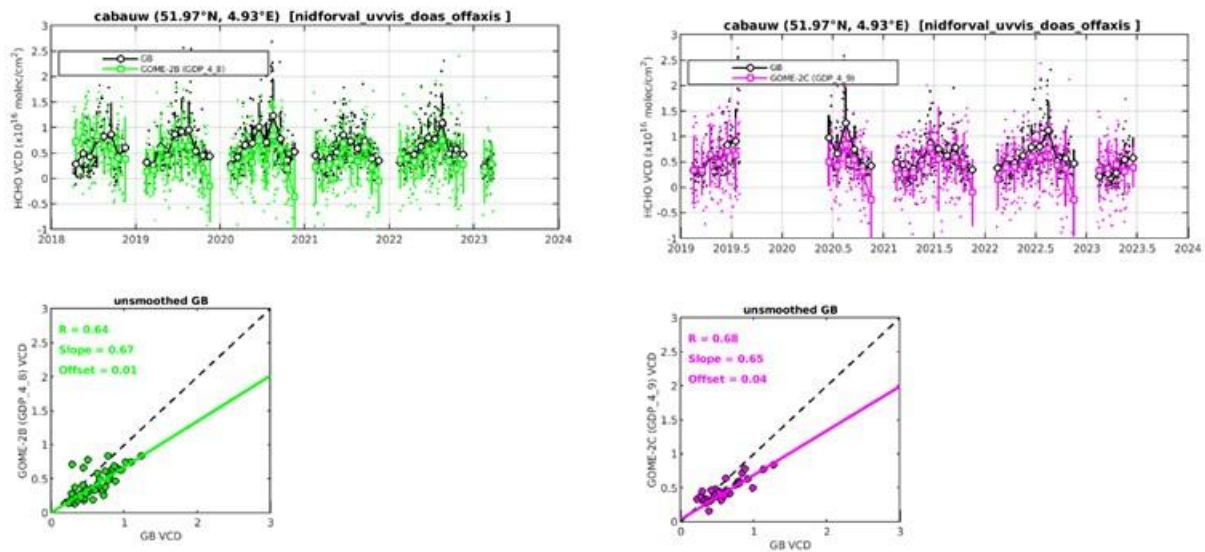
Figure 7.10. Illustration for the Cabauw MAXDOAS versus GOME-2B GDP-4.8 (left) and GOME-2C GDP-4.9 (right) HCHO comparisons.

Table 7.12. Summary of the mean biases (SAT-GB, in 10^{15} molec/cm^2) between GOME-2B/C and MAX-DOAS HCHO VCDs. The values in parentheses correspond to the mean relative biases (in %) and R is the correlation coefficients and S the slope of the linear regression of the monthly mean points. Only the first two rows are stations with recent data, the others are given as examples of past results.

	GOME-2B	GOME-2C
CABAUW **(51.97°N, 4.93°E)** **(whole period: 04/2018 – 05/2023)**	-1.6 ± 2 (-32 ± 5) R = 0.64, S=0.67	-1.6 ± 2 (-28 ± 44) R = 0.68, S = 0.65
DE BILT **(52.10°N, 5.18°E)** **(whole period: 05/2018 – 05/2023)**	-2.1 ± 2.3 (-36 ± 54) R = 0.68, S = 0.61	-1.5 ± 2.4 (-26 ± 78) R = 0.64, S = 0.54
UCCLE-SG **(50.8°N, 4.3°E)** **(whole period: 02/2017 – 12/2019)**	0.3 ± 1.6 (7 ± 52) R = 0.75, S = 0.96	-
With smoothing	1.6 ± 1.7 (49 ± 75) R = 0.76, S = 1.34	-
REUNION MAIDO **(20.9°S, 55.3°E)** **(whole period: 06/2018 – 11/2019)**	2.1 ± 0.8 (94 ± 54) R = 0.84, S = 1.17	-
With smoothing	1.7 ± 0.8 (68 ± 43) R = 0.69, S = 1.29	-

XIANGHE **(39.7°N, 117.0°E)** **(whole period: 03/2010 – 12/2021)**	-6.4 ± 2.7 (-48 ± 16) R = 0.88, S = 0.67	-8.9 ± 2.6 (-60 ± 21) R = 0.82, S = 0.76
With smoothing	0.59 ± 2.2 (-8 ± 31) R = 0.88, S = 1.19	-2.4 ± 2.7 (-29 ± 37) R = 0.79, S = 1.40
BUJUMBURA **(3.0°S, 29.0°E)** **(whole period: 11/2013 – 07/2017)**	-4.4 ± 2.2 (-32 ± 10) R = 0.88, S = 0.52	-
With smoothing	0.3 ± 2.0 (3.2 ± 25) R = 0.72, S = 0.65	-
OHP **(whole period: 08/2014 – 03/2017)**	0.3 ± 1.1 (4.2 ± 21) R = 0.90, S = 0.75	-
With smoothing	103.51 ± 1.0 (17 ± 22) R = 0.86, S = 1.01	-
REUNION LEPORT **(20.9°S, 55.3°E)** **(whole period: 04/2016 – 12/2017)**	103.51 ± 0.8 (39 ± 26) R = 0.80, S = 1.56	-
With smoothing	2.6 ± 0.1 (180 ± 56) R = 0.78, S = 2.83	-
UCCLE-miniDOAS **(50.8°N, 4.3°E)** **(whole period: 04/2011 – 05/2015)**	-0.6 ± 1.6 (-9.4 ± 29) R = 0.76, S = 0.89	-
With smoothing	-0.4 ± 1.7 (7.1 ± 34) R = 0.73, S = 0.88	-

Results obtained at Cabauw and De Bilt confirm that both satellite instruments capture well the HCHO VCD seasonality. Results for GOME-2B and GOME-2C are similar (as shown also in the past for Xianghe), with absolute and relative differences are slightly larger than GOME-2B. Results for the whole period (shown here) and for the last 12 months do not show large differences (not shown here, see the different figures for each stations on the BIRA validation web server). In Reunion the signal is very small (less than ~0.5×10^{16} molec/cm²) and is more difficult to have firm conclusions.

A significant bias exists between GOME-2B/C and MAX-DOAS observations at the some of the stations (up to 50 %), but as already shown in the GDP-4.8 validation report, for some stations this bias can be significantly reduced when smoothing the MAX-DOAS profiles with the satellite column averaging kernels (see also values with smoothing in Table 7.12).

Status of GOME-2B and GOME-2C total BrO

GOME-2B/C total columns of BrO from GDP-4.8 (4.9 in the case of GOME-2C) operational product are usually compared to ground-based UV-visible zenith-sky measurements at Harestua, Norway (60°N, 11°E), as done in previous validation report. The ground-based columns are derived

from the vertical profiles retrieved by applying an OEM (Optimal Estimation Method) –based profiling technique to zenith-sky measurements at sunrise (Hendrick *et al.*, 2007). The instrument was temporarilly off due to problems at the Harestua obervatory since 09/12/2022 and is now back in operations since the end of April 2023 with a change of management at the Harestua Solar Observatory. Moreover, due to long-period sickness of key personnel, the ground-based BrO data could not yet be analyzed and this comparison with the GOME-2 instruments could not be updated for this report. We leave the results and discussion of the Operations Report 1/2022.

The sensitivity of these measurements to the troposphere is increased by using a fixed reference spectrum corresponding to clear-sky noon summer conditions for the spectral analysis. In order to ensure the photochemical matching between satellite and ground-based observations, sunrise ground-based columns have been photochemically converted to the satellite overpass SZAs using a stacked box photochemical model (Hendrick *et al.*, 2007 and 2008).

Comparison results (150 km overpasses) for GOME-2B and GOME-2C are shown in Figure 7.11 and Figure 7.12, respectively.

Mean biases values between GOME-2B/C and ground-based data are of -15 ± 11 % and -9 ± 10 %. GOME-2B/C BrO columns are thus all within the target accuracy of 30 % and also within the optimal accuracy of 15 %, except GOME-2B which is slightly above the required optimal accuracy threshold.
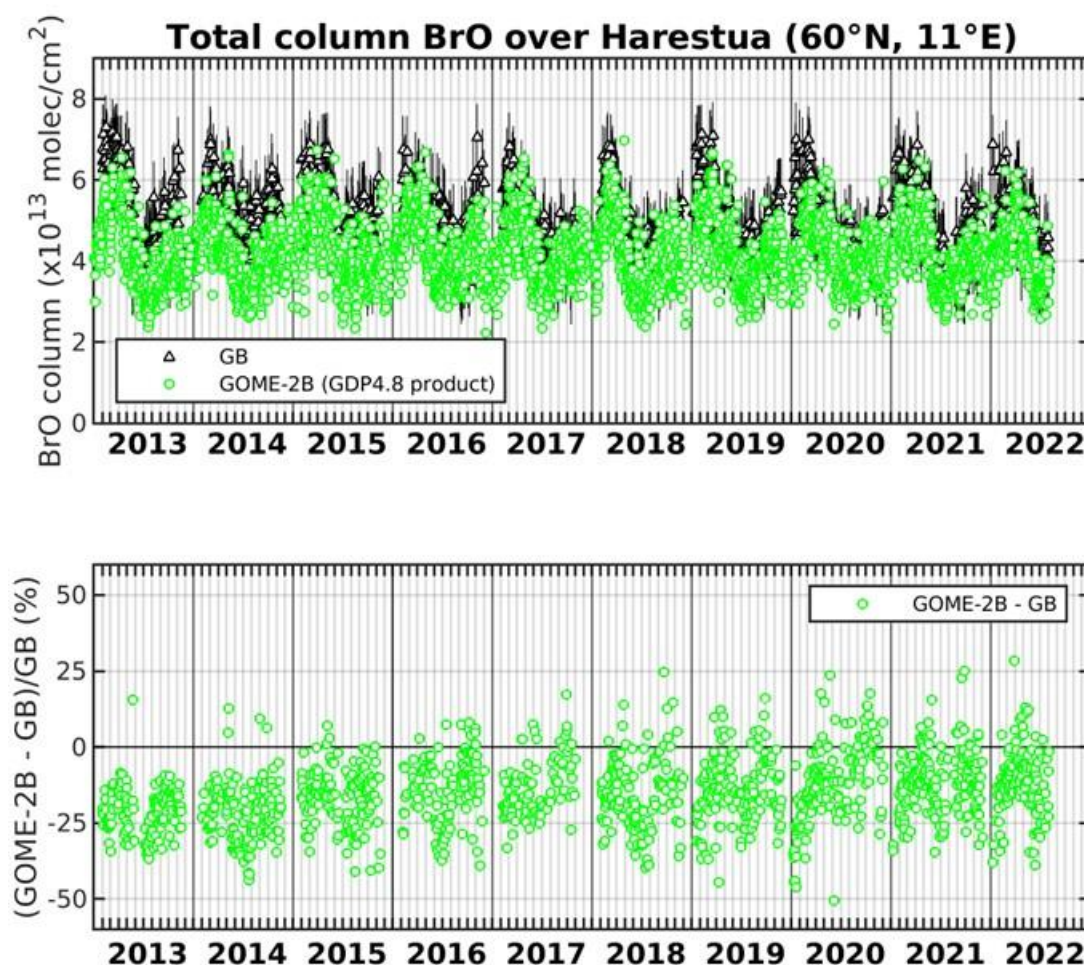
Figure 7.11. Comparison between GOME-2B GDP-4.8 and ground-based total BrO columns at Harestua (60°N, 11°E). The relative differences appear in the lower plot.
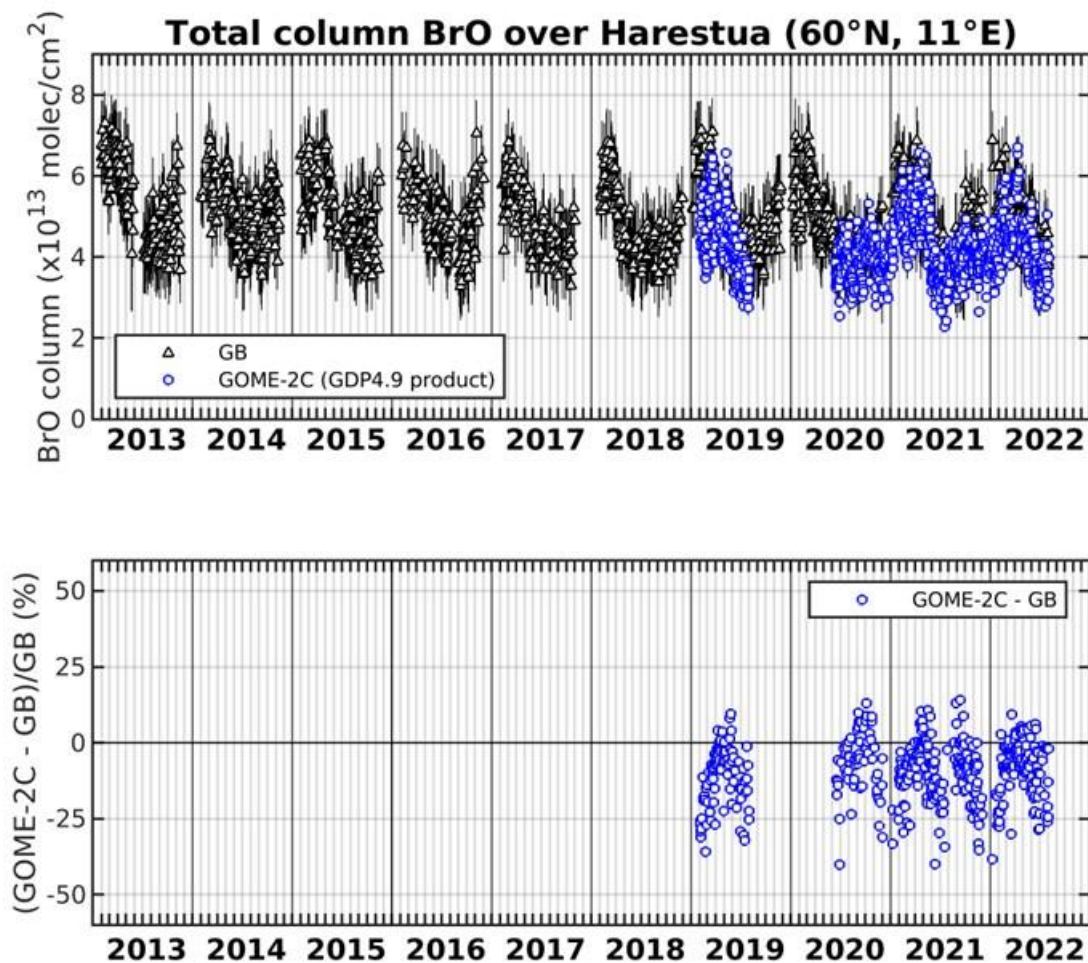
Figure 7.12. Comparison between GOME-2C GDP-4.9 and ground-based total BrO columns at Harestua (60°N, 11°E). The relative differences appear in the lower plot.

Status of GOME-2B and GOME-2C SO$_2$

GOME-2 SO$_2$ GDP-4.8 continues to be used for the near-real-time observation of volcanic activity within the SACS service. The Support to Aviation Control Service (SACS) hosted by the Royal Belgian Institute for Space Aeronomy (BIRA-IASB) aims at supporting the Volcanic Ash Advisory Centers, like Toulouse VAAC and London VAAC. This is achieved by delivering near real-time data of SO$_2$ and aerosols derived from satellite measurements regarding volcanic emissions by UV-VIS (OMI, GOME-2A and GOME-2B composite until 31 March 2021 and GOME-2B and GOME-2C composite since then, OMPS, TROPOMI) and infrared (AIRS, IASI-A, IASI-B) instruments. In case of volcanic eruptions, notifications are sent out by email to interested parties. The SACS notification archive service gathers all the notifications; the results can be found here.

In the first half of 2023, SACS reported only two clusters of cases where the GOME-2B/C instruments detected significant SO$_2$, as shown in Figure 7.13. In mid-April, a strong eruption in Siveluch, Kamchatka Peninsula in eastern Russia, while at the end of May, a relatively smaller eruption of Popocatepl were observed. Similar SO$_2$ levels and alerts are seen by GOME-2B and GOME-2C, with some small differences due to differences of the maximum SO$_2$ levels.
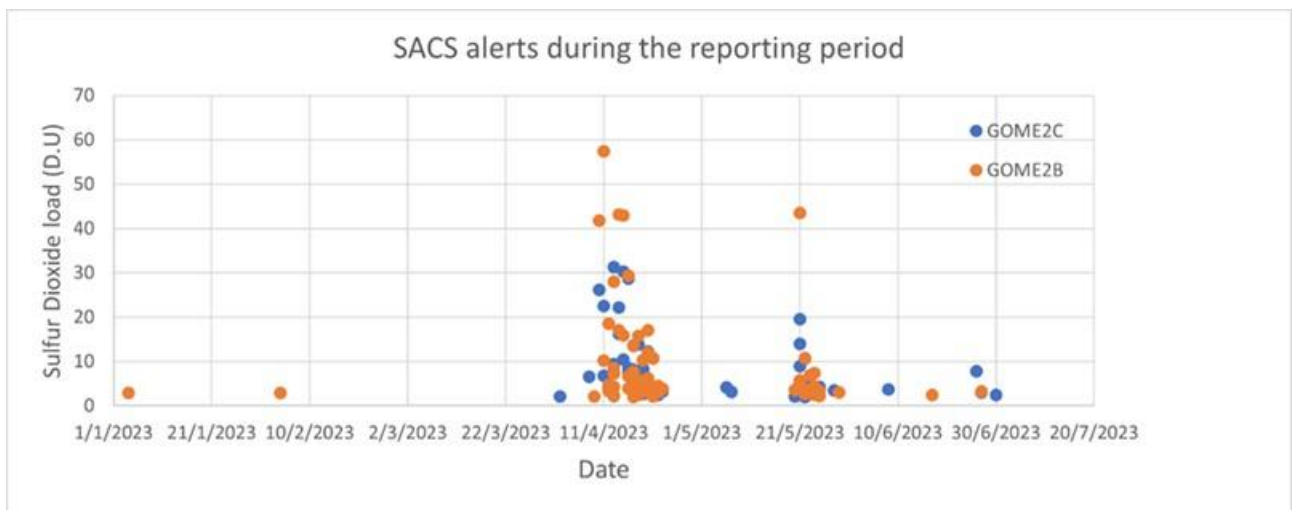
Figure 7.13. GOME2B [orange] and GOME2C [blue] SACS alerts during the reporting period as a function of the SO₂ load observed.

In Figure 7.14 two eruptive days during the reporting period are presented, for the onset of the Siveluch eruption on the 12th of April and the continuation of the phenomenon on the 14th of April 2023 respectively. The GOME2-B/C combined product appears to capture the event very well, both in terms of sulphur dioxide load and location of the volcanic SO2 plume.
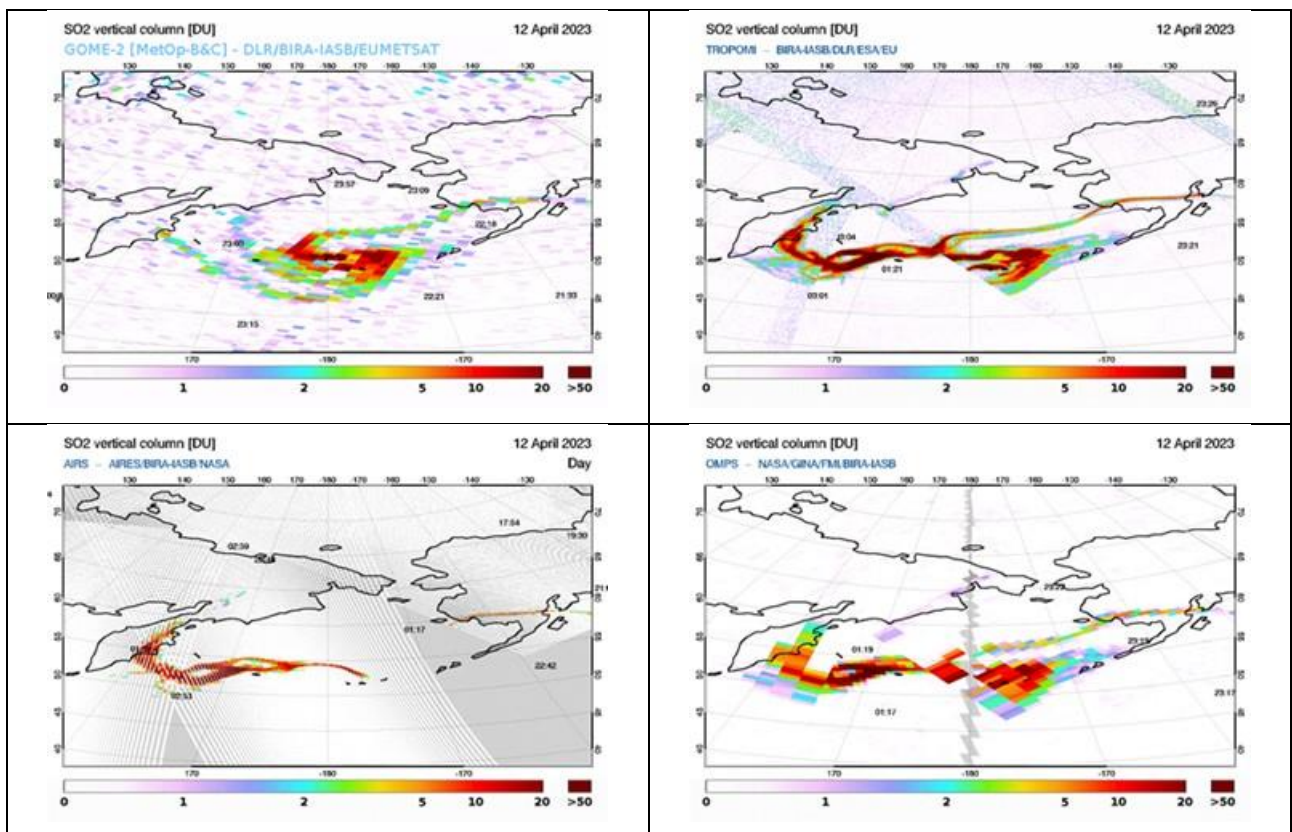
Figure 7.14. Shiveluch eruption on the 12th of April 2023, sensed by GOME2-B/C [upper left], S5P/TROPOMI [upper right], AIRS [bottom left] and OMPS/NPP [bottom right] from the SACS monitoring pages.
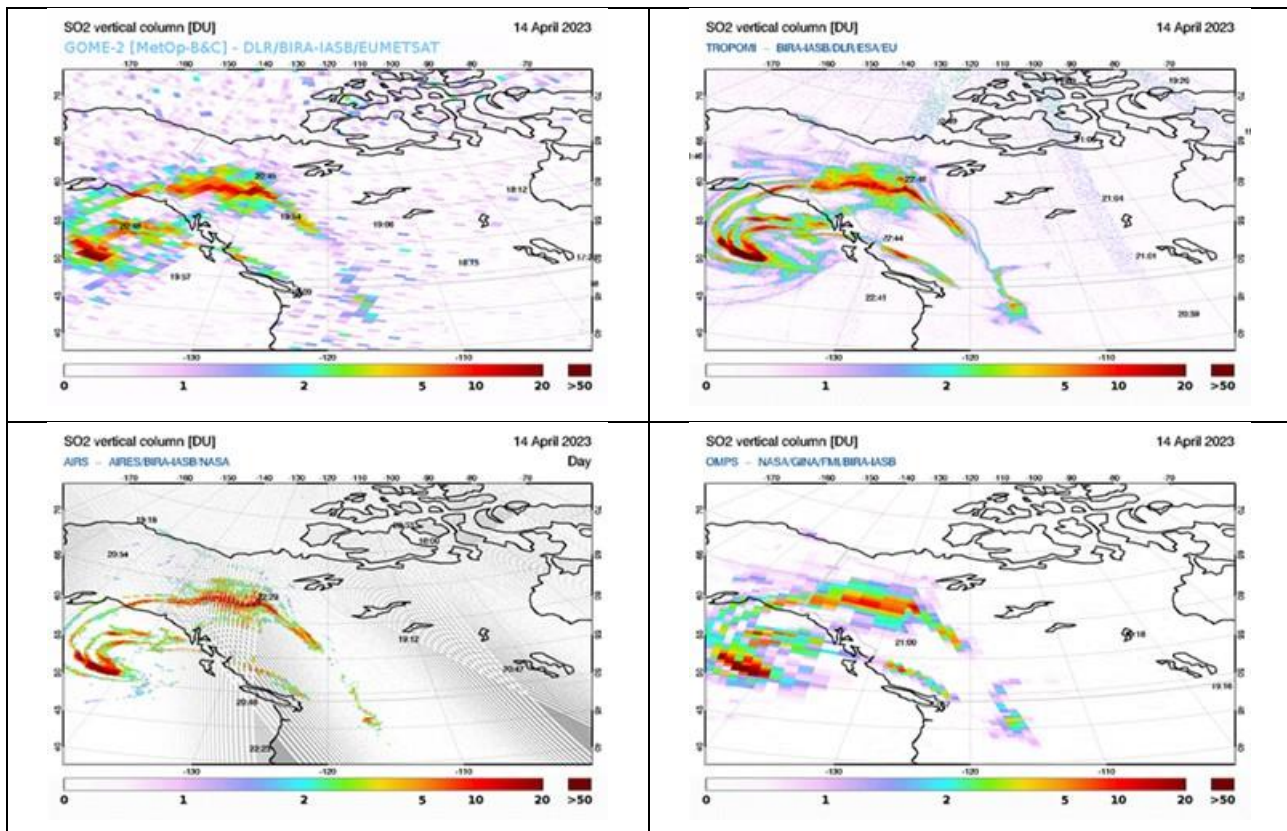
Figure 7.15. As Figure 7.14, but for the evolution of the Shiveluch eruption, on the 14th of April from the SACS monitoring pages.

The coherence of the GOME-2B/C measurements with the other morning instruments (Figure 7.14) is clear, as is the temporal evolution with the afternoon platform instruments (Figure 7.15).

As discussed in the previous Operations Reports, the plan for the improvement of the SO2 GOME-2 products is to follow BIRA-IASB recommendations and bring the GDP SO2 algorithm consistent to the TROPOMI product (Theys *et al.*, 2017). The current operational GOME-2C SO2 algorithm (GDP 4.9) has an improved fitting-window, but unfortunately this fitting window can not be applied to GOME-2B due to instrument- and L1B data degradation.

The quality of the GOME-2B SO2 retrieval can be improved with a 3-fit window algorithm approach (like in TROPOMI SO2 retrieval), which is planned to be implemented in the CDOP-4 for the NRT/offline GOME-2 SO2 products, as well as for the reprocessing.

References:

Clémer, K., Van Roozendael, M., Fayt, C., Hendrick, F., Hermans, C., Pinardi, G., Spurr, R., Wang, P., and De Mazière, M.: Multiple wavelength retrieval of tropospheric aerosol optical properties from MAXDOAS measurements in Beijing, Atmos. Meas. Tech., 3, 863-878, 2010. https://doi.org/10.5194/amt-3-863-2010

De Smedt, I., Stavrakou, T., Hendrick, F., Danckaert, T., Vlemmix, T., Pinardi, G., Theys, N., Lerot, C., Gielen, C., Vigouroux, C., Hermans, C., Fayt, C., Veefkind, P., Müller, J.-F., and Van Roozendael, M.: Diurnal, seasonal and long-term variations of global formaldehyde columns inferred from combined OMI and GOME-2 observations, Atmos. Chem. Phys., 15, 12519-12545, 2015. https://doi.org/10.5194/acp-15-12519-2015

De Smedt, I., Pinardi, G., Vigouroux, C., Compernolle, S., Bais, A., Benavent, N., Boersma, F., Chan, K.-L., Donner, S., Eichmann, K.-U., Hedelt, P., Hendrick, F., Irie, H., Kumar, V., Lambert, J.-C., Langerock, B., Lerot, C., Liu, C., Loyola, D., Piters, A., Richter, A., Rivera Cárdenas, C., Romahn, F., Ryan, R. G., Sinha, V., Theys, N., Vlietinck, J., Wagner, T., Wang, T., Yu, H., and Van Roozendael, M.: Comparative assessment of TROPOMI and OMI formaldehyde observations and validation against MAX-DOAS network column measurements, Atmos. Chem. Phys., 21, 12561–12593, 2021.
https://doi.org/10.5194/acp-21-12561-2021

Gielen, C., Van Roozendael, M., Hendrick, F., Pinardi, G., Vlemmix, T., De Bock, V., De Backer, H., Fayt, C., Hermans, C., Gillotay, D., and Wang, P.: A simple and versatile cloud-screening method for MAX-DOAS retrievals, Atmos. Meas. Tech., 7, 3509–3527, 2014.
https://doi.org/10.5194/amt-7-3509-2014

Hendrick, F.M., Van Roozendael, M., Chipperfield, M.P., Dorf, M., Goutail, F., Yang, X., Fayt, C., Hermans, C., Pfeilsticker, K., Pommereau, J.-P., Pyle, J.A., Theys, N., and De Maziere, M.: Retrieval of stratospheric and tropospheric BrO profiles and columns using ground-based zenith-sky DOAS observations at Harestua, 60° N., Atmos. Chem. Phys., 7, 4869-4885, 2007.
https://doi.org/10.5194/acp-7-4869-2007

Hendrick, F., Johnston, P.V., De Mazière, M., Fayt, C., Hermans, C., Kreher, K., Theys, N., Thomas, A., and Van Roozendael, M.: One-decade trend analysis of stratospheric BrO over Harestua (60°N) and Lauder (45°S) reveals a decline, Geophys. Res. Letters, 35, L14801, 2008.
https://doi.org/10.1029/2008gl034154

Hendrick, F., Müller, J.-F., Clémer, K., Wang, P., De Mazière, M., Fayt, C., Gielen, C., Hermans, C., Ma, J.Z., Pinardi, G., Stavrakou, T., Vlemmix, T., and Van Roozendael, M.: Four years of ground-based MAX-DOAS observations of HONO and NO2 in the Beijing area, Atmos. Chem. Phys., 14, 765–781, 2014.
https://doi.org/10.5194/acp-14-765-2014

Pinardi, G., Van Roozendael, M., Lambert, J.-C., Granville, J., Hendrick, F., Tack, F., Yu, H., Cede, A., Kanaya, Y., Irie, I., Goutail, F., Pommereau, J.-P., Pazmino, A., Wittrock, F., Richter, A., Wagner, T., Gu, M., Remmers, J., Friess, U., Vlemmix, T., Piters, A., Hao, N., Tiefengraber, M., Herman, J., Abuhassan, N., Bais, A., Kouremeti, N., Hovila, J., Holla, R., Chong, J., Postylyakov, O., Ma, J.: GOME-2 total and tropospheric NO_2 validation based on zenith-sky, direct-sun and multi-axis DOAS network observations, Proceeding of the EUMETSAT conference, 22-26 September 2014, Geneva, Switzerland.

Pinardi, G., Van Roozendael, M., Hendrick, F., Theys, N., Abuhassan, N., Bais, A., Boersma, F., Cede, A., Chong, J., Donner, S., Drosoglou, T., Frieß, U., Granville, J., Herman, J. R., Eskes, H., Holla, R., Hovila, J., Irie, H., Kanaya, Y., Karagkiozidis, D., Kouremeti, N., Lambert, J.-C., Ma, J., Peters, E., Piters, A., Postylyakov, O., Richter, A., Remmers, J., Takashima, H., Tiefengraber, M., Valks, P., Vlemmix, T., Wagner, T., and Wittrock, F.: Validation of tropospheric NO2 column measurements of GOME-2A and OMI using MAX-DOAS and direct sun network observations, Atmos. Meas. Tech., 13, 6141-6174, 2020.
https://doi.org/10.5194/amt-13-6141-2020

Richter, A., Behrens, L., Hilboll, A., Munassar, S., Burrows, J.P., Pinardi, G., and Van Roozendael, M.: Cloud effects on satellite retrievals of tropospheric NO2 over China, oral presentation at the DOAS workshop, September 2017, Yokohama, Japan.

Theys, N., De Smedt, I., Yu, H., Danckaert, T., van Gent, J., Hörmann, C., Wagner, T., Hedelt, P., Bauer, H., Romahn, F., Pedergnana, M., Loyola, D., and Van Roozendael, M.: Sulfur dioxide retrievals from TROPOMI onboard Sentinel-5 Precursor: algorithm theoretical basis, Atmos. Meas. Tech., 10, 119-153, 2017.
https://doi.org/10.5194/amt-10-119-2017

Verhoelst, T., Compernolle, S., Pinardi, G., Lambert, J.-C., Eskes, H. J., Eichmann, K.-U., Fjæraa, A. M., Granville, J., Niemeijer, S., Cede, A., Tiefengraber, M., Hendrick, F., Pazmiño, A., Bais, A., Bazureau, A., Boersma, K. F., Bognar, K., Dehn, A., Donner, S., Elokhov, A., Gebetsberger, M., Goutail, F., Grutter de la Mora, M., Gruzdev, A., Gratsea, M., Hansen, G. H., Irie, H., Jepsen, N., Kanaya, Y., Karagkiozidis, D., Kivi, R., Kreher, K., Levelt, P. F., Liu, C., Müller, M., Navarro Comas, M., Piters, A. J. M., Pommereau, J.-P., Portafaix, T., Prados-Roman, C., Puentedura, O., Querel, R., Remmers, J., Richter, A., Rimmer, J., Rivera Cárdenas, C., Saavedra de Miguel, L., Sinyakov, V. P., Stremme, W., Strong, K., Van Roozendael, M., Veefkind, J. P., Wagner, T., Wittrock, F., Yela González, M., and Zehner, C.: Ground-based validation of the Copernicus Sentinel-5P TROPOMI NO2 measurements with the NDACC ZSL-DOAS, MAX-DOAS and Pandonia global networks, Atmos. Meas. Tech., 14, 481–510, 2021.
https://doi.org/10.5194/amt-14-481-2021

Vlemmix, T., Hendrick, F., Pinardi, G., Smedt, I., Fayt, C., Hermans, C., Piters, A., Wang, P., Levelt, P, and Van Roozendael, M.: MAX-DOAS observations of aerosols, formaldehyde and nitrogen dioxide in the Beijing area: comparison of two profile retrieval approaches, Atmos. Meas. Tech., 2, 941–963, 2015.
https://doi.org/10.5194/amt-8-941-2015

Wang, T., Hendrick, F., Wang, P., Tang, G., Clémer, K., Yu, H., Fayt, C., Hermans, C., Gielen, C., Müller, J.-F., Pinardi, G., Theys, N., Brenot, H., and Van Roozendael, M.: Evaluation of tropospheric SO2 retrieved from MAX-DOAS measurements in Xianghe, China, Atmos. Chem. Phys., 14(20), 11149-11164, 2014.
https://doi.org/10.5194/acp-14-11149-2014

7.3.1. Online quality monitoring

Online quality monitoring plots are continuously generated at DLR and published for O_3, NO_2, BrO, HCHO, SO_2, H2O products as described in Section 7.1.3.

BIRA-IASB provides quality assessment (QA) pages for vertical column amounts of NO_2, HCHO, BrO and SO_2, derived from GOME-2B and GOME-2C. The goal is to provide an easy tool to quickly spot anomalies and trends in the L2 data, by selecting and examining geographical regions of interest. These pages are available under https://cdop.aeronomie.be/quality-assessment/.

The monitored L2 is provided by DLR with precessor version GDP 4.8 for GOME-2B and GDP 4.9 for GOME-2C.

System developments:

- The GOME-2 monitoring page shows time-series for Metop-B and Metop-C. Metop-A data is kept internally for comparison reasons.
- The current monitoring system, based on data storage in an SQL database, remains slow in use. As mentioned in the previous report, a new system has been under development and has shown to be much faster. Over summer 2023, some delays occurred in the finalization of this system and it is not foreseen to implement this in the second half of the year.

Monitoring status:

SO₂

In the case of SO$_2$, the available geographical regions of interest are either locations with known outgassing volcanoes or locations with strong anthropogenic sources of SO$_2$. The resulting graphs show a history of monthly average values over the selected region.

In Figure 7.16 and Figure 7.17, two relevant panels are presented for the time period 01/01/2022 – 31/12/2022. In the upper panels, the SO$_2$ fitting RMS is shown, an important parameter which acts as immediate indicator to the stability of the instruments/algorithms. In the bottom panels, the total vertical SO$_2$ column is presented, alongside other metrics, explained in the figure caption.
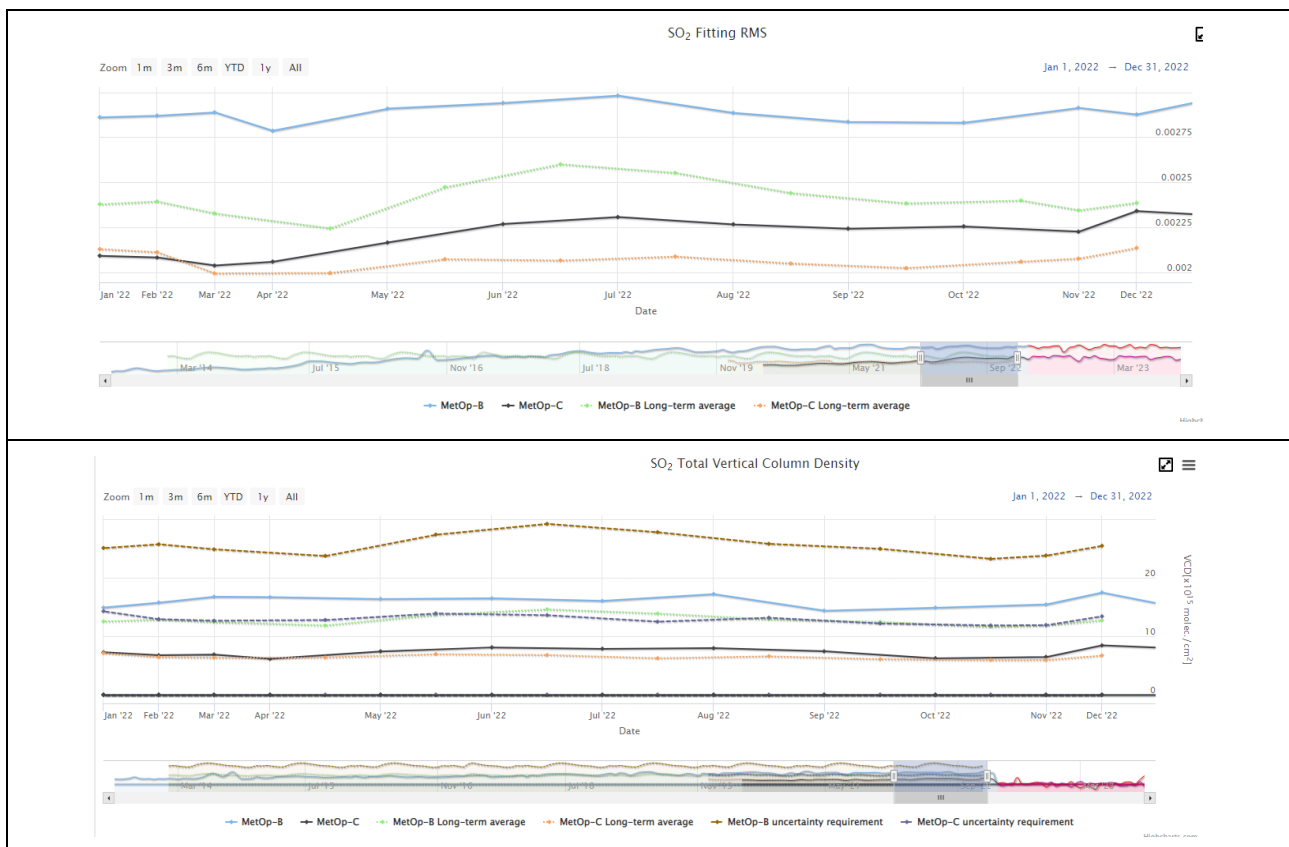
Figure 7.16. The behaviour of the GDP4.8 GOME2B [blue curve] & GOME2C [black curve] 6km plume height SO₂ products between 01/01/2022 and 31/12/2022 over the Democratic Republic of Congo volcanoes. Upper panel, the SO₂ fitting RMS is shown and in the bottom panel, the total vertical SO₂ column. The equivalent long-term average is also provided [see insert legend.]
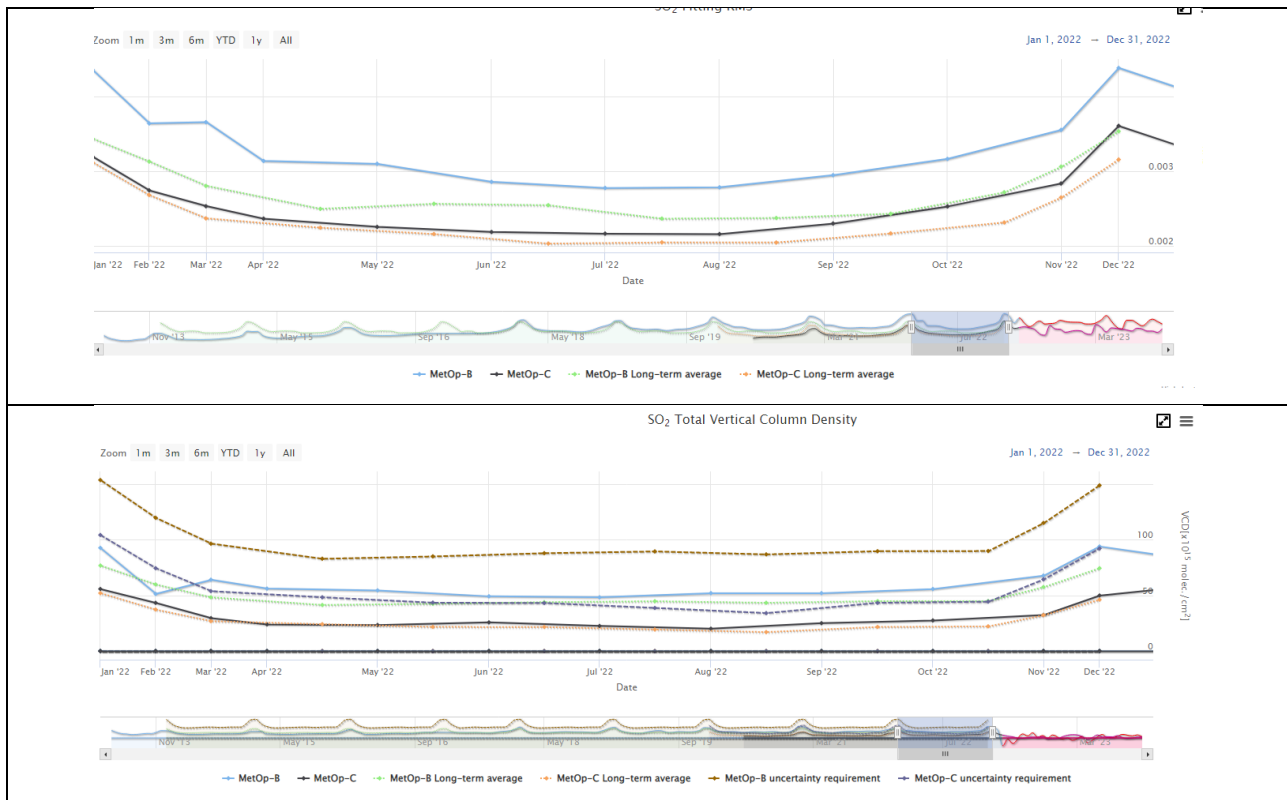
Figure 7.17. The behaviour of the GDP4.8 GOME2B [blue curve] & GOME2C [black curve] 1km plume height SO₂ products between 01/01/2022 and 31/12/2022 over the North China Plane. Upper panel, the SO₂ fitting RMS is shown and in the bottom panel, the total vertical SO₂ column. The equivalent long-term average is also provided [see insert legend.]

From Figure 7.16 and Figure 7.17, upper panels, no spurious jumps or artefacts are observed during 2022 for either the anthropogenic or the volcanic locations in the SO₂ fitting RMS. However, not only it is said that RMS is ~20-25% larger for GOME-2B than GOME-2C, but it is also equally larger from its long-term average. This points to a possible degradation effect in the GOME-2B L1b data which also affects the L2 data, as shown in Figure 7.16 and Figure 7.17, lower panels. GOME-2B has provided far larger (more than 50 %) SO₂ columnar estimates than GOME-2C and ~20-25 % larger than the long-term average.

Both these issues are cause for concern and merit further investigation from the DLR L2 algorithm team. Currently, GOME-2 SO2 retrieval uses a one fit-window approach with an improved fit-window for GOME-2C (which cannot be applied to GOME-2B due to L1b data degradation effects).

The overall quality of GOME-2B and GOME-2C SO2 products can be improved with a 3-fit window retrieval approach (as for TROPOMI SO2 retrieval), which is planned in the CDOP-4 for the NRT/offline products, as well as for the reprocessing.

NO₂, HCHO, and BrO

The other three trace gaces monitored through the Quality Assessment page do not show the same discrepancy in retrieved column amount between GOME-2B and GOME-2C as is the case for SO₂. When observing the full time-series, column amounts between the two instruments agree quite well. Some examples are depicted in Figure 7.18. For NO₂, the tropospheric column amounts of both sensors show the expected annual cycle and show no systematic mutual offset (panel a, situation over northern India). Indications of instrumental degradation are visible in the fit residual (RMS,

panel b) of both instruments and for GOME-2C the RMS for the first time raises above the long-term average for the period of the current report. On the other hand, the raise of GOME-2B RMS seems to flatten out over the last few years. For NO_2, similar patterns are observed over other geographical regions (not shown here).

Consistent patterns of total column amounts are also observed for HCHO (panel c, Guatemala). There, however, the increase of the RMS signal for GOME-2B seems to continue also in recent years, something that is also observed for BrO (not shown), be it less pronounced.

(a)

(b)

(c)
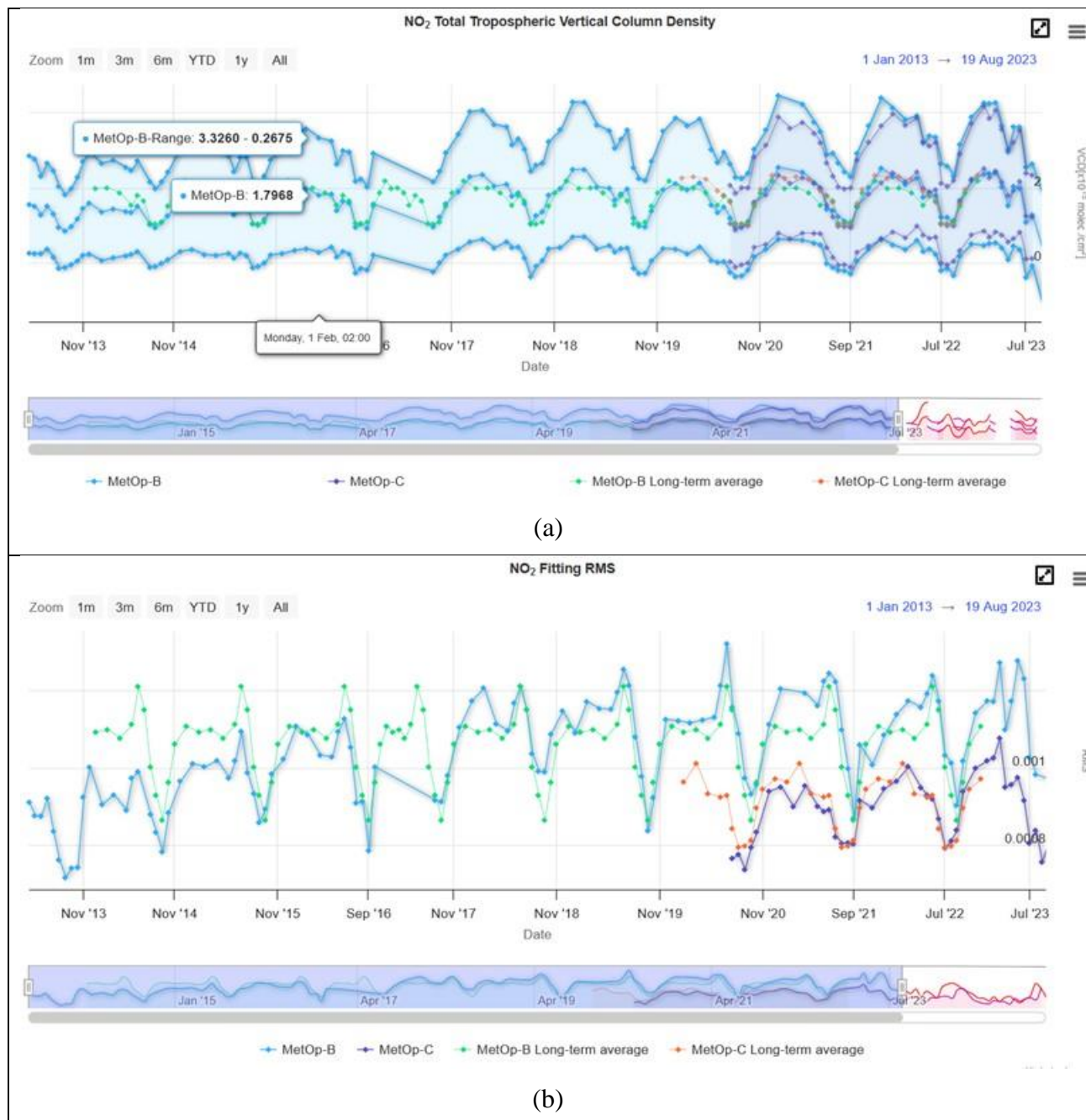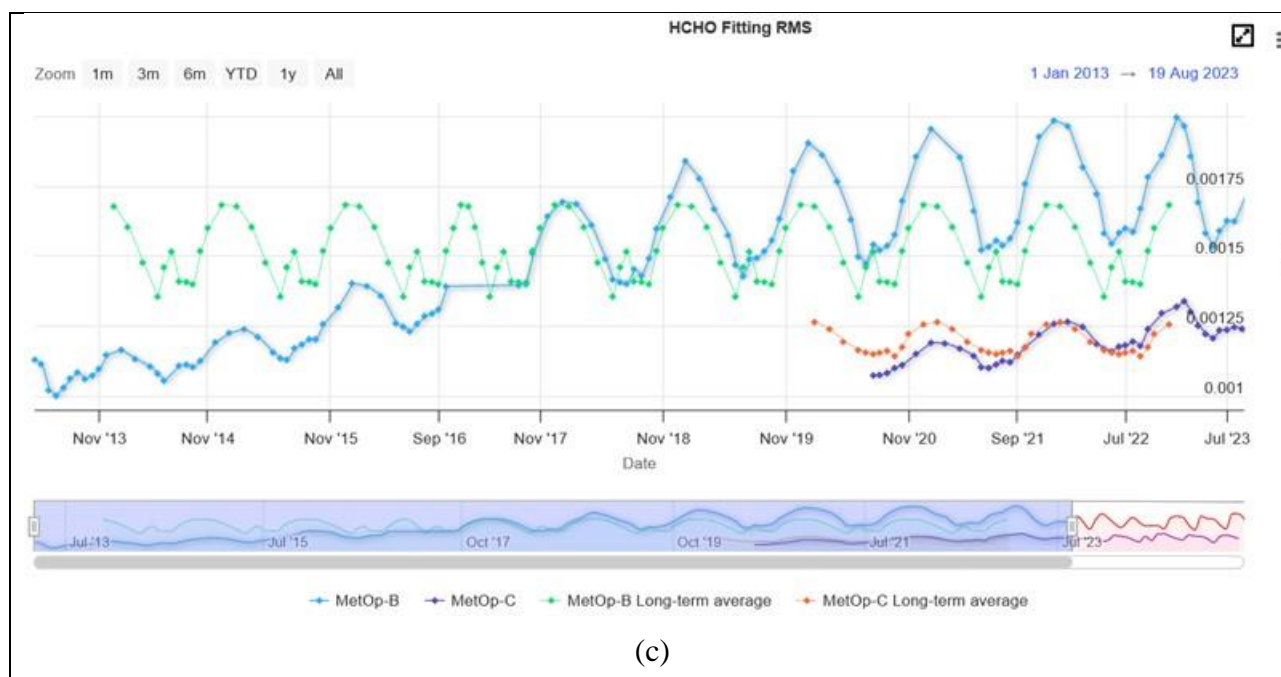
Figure 7.18. Examples of time series from the QA monitoring page. a: NO₂ tropospheric column over India. b: NO₂ fitting RMS over India. c: HCHO fitting RMS over Guatemala.

7.4. Ozone profile products

Table 7.13. Validation status of ozone profile products

Product Identifier	Product Name	Accuracy	Reference	Validating Institute	Correlative data sources
O3M-47.1	NRT high-resolution ozone profile	Fulfils threshold accuracy requirements	RD8	KMI DWD	Ozonesonde data from SHADOZ, NDACC, NILU and WOUDC Lidar/microwave data from NDACC
O3M-311			RD26		
O3M-39	Offline high-resolution ozone profile	Fulfils threshold accuracy requirements	RD7	KMI DWD	Ozonesonde data from SHADOZ, NDACC, NILU and WOUDC Lidar/microwave data from NDACC
O3M-48			RD8		
O3M-312			RD26		

Validation results can be found in more detail on the at AC SAF validation & quality assessment website.

Validation activities summary:

This summary contains validation results for the GOME-2B and GOME-2C high-resolution (HR) ozone profile products, retrieved by the Ozone Profile Retrieval Algorithm (OPERA) at KNMI. This validation section focuses on the time period July 2022 – June 2023.

The authors of this summary are Dr. Andy Delcloo from KMI and Dr. Peggy Achtert from DWD. More information on how these values are extracted is available in the validation report.

There is no material difference in the content of the NRT vs. the offline vertical ozone profile data product, other than its size. The offline file is a concatenation of the NRT L2 PDUs for a particular orbit. While the validation partners are provided the L2 PDUs that were sent out in NRT for their validation, it makes no difference for the validation itself.

To report the skill scores of GOME-2 ozone profile products in a more condensed way, the statistics for the different output levels of GOME-2 are reduced to two layers: Lower Stratosphere (until an altitude of 30 km) and Upper Stratosphere (up to an altitude of 50 km).

The validation for the lower stratosphere is made with ozonesonde data, for the upper stratosphere with lidar, FTIR and/or microwave data. The stations used in this validation for the FTIR/lidar/microwave data are the Network for the Detection of Atmospheric Composition Change (NDACC) stations of Bern (microwave), Ny Ålesund (microwave, FTIR), Thule (FTIR), Payerne (microwave), Hohenpeissenberg (lidar), Table Mountain (lidar), Mauna Loa (microwave/lidar), Eureka (lidar), and Lauder (FTIR, lidar).

The collocation data used for the validation using ozonesonde data are shown in Figure 7.19.
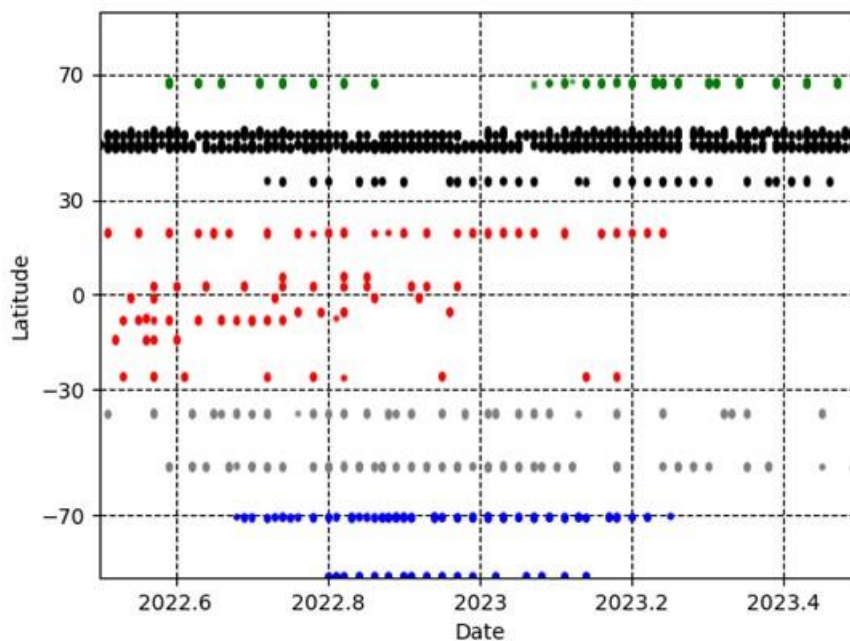

Figure 7.19. Collocation data for the validation with ozonesonde data for the time period July 2022 – June 2023.

Table 7.14 shows an overview of the obtained results for the time period July 2022 – June 2023 only for the lower and the higher stratosphere, not taking into account the tropospheric ozone column products since a dedicated product is discussed earlier in this report. The statistics for the lower stratosphere are obtained by KMI, the statistics for the higher stratosphere by DWD.

Table 7.14. Absolute Differences (AD), Relative Differences (RD) and standard deviation (STDEV) are shown on the accuracy of GOME-2B/C HR ozone profile products for the lower and the higher stratosphere for five different latitude belts for the time period July 2022 – June 2023.

	GOME-2B HR					
	Lower Stratosphere			Upper Stratosphere		
	AD	RD	STDEV	AD	RD	STDEV
	(DU)	(%)	(%)	(DU)	(%)	(%)
Northern Polar Region	0.7	0.3	9.6	-8.5	-13.5	8.7
Northern Mid-Latitudes	2.2	1.2	9.9	-2.6	-0.8	17.6
Tropical Region	4.9	3.6	5.6	-	-	-
Southern Mid-Latitudes	11.7	6.6	10.5	-10.8	-17.9	6.6
Southern Polar Region	7.9	13.5	65.5	-	-	-
	GOME-2C HR					
	Lower Stratosphere			Upper Stratosphere		
	AD	RD	STDEV	AD	RD	STDEV
	(DU)	(%)	(%)	(DU)	(%)	(%)
Northern Polar Region	3.4	1.3	9.8	-9.2	-13.7	8.3
Northern Mid-Latitudes	1.9	1.6	8.5	-3.2	-2.8	14.7
Tropical Region	0.5	0.3	6.3	-	-	-
Southern Mid-Latitudes	11.4	6.9	10.2	-13.0	-19.4	6.9
Southern Polar Region	2.9	19.2	54.4	-	-	-

The target value (15 % accuracy) is met in both lower and upper stratosphere for all belts under consideration for Metop-B and Metop-C. The discrepancy is highest at high-latitude.

More detailed ozone profile validation results can also be found on the AC SAF ozone profile validation website.

7.4.1. Online quality monitoring

Timeline of the vertically integrated Metop-B ozone profile with respect to time is presented in Figure 7.20.

More information and images at the following web addresses
https://www.temis.nl/acsaf/timeseries.php?sat=metopa
https://www.temis.nl/acsaf/timeseries.php?sat=metopb
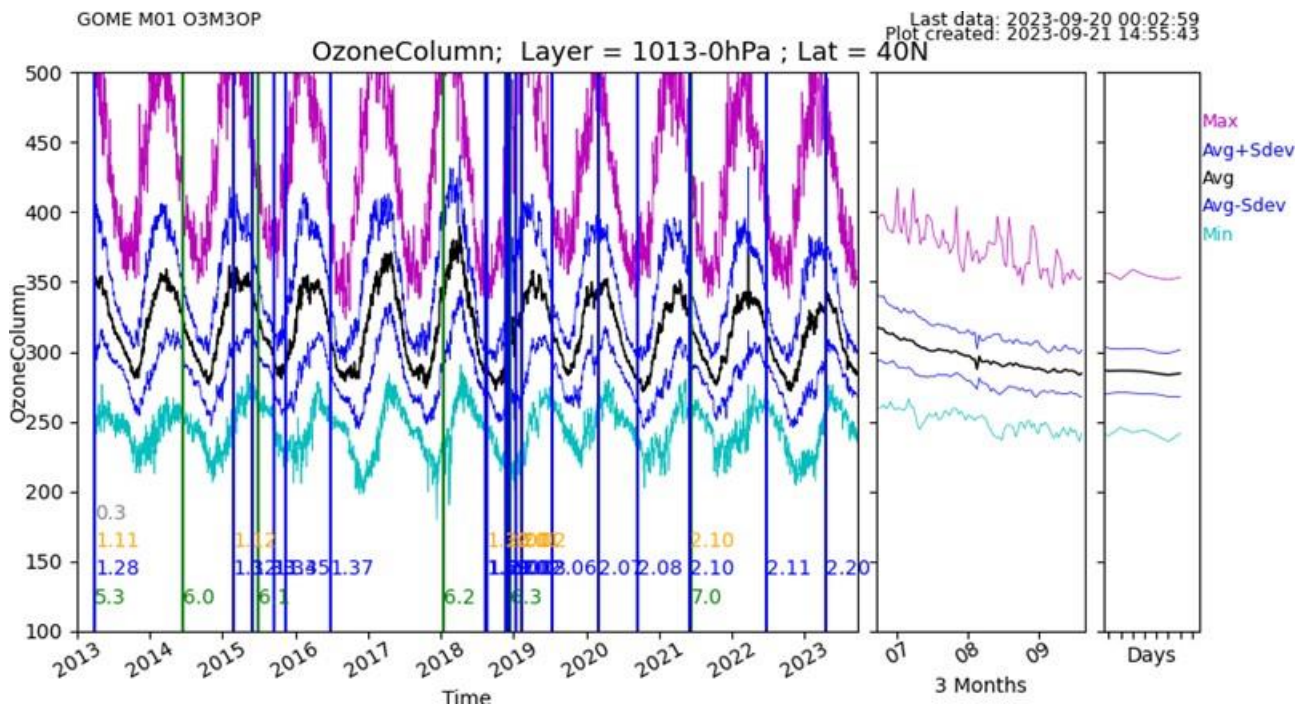https://www.temis.nl/acsaf/timeseries.php?sat=metopc

Figure 7.20. Timeline of vertically integrated Metop-B ozone profiles (=total ozone columns) and changes in data processor (vertical lines). The changes in late 2018 / early 2019, including the improved degradation correction, have resulted in much better ozone profiles and have also affected the total ozone columns shown here.

Legend of the coloured vertical lines:

> ➢ Green: PPF version
> ➢ Blue: Software version (PGE)
> ➢ Orange: Algorithm version
> ➢ Grey: Config version

7.5. Aerosol products

Table 7.15. Validation status of aerosol products

Product Identifier	Product Name	Accuracy	Reference	Validating Institute	Correlative data sources
O3M-78	NRT absorbing aerosol height	Fulfils threshold accuracy requirement	RD32	KMI, AUTH	CALIOP, EARLINET
O3M-364					
O3M-72.1	NRT absorbing aerosol index from PMDs	Fulfils threshold accuracy requirement	RD14	KNMI	Comparisons with other satellite instruments: SCIAMACHY, OMI, and intercomparison of GOME-2A with GOME-2B
O3M-362			RD33		Comparisons with the AAI products from GOME-2A and GOME-2B
O3M-69	Offline absorbing aerosol height	Fulfils threshold accuracy requirements	RD32	KMI, AUTH	CALIOP, EARLINET
O3M-79					
O3M-365					
O3M-63.1	Offline absorbing aerosol index from PMDs	Fulfils threshold accuracy requirements	RD14	KNMI	Comparisons with other satellite instruments: SCIAMACHY, OMI, and intercomparison of GOME-2A with GOME-2B
O3M-73.1					
O3M-363			RD33		Comparisons with the AAI products from GOME-2A and GOME-2B

Validation activities summary:

This summary contains validation results for the GOME-2A, GOME-2B and GOME-2C Absorbing Aerosol Height (AAH) products and is made available by the validation teams of AUTH and KMI. More information on how these values are extracted is available in the validation report [validation report](#).

AAH is a new operational AC SAF product for aerosol layer height detection, developed by KNMI within the AC SAF. It uses the AAI as an indicator to derive the actual height of the absorbing aerosol layer in the O_2-A band using the Fast Retrieval Scheme for Clouds from the Oxygen A band (FRESCO) algorithm (Wang *et al*., 2012; Tilstra *et al*., 2020). The AAH reported by GOME-2 onboard Metop-A, Metop-B and Metop-C, between 2007 and 2019, has been validated by AUTH against ground-based lidar data from the European Aerosol Research Lidar Network (EARLINET) database and by KMI against CALIOP aerosol layer height (De Bock, *et al*. 2020; Michailidis *et al*., 2021).

AUTH results:

A wide selection of lidar stations (first column of Table 7.16 was made in order to examine the behaviour of the comparisons for different common aerosol loads around Europe. The total number

of carefully screened collocations with the EARLINET lidar measurements was 271 for the three GOME-2 instruments, from the beginning of each mission to the reporting period. On average, the mean absolute bias (GOME-2 minus EARLINET lidar height) was found to be -0.3 ± 1.93 km, with a near-Gaussian distribution and minimum and maximum differences of ~ ±5 km. On a per station basis, and with a couple of exceptions, their mean biases fall in the ±1 km range, with an associated standard deviation between 0.6 – 2.4 km.

Table 7.16. Summary of statistics for the comparisons between GOME-2 AAH and LIDAR ALH for all stations

EARLINET Station	N	Statistical parameters (in km)			
		Mean absolute bias	Std	Min	Max
Antikythera, Greece	12	-2.15	1.58	-4.27	0.55
Athens, Greece	3	-2.00	1.38	-3.60	-1.06
Barcelona, Spain	36	-0.44	1.86	-4.66	2.86
Belsk, Poland	28	0.11	1.50	-3.11	3.24
Bucharest, Romania	19	-0.07	2.08	-4.81	3.37
Évora, Portugal	10	-0.09	1.98	-1.64	3.31
Granada, Spain	51	-0.6	1.86	-3.73	4.42
Lecce, Italy	18	-0.24	1.14	-3.47	2.05
Limassol, Cyprus	28	0.08	2.42	-4.08	4.43
Minsk, Belarus	5	0.56	0.61	-0.05	1.51
Potenza, Italy	12	-1.57	1.32	-3.49	1.17
Thessaloniki, Greece	41	0.02	1.87	-4.71	5.23
Warsaw, Poland	8	0.80	1.50	1.08	2.15
Summary	**271**	**-0.3**	**1.93**	**-4.81**	**5.23**

In Figure 7.21, the histogram of absolute differences between GOME-2 and EARLINET aerosol layer heights, calculated for all collocated cases is shown, with the associated statistics. The associated Absorbing Aerosol Index (AAI) value is color-coded. In the right panel, the scatter plot between GOME-2 AAH and aerosol layer height from EARLINET stations, for the totality of collocated cases is presented.
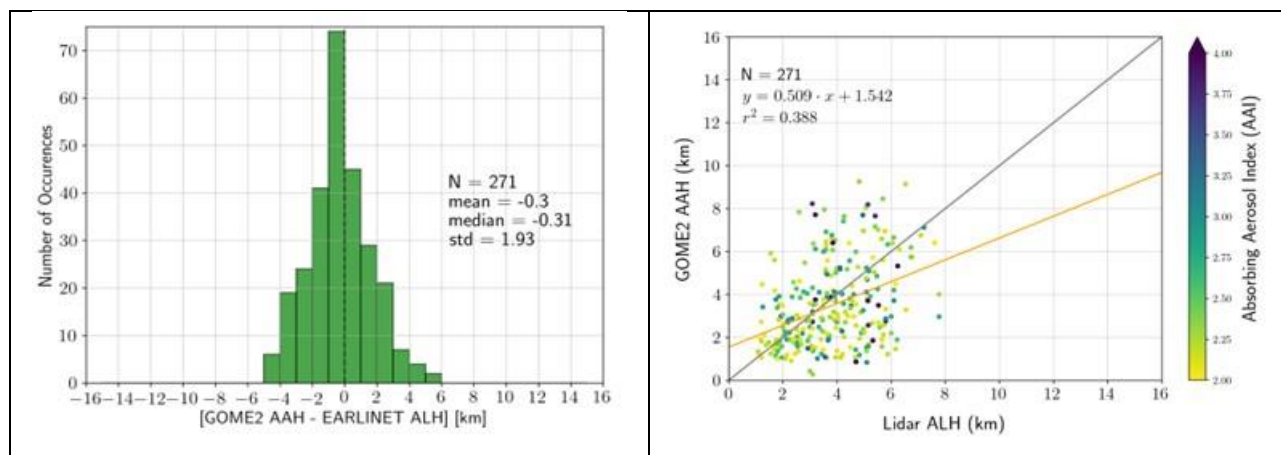
Figure 7.21. Histogram of absolute differences between GOME-2 AAH and aerosol layer height obtained from EARLINET backscatter profiles (using the WCT method), calculated for all collocated cases. The associated AAI value is color-coded. Right: Scatter plot between GOME-2 AAH and aerosol layer height from EARLINET stations, for the total of collocated cases.

Considering the possible temporal collocation mismatch and the spatial difference between the satellite pixel size and the point view of the ground-based observations, these results are quite promising and demonstrate that stable aerosol layers are well captured by the satellite sensors. The official AC SAF requirements for the accuracy of the GOME-2 AAH product state that, for heights <10 km, the threshold accuracy is 3 km, the target accuracy is 2 km, and the optimal accuracy is 1 km. This validation effort shows that for all cases the target accuracy is met, see Table 7.17. For the different regimes, which relate to the degree of cloud cover, please refer to the validation report and Michailidis *et al.*, 2021.

Table 7.17. Percentage of collocated lidar & GOME-2 AAH cases that fulfil the optimal accuracy criteria (first row), the target criteria (second row), the threshold criteria (third row) for Regime A in the first column, Regime B in the second, Regime C in the third and the totality of the collocations in the final column. The regimes are related to the degree of cloud cover.

	Regime A (133 cases)	Regime B (125 cases)	Regime C (13 cases)	Total (271 cases)
Optimal (1 km)	37.9 %	58.2 %	36.6 %	46.9 %
Target (2 km)	55.5 %	78.9 %	54.5 %	66.5 %
Threshold (3 km)	66.4 %	89.5 %	91.2 %	78.6 %

KMI results:

At the time of writing this report, there was no updated AAH reference data available. Therefore, all the results are as in AC SAF Operations Report 1/2021.

KMI validated the AAH only for specific case studies related to volcanic eruptions. AAH values are only included in the analysis if the corresponding AAI is higher than 4. CALIOP and GOME data are compared when the distance between both overpasses is maximum 100 km. There is currently no constraint on the time difference between both overpasses.

Compared to the results shown in the validation report, new data has been added to the study (i.e. Fournaise de la Piton 11-12 February 2020, Karymsky 1-2 April 2020, Kavachi 16 March 2020 and Kikai 29-30 April 2020) in this report. The updated results are summarized in Table 7.18.

Overall, just about 50-60 % of the AAH pixels from GOME-2A, GOME-2B and GOME-2C reach the threshold requirements (see Table 7.18 and Figure 7.22). The optimal requirement threshold is reached for GOME-2A, GOME-2B and GOME-2C in 18 %, 25 % and 24 % of the cases, respectively (when comparing the AAH with the minimum CALIOP layer height). If only the tropospheric aerosol species (as defined by CALIOP) are studied, the results improve. This can also be seen in Table 7.18 (values in brackets).

Table 7.18. Percentage of data for each GOME-2 instrument that reached the threshold, target and optimal accuracy requirements. Values obtained when only considering the tropospheric aerosol species are shown in brackets

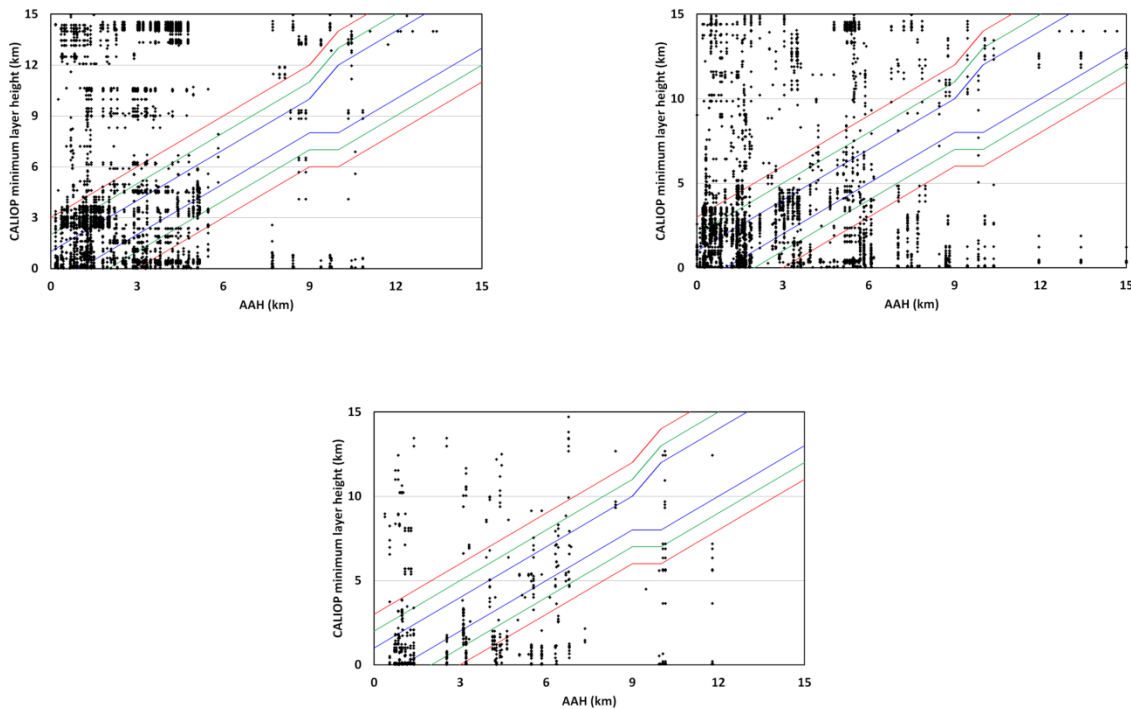| GOME-2A				
		Layer height <10 km	**Layer height >10 km**	**Total**
Threshold	**AAH-minC**	56.0 % (69.6 %)	53.1 % (26.4 %)	55.9 % (68.9 %)
	AAH-maxC	56.4 % (69.5 %)	46.8 % (23.6 %)	56.2 % (68.7 %)
Target	**AAH-minC**	39.0 % (48.5 %)	43.5 % (19.1 %)	39.1 % (48.0 %)
	AAH-maxC	38.0 % (46.9 %)	32.4 % (23.6 %)	37.9 % (46.3 %)
Optimal	**AAH-minC**	17.3 % (21.5 %)	29.9 % (10.0 %)	17.6 % (21.3 %)
	AAH-maxC	18.1 % (22.3 %)	15.6 % (10.0 %)	18.1 % (22.1 %)
GOME-2B				
		Layer height <10 km	**Layer height >10 km**	**Total**
Threshold	**AAH-minC**	51.8 % (53.6 %)	22.9 % (11.7 %)	50.9 % (51.6 %)
	AAH-maxC	52.6 % (54.4 %)	20.6 % (10.2 %)	51.6 % (52.2 %)
Target	**AAH-minC**	42.9 % (44.5 %)	20.6 % (5.60 %)	42.2 % (42.6 %)
	AAH-maxC	37.0 % (38.3 %)	17.1 % (7.90 %)	36.4 % (36.8 %)
Optimal	**AAH-minC**	25.1 % (26.0 %)	17.1 % (3.40 %)	24.8 % (24.9 %)
	AAH-maxC	20.5 % (33.1 %)	16.5 % (3.00 %)	20.4 % (31.6 %)
GOME-2C				
		Layer height <10 km	**Layer height >10 km**	**Total**
Threshold	**AAH-minC**	50.8 % (50.8 %)	0.0 % (0.0 %)	46.8 % (46.8 %)
	AAH-maxC	57.1 % (57.1 %)	0.0 % (0.0 %)	52.9 % (52.9 %)
Target	**AAH-minC**	42.2 % (42.2 %)	0.0 % (0.0 %)	38.8 % (38.8 %)
	AAH-maxC	49.1 % (49.1 %)	0.0 % (0.0 %)	45.2 % (45.2 %)
Optimal	**AAH-minC**	26.3 % (26.3 %)	0.0 % (0.0 %)	24.1 % (24.1 %)
	AAH-maxC	34.5 % (34.5 %)	0.0 % (0.0 %)	31.6 % (31.6 %)

Figure 7.22. Requirement plots for GOME-2A (upper left), GOME-2B (upper right) and GOME-2C (lower middle).The red, green and blue lines represent the threshold, target and optimal requirements. CALIOP pixels are only shown up to a height of 15 km, which is the detection limit of GOME-2.

References:

Michailidis, K., Koukouli, M.-E., Siomos, N., Balis, D., Tuinder, O., Tilstra, L. G., Mona, L., Pappalardo, G. and Bortoli, D.: First validation of GOME-2/MetOp absorbing aerosol height using EARLINET lidar observations, Atmos. Chem. Phys., 21, 3193–3213, 2021. https://doi.org/10.5194/acp-21-3193-2021

Tilstra, L. G., Tuinder, O., Wang, P. and Stammes, P.: ALGORITHM THEORETICAL BASIS DOCUMENT GOME-2 Absorbing Aerosol Height, SAF/AC//KNMI/ATBD/005, 1.4, Royal Netherlands Meteorological Institute, de Bilt, 2019. https://acsaf.org/docs/atbd/Algorithm_Theoretical_Basis_Document_AAH_Apr_2019.pdf, last access: 31 March 2021.

Wang, P., Tuinder, O. N. E., Tilstra, L. G., De Graaf, M. and Stammes, P.: Interpretation of FRESCO cloud retrievals in case of absorbing aerosol events, Atmos. Chem. Phys., 12(19), 9057–9077, 2021. https://doi.org/10.5194/acp-12-9057-2012

De Bock, V., A. Delcloo, K. Michailidis, M. Koukouli and D. Balis, ACSAF Absorbing Aerosol Height products validation report, SAF/AC/AUTH-RMI/VR/001, 1/2020, 3 July 2020. https://acsaf.org/docs/vr/Validation_Report_AAH_Jul_2020.pdf, last access: 31 March 2021.

7.5.1. Online quality monitoring

The online quality monitoring of the AAI in this section show (left duo-plot) the radiance corrections for the PMD-AAI at 340 and 380 nm, and (right duo-plot) the uncorrected residue, and the corrected residue. The rightmost plot is the result of all the corrections and should stay more or less flat when seasonal cycles and differences are removed.

The break in the curves of the latter plot in August 2018 is caused by the introduction of a combination of the 'End-of-Orbit' corrections and a flattening of the AAI across the swath.
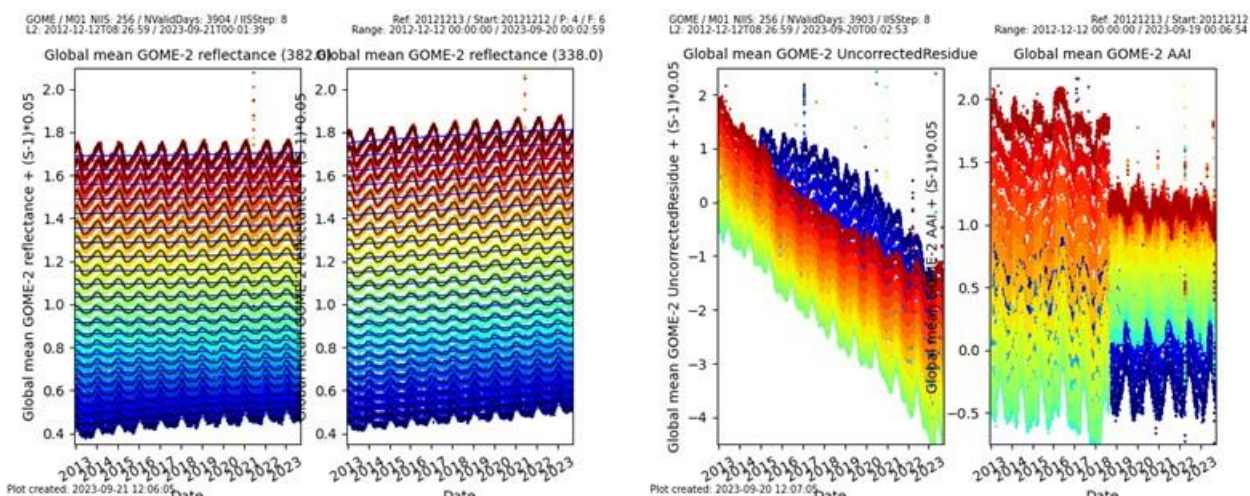

Figure 7.23. Timeline of global mean reflectances at 340 and 380 nm (left) and the uncorrected and corrected AAI from the PMDs of Metop-B.

7.6. UV products

Table 7.19. Validation status of UV products

Product Identifier	Product Name	Accuracy	Reference	Validating Institute	Correlative data sources
O3M-409	NRT UV index, clear-sky	Fulfils threshold accuracy requirements	RD9	DMI	WOUDC, NEUBrew, NSF
O3M-410	NRT UV index, cloud-corrected				
O3M-450 – O3M-464	Offline surface UV	Fulfils target accuracy requirements	RD15	FMI	Brewers and SUV-spectroradiometers from WOUDC, NEUBrew, NSF, NOAA, AUTH and FMI

7.6.1. Online quality monitoring

NUV:

Online quality monitoring of the NRT UV index is found on NUV web page. It can be traced that the quality of the NUV products is stable since the last validation. No problems with the data quality was found in the reporting period.

OUV:

Online quality monitoring of offline surface UV has not shown any unexpected, permanent changes in the monitoring value after the latest validation, indicating that the product accuracy has remained within requirements also during the reporting period. The latest OUV validation reports were published in February 2009 covering June 2007 – May 2008 (Metop-A data) and in February 2015 covering June 2012 – May 2013 (Metop-B data).

Figure 7.24 presents the long-term monitoring graph of OUV, which illustrates seasonal variation of **global average of erythemal daily dose** (yellow markers). Any sudden changes would indicate problems with data quality. Additionally, six-month average values (January – June and July – December) are represented by red markers.
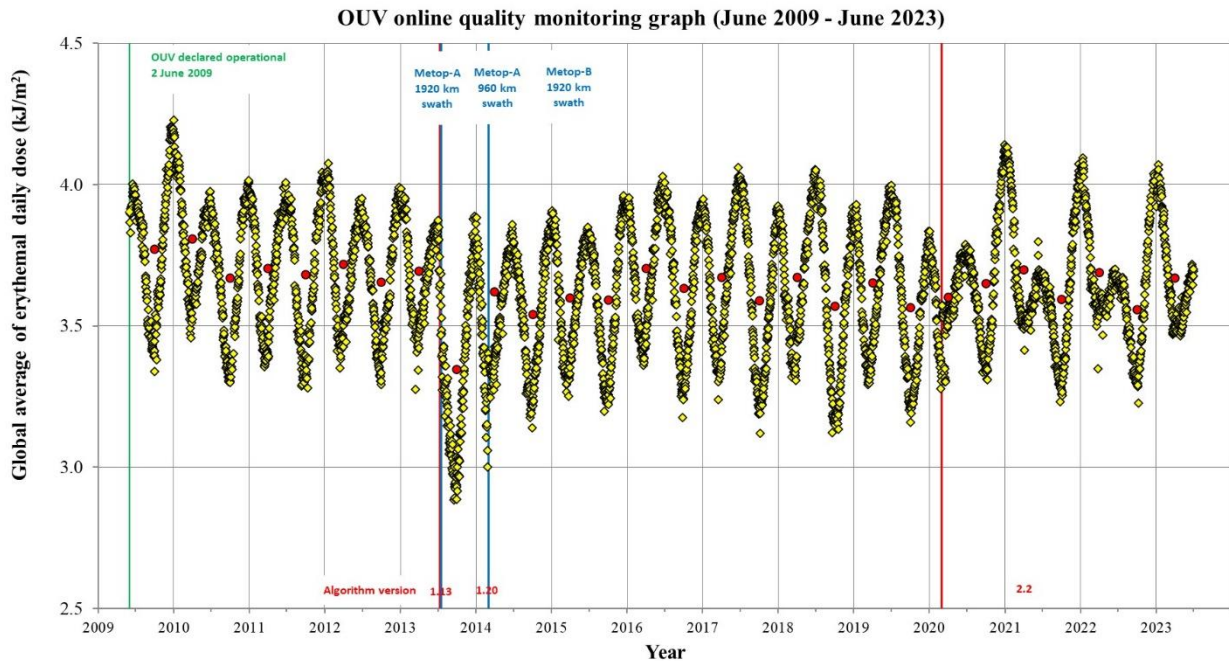

Figure 7.24. OUV long-term monitoring graph.

NOTES:

- GOME-2A was switched from nominal swath width (1920 km) to reduced swath width (960 km) 15 July 2013. The effect to OUV monitoring values can be clearly seen as more wide-spread global average values of erythemal daily dose. This is due to the dominance of lower EDD values in high latitudes when the satellite coverage near the equator is poor due to narrower swath width.

- OUV data processing was switched to use Metop-B data having nominal swath width of 1920 km 1 March 2014

- OUV data processing was switched to use Metop-B+C data 1 March 2020

7.7. IASI NRT products

Table 7.20. Online quality monitoring of the IASI CO, SO2, O3 and HNO3 products

Product Identifier	Product Name	Accuracy	Reference	Validating Institute	Correlative data sources
O3M-80	IASI NRT CO	Fulfils threshold accuracy requirement	RD20	LATMOS	FTIR NDACC, MOPITT
O3M-57	IASI NRT SO2	Fulfils threshold accuracy requirement	RD22	AUTH, BIRA-IASB, LATMOS, ULB	MAXDOAS
O3M-44 O3M-49	IASI NRT O3	Fulfils threshold accuracy requirement	RD35	AUTH, KMI, DWD	GOME-2, balloon sonde, lidar and microwave radiometer, Brewer and Dobson
O3M-81	IASI NRT HNO3	Fulfils threshold accuracy requirement	RD36	BIRA-IASB	FTIR NDACC (only available in 2021)

IASI NRT O3 and IASI NRT HNO3 products have been released by EUMETSAT as 'operational' on 18 May 2022.

IASI online quality monitoring is performed at ULB and LATMOS.

IASI NRT CO online monitoring:
https://atmosphere.copernicus.eu/charts/packages/cams_monitoring/

Dissemination monitoring activities summary:

IASI CO:

The IASI NRT CO product (v6.3) has been declared operational on 2 March 2017. Here we present statistical results when comparing the EUMETSAT product disseminated by EUMETCast in BUFR format (COX) with the native product produced at ULB (FORLI-CO v20191122) for 6 days representative of 6 months: January 15th, February 15th, March 15th, April 15th, May 15th and June 15th, 2023, for Metop-B and Metop-C. This allows monitoring if any discrepancy occurs between the two, EUMETSAT and native, products. So far, the discrepancies are found within the numerical errors inherent to the use of different IT infrastructure.

CO total column and profiles are investigated. Statistics between COX data and FORLI-CO data (v20191122) are presented in Table 7.21. Profiles correlation ("Correlation") score is computed using the discreet cross correlation integral between two profiles, normalized by the square root of the product of their auto-correlation integral. Score of 1 is expected for perfectly matching profiles, 0 for unrelated ones. Absolute and relative differences are calculated for the total columns. These tables are extracted from the Daily Reports prepared by Daniel Hurtmans at ULB.

Table 7.21. Statistics between COX data and FORLI-CO data for 6 days: January 15th, February 15th, March 15th, April 15th, May 15th and June 15th, 2023.

15/01/2023:

		IASI-b		IASI-c	
		Native	COX	Native	COX
Individual Pixels		547411	546796	554041	553518
Common Pixels		546345 (99.81%)		553096 (99.83%)	
Correlation	Mean	0.9997±0.0007		0.9997±0.0008	
	Max	1.0000		1.0000	
	Min	0.8134		0.7238	
Total Column Differences	Mean (10^{19} mol/cm^2)	0.0042±0.0034		0.0042±0.0034	
	Max (10^{19} mol/cm^2)	0.2319		0.2785	
	Min (10^{19} mol/cm^2)	-0.0749		-0.2298	
Total Column Relative Differences	Mean (%)	2.4227±1.3629		2.4106±1.3763	
	Max (%)	48.5343		56.5865	
	Min (%)	-22.2263		-27.1136	

15/02/2023:

		IASI-b		IASI-c	
		Native	COX	Native	COX
Individual Pixels		572981	574181	561253	563731
Common Pixels		570268 (99.32%)		557662 (98.92%)	
Correlation	Mean	0.9997±0.0008		0.9997±0.0006	
	Max	1.0000		1.0000	
	Min	0.7819		0.8514	
Total Column Differences	Mean (10^{19} mol/cm^2)	0.0043±0.0054		0.0043±0.0049	
	Max (10^{19} mol/cm^2)	0.8987		0.7184	
	Min (10^{19} mol/cm^2)	-0.1833		-0.3288	
Total Column Relative Differences	Mean (%)	2.3938±1.4062		2.4090±1.3673	
	Max (%)	59.0870		70.2567	
	Min (%)	-54.5107		-48.9163	

15/03/2023:

		IASI-b		IASI-c	
		Native	COX	Native	COX
Individual Pixels		605369	604836	602750	602329
Common Pixels		604373 (99.84%)		601864 (99.85%)	
Correlation	Mean	0.9997±0.0007		0.9997±0.0005	
	Max	1.0000		1.0000	
	Min	0.7570		0.9604	
Total Column Differences	Mean (10^{19} mol/cm^2)	0.0049±0.0049		0.0048±0.0039	
	Max (10^{19} mol/cm^2)	2.2537		0.6008	
	Min (10^{19} mol/cm^2)	-0.5402		-0.3811	
Total Column Relative Differences	Mean (%)	2.5631±1.3222		2.5422±1.2947	
	Max (%)	60.4023		60.8980	
	Min (%)	-50.6837		-18.4569	

15/04/2023:

		IASI-b		IASI-c	
		Native	COX	Native	COX
Individual Pixels		592951	592082	590165	589493
Common Pixels		591543 (99.76%)		588973 (99.80%)	
Correlation	Mean	0.9996±0.0010		0.9996±0.0011	
	Max	1.0000		1.0000	
	Min	0.7366		0.6218	
Total Column Differences	Mean (10^{19} mol/cm^2)	0.0050±0.0068		0.0051±0.0058	
	Max (10^{19} mol/cm^2)	1.1896		2.0584	
	Min (10^{19} mol/cm^2)	-3.6716		-1.1518	
Total Column Relative Differences	Mean (%)	2.6234±1.3594		2.6430±1.3453	
	Max (%)	81.1373		82.0749	
	Min (%)	-95.6076		-66.6633	

15/05/2023:

		IASI-b		IASI-c	
		Native	COX	Native	COX
Individual Pixels		550867	549757	553114	551974
Common Pixels		549298 (99.72%)		551469 (99.70%)	
Correlation	Mean	0.9996±0.0017		0.9996±0.0016	
	Max	1.0000		1.0000	
	Min	0.4305		0.6077	
Total Column Differences	Mean (10^{19} mol/cm^2)	0.0052±0.0059		0.0050±0.0059	
	Max (10^{19} mol/cm^2)	1.0805		0.8845	
	Min (10^{19} mol/cm^2)	-1.4224		-1.7220	
Total Column Relative Differences	Mean (%)	2.7074±1.5125		2.6891±1.6746	
	Max (%)	74.2631		53.2355	
	Min (%)	-450.0795		-489.1307	

15/06/2023:

		IASI-b		IASI-c	
		Native	COX	Native	COX
Individual Pixels		583361	583455	488254	487477
Common Pixels		580649 (99.52%)		487056 (99.75%)	
Correlation	Mean	0.9995±0.0016		0.9996±0.0014	
	Max	1.0000		1.0000	
	Min	0.8359		0.4912	
Total Column Differences	Mean (10^{19} mol/cm^2)	0.0050±0.0048		0.0049±0.0043	
	Max (10^{19} mol/cm^2)	1.4597		0.2716	
	Min (10^{19} mol/cm^2)	-0.7987		-1.2471	
Total Column Relative Differences	Mean (%)	2.7131±1.3437		2.6510±1.5489	
	Max (%)	76.0878		40.1949	
	Min (%)	-84.6415		-565.7994	

Figure 7.25 – Figure 7.30 show the correlation plots for total column between COX data and FORLI-CO for each platform. No critical deviation was found for these dates.
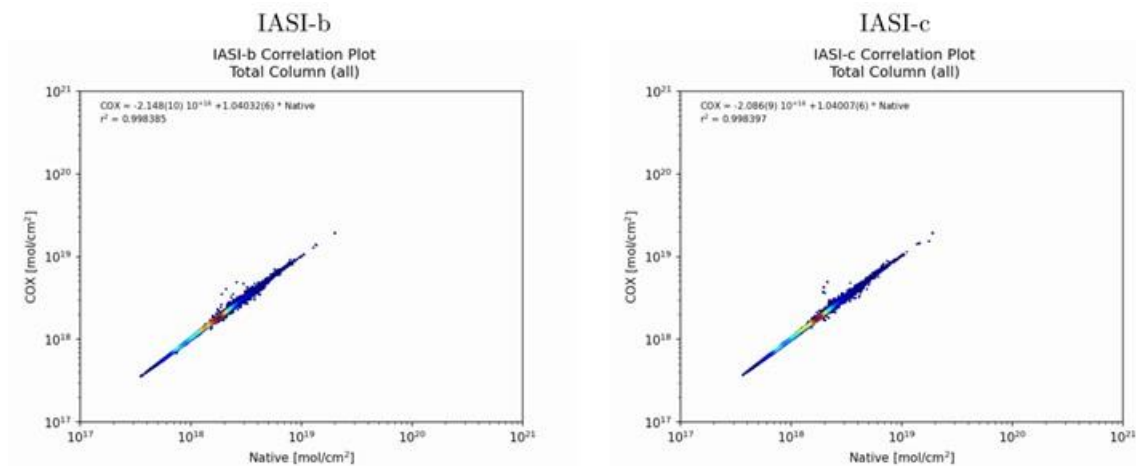
Figure 7.25. Correlation plots for total column between COX data and FORLI-CO for each platform for 15/01/2023. X-axis corresponds to native data (mol/cm^2) and Y-axis corresponds to COX data (mol/cm^2).
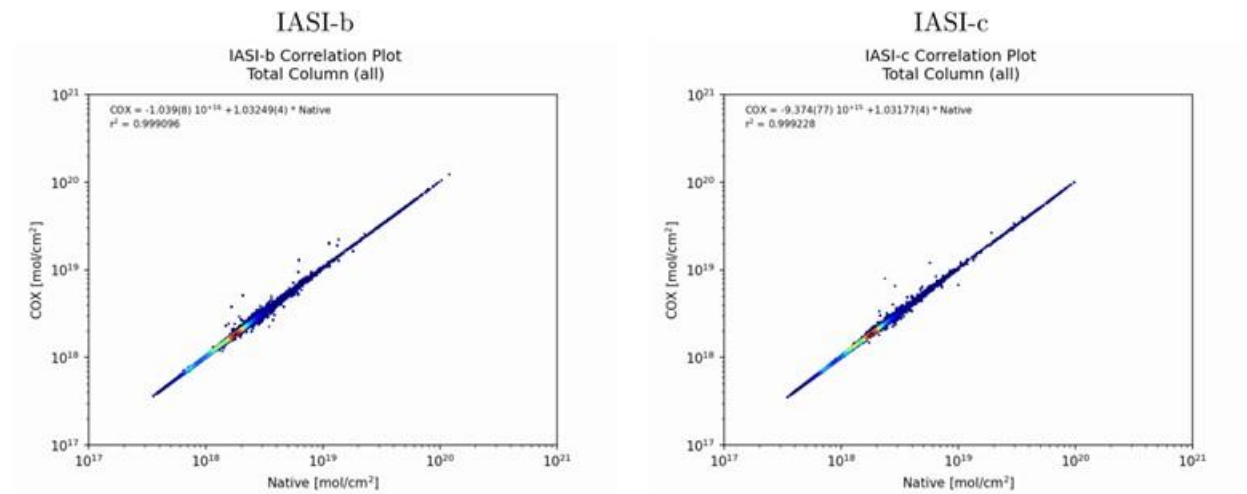
Figure 7.26. Same as Figure 7.25 but for 15/02/2023.
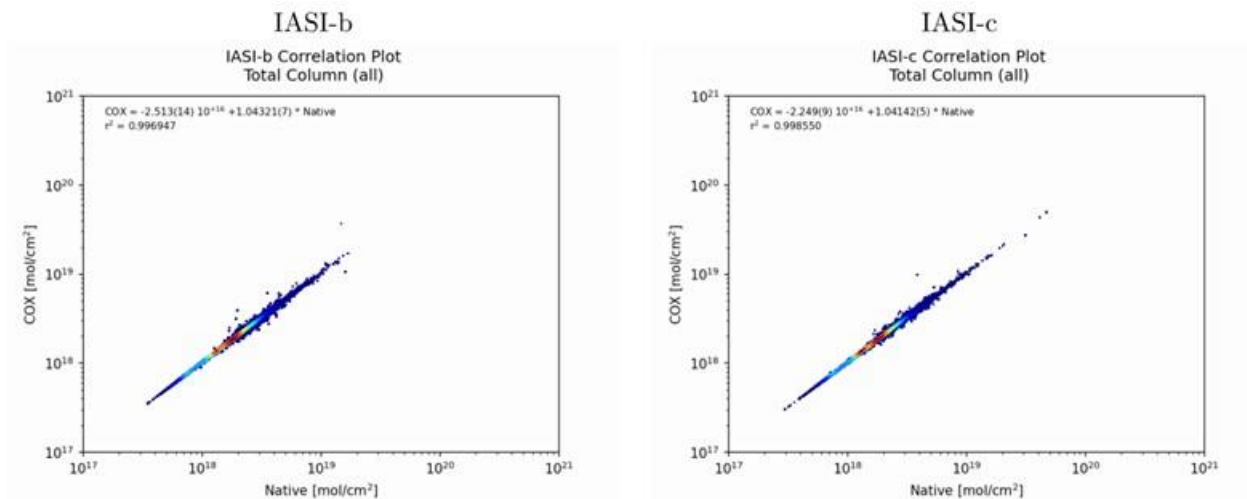
Figure 7.27. Same as Figure 7.25 but for 15/03/2023.
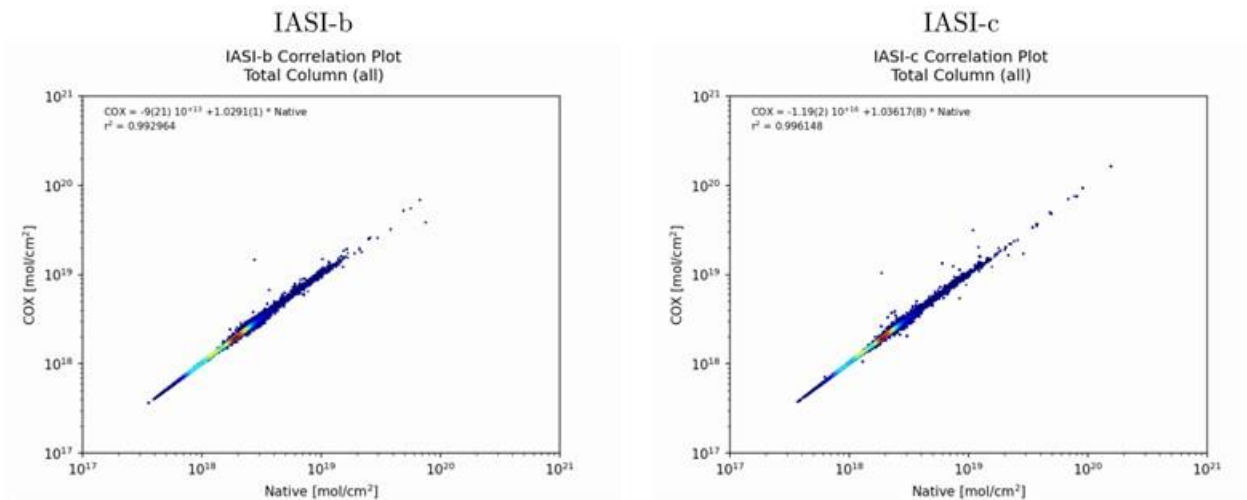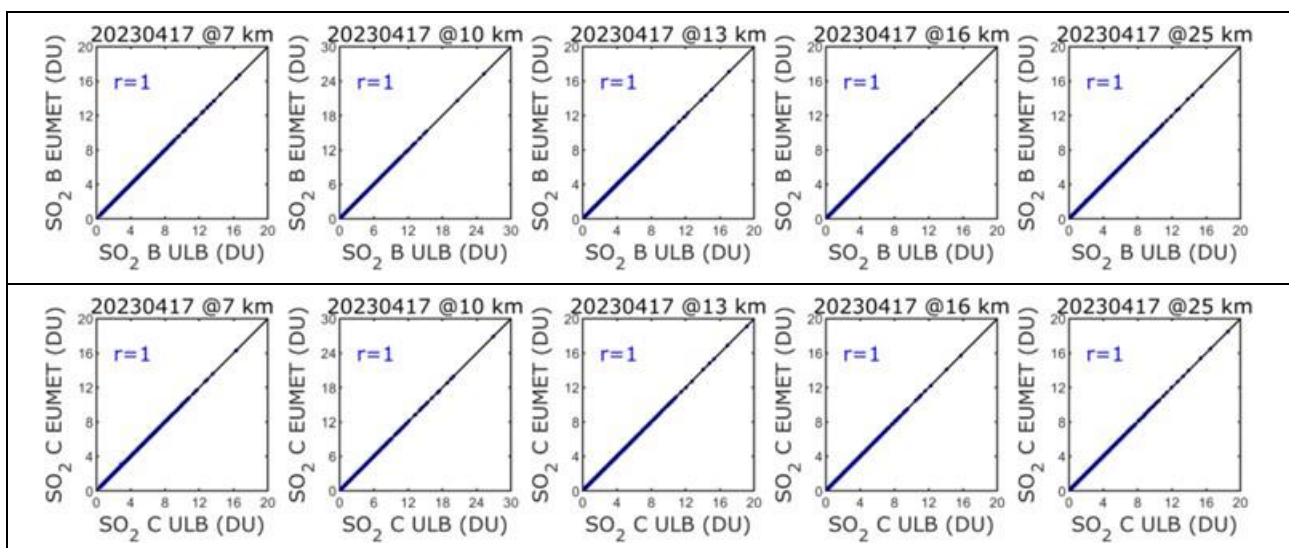
Figure 7.28. Same as Figure 7.25 but for 15/04/2023.
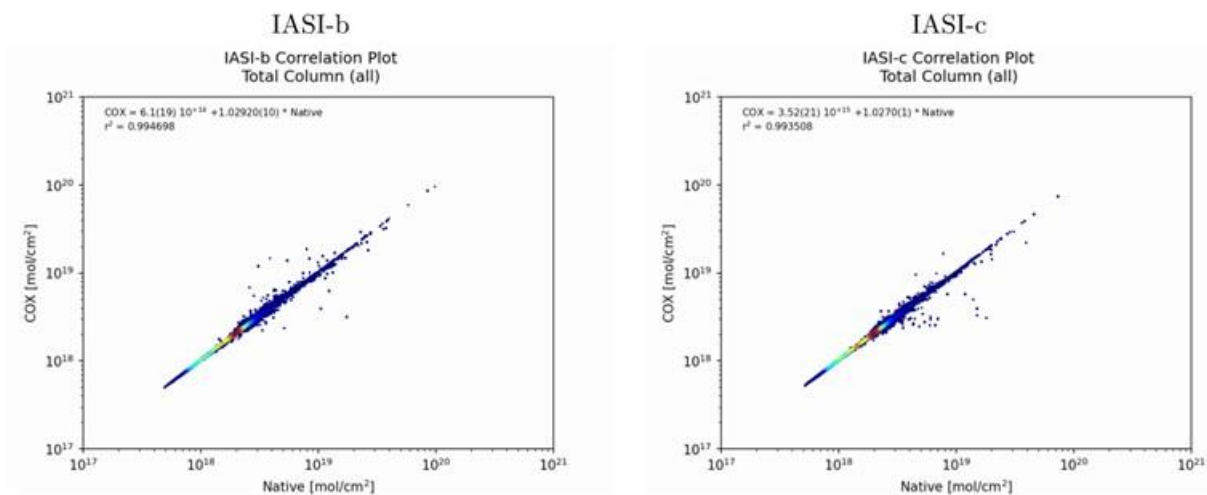
Figure 7.29. Same as Figure 7.25 but for 15/05/2023.
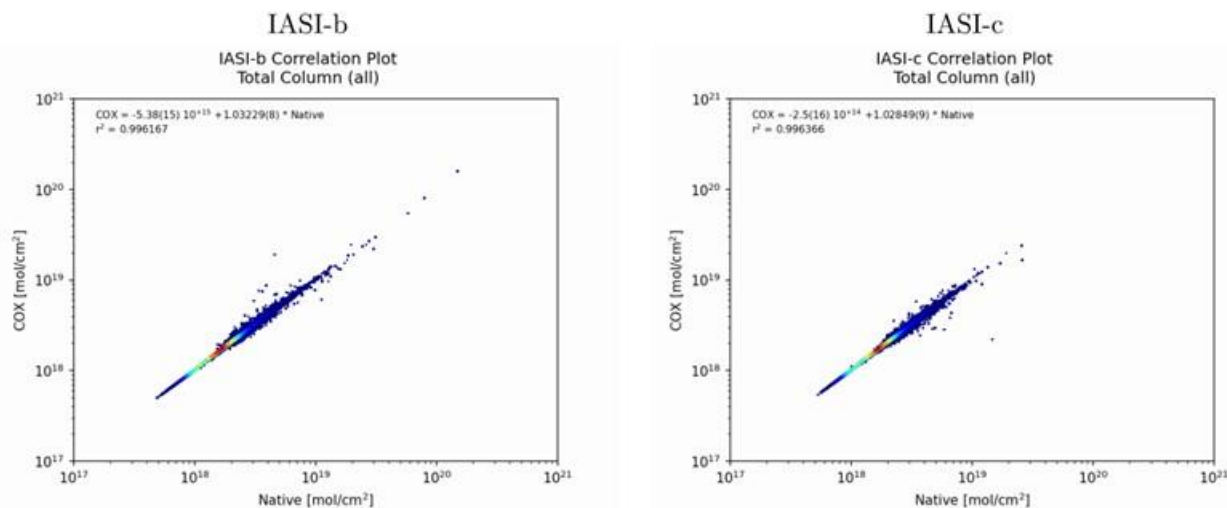

Figure 7.30. Same as Figure 7.25 but for 15/06/2023.

Note that a frequency distribution of the correlation coefficients (separated for each platform) will be provided when EUMETSAT will update the IASI CO retrieval algorithm at the EUMETSAT facilities. (In response to Action 3 (OR-9)).

IASI SO2:

The IASI BRESCIA SO2 retrieval algorithm has been implemented in the PPF v6.3 at EUMETSAT (operational release on 18/04/2018). Here we compare the EUMETSAT product disseminated by EUMETCast in BUFR format (SO2 EUMET) with the native product produced at ULB (SO2 ULB) for five days between April and May 2023, for Metop-B and Metop-C. We choose to study 14/04/2023, 17/04/2023, 21/04/2023, 24/05/2023 and 25/05/2023 (no volcanic eruptions occurred during the other months of the January-June 2023 period).

Online quality monitoring for SO2 for five estimated altitudes:

For each of the five days, scatterplots for the different estimated altitudes (7, 10, 13, 16 and 25 km) are presented (Figure 7.31 – Figure 7.35). The data have been filtered following the recommendations of the Product User Manual (Section 5.2.2, i.e. we kept the pixels in the

neighbourhood (± 10 degrees) of SO2_BT_DIFFERENCE > 1K pixels, and did not use the pixels with a SO2_BT_DIFFERENCE < 0.4K.

We recall here that when the IASI L2 pressure and temperature profiles are not available, ECMWF forecasts (3h, interpolated in time and space) data are used in the EUMETSAT API. These pixels are flagged with SO2_QFLAG = 11 and are not part of the comparison.

Correlation coefficients (in blue) are ~1.

So far, the discrepancies are found within the numerical errors inherent to the use of different IT infrastructure.
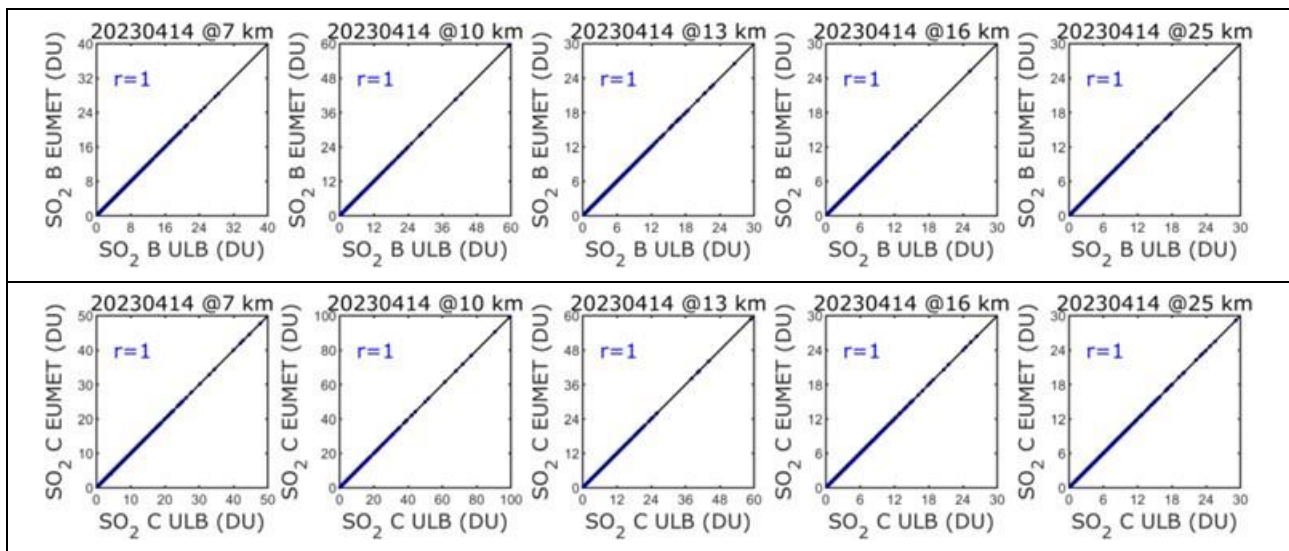
Figure 7.31. Scatterplots for Metop-B (top) and Metop-C (bottom): SO2 EUMET versus SO2 ULB for 14/04/2023, for the five estimated altitudes (7, 10, 13, 16 and 25 km).

Figure 7.32. Same as Figure 7.31 but for 17/04/2023.
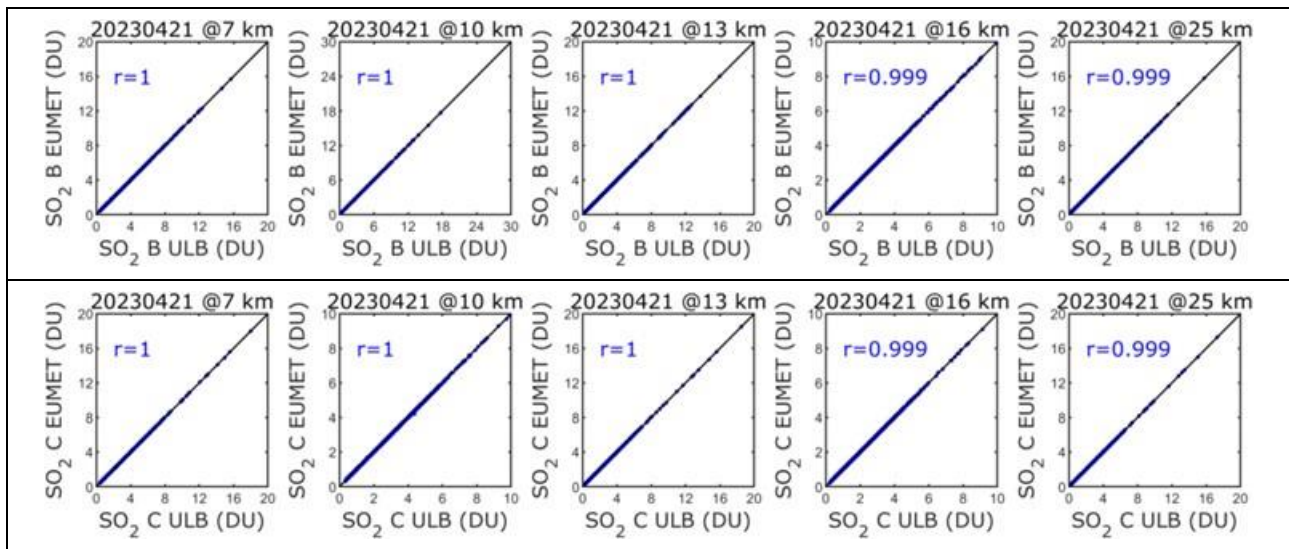
Figure 7.33. Same as Figure 7.31 but for 21/04/2023.
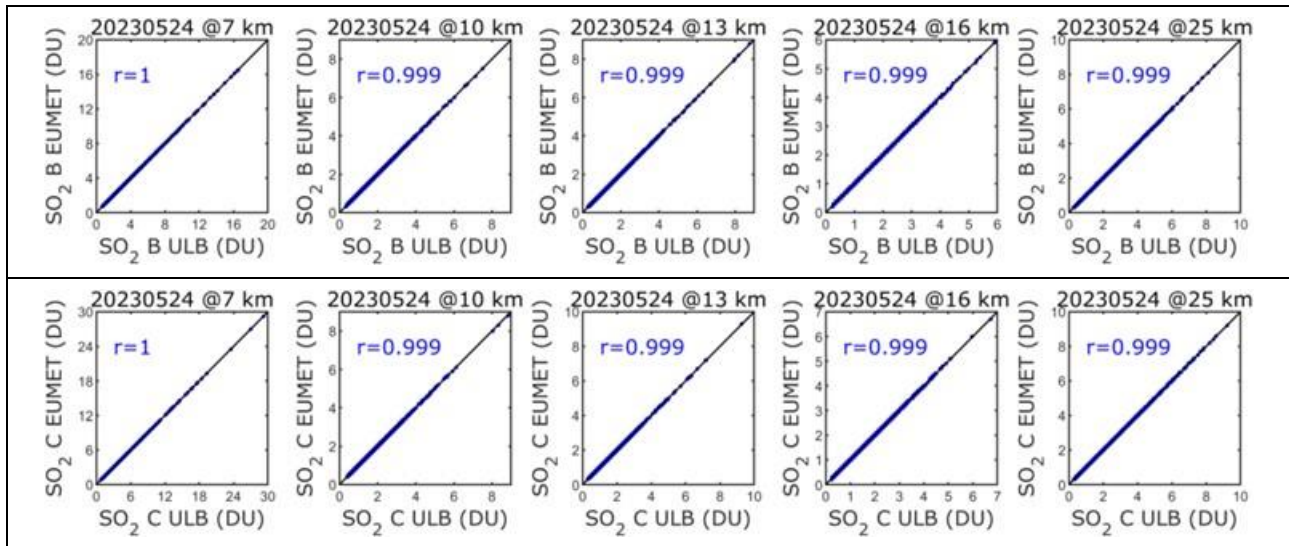
Figure 7.34. Same as Figure 7.31 but for 24/05/2023.
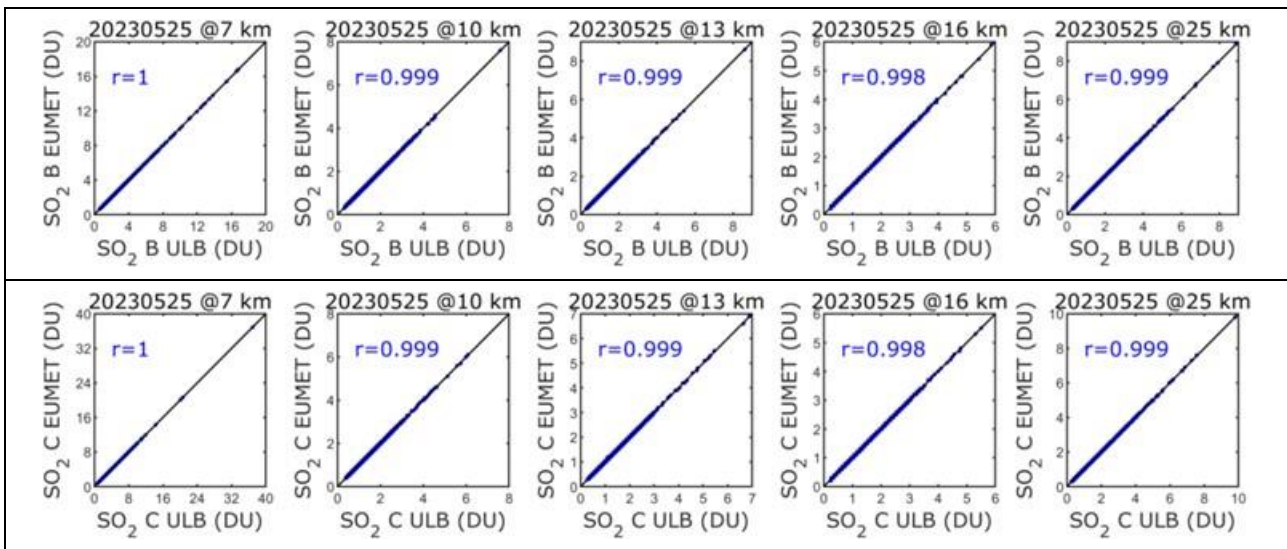
Figure 7.35. Same as Figure 7.31 but for 25/05/2023.

Online quality monitoring for SO2_ALTITUDE and SO2_COL:

Although the two products SO2_ALTITUDE (estimated altitude of the SO_2 plume) and SO2_COL (SO_2 column at the estimated altitude) are operational since May 2021 **the EUMETSAT and the ULB algorithms versions are different,** with the ULB version being the latest version of the algorithm**. As said in the previous report, the EUMETSAT and ULB products are not the same and the comparison shows differences**. We showed one plot as an example in the previous report. Here, we show the scatter plots for five dates (14/04/2023, 17/04/2023, 21/04/2023, 24/05/2023 and 25/05/2023), for Metop-B and C (Figure 7.36 – Figure 7.40) . Daniel Hurtmans provided an updated version of the Brescia algorithm (including the SO_2 altitude) for implementation to EUMETSAT, in order for the two versions to be the same. We are waiting for an update from EUMETSAT.
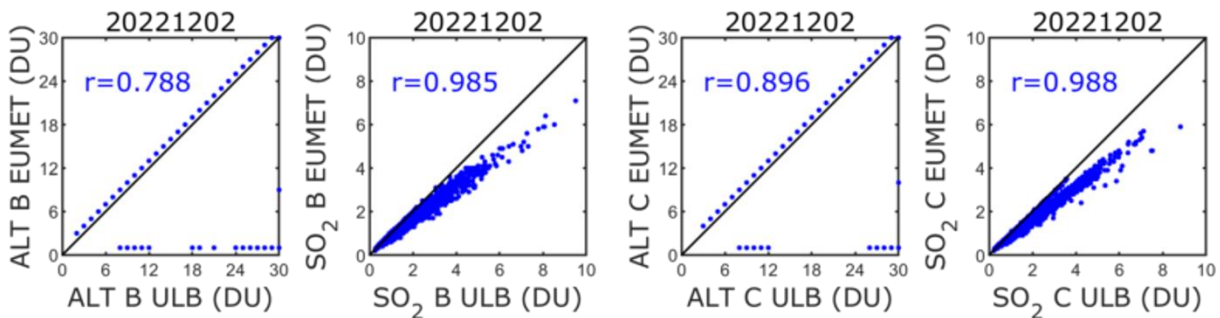

Figure 7.36. Scatterplots for Metop-B and Metop-C : SO2_ALTITUDE EUMET versus SO2_ALTITUDE ULB, as well as SO2_COL EUMET versus SO2_COL ULB, for 14/04/2023.
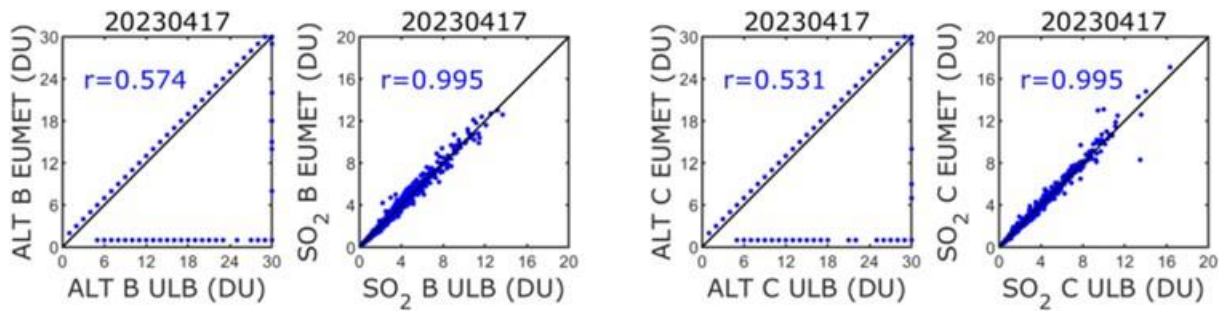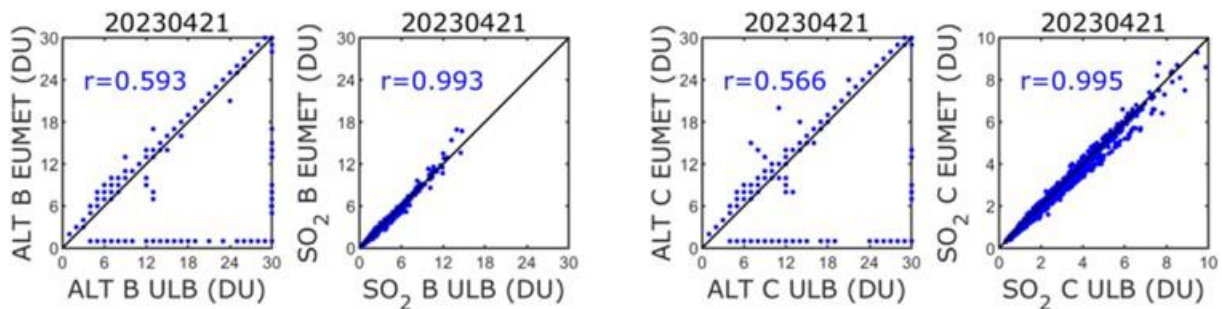
Figure 7.37. Same as Figure 7.36 but for 17/04/2023.
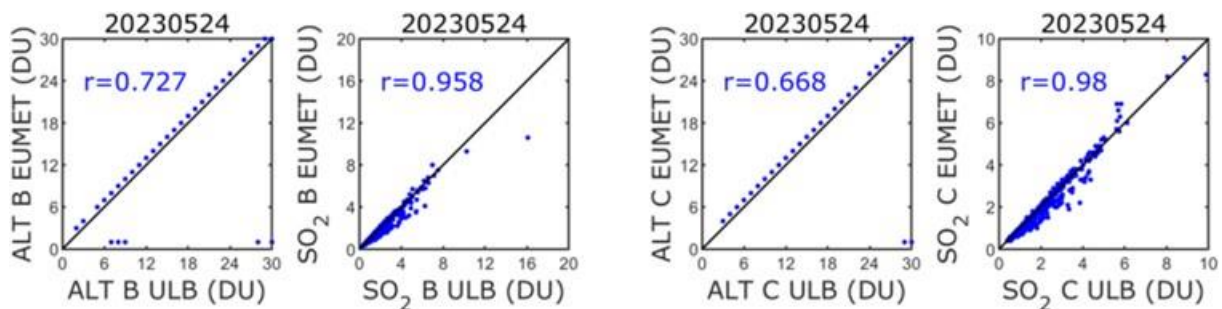

Figure 7.38. Same as Figure 7.36 but for 21/04/2023.

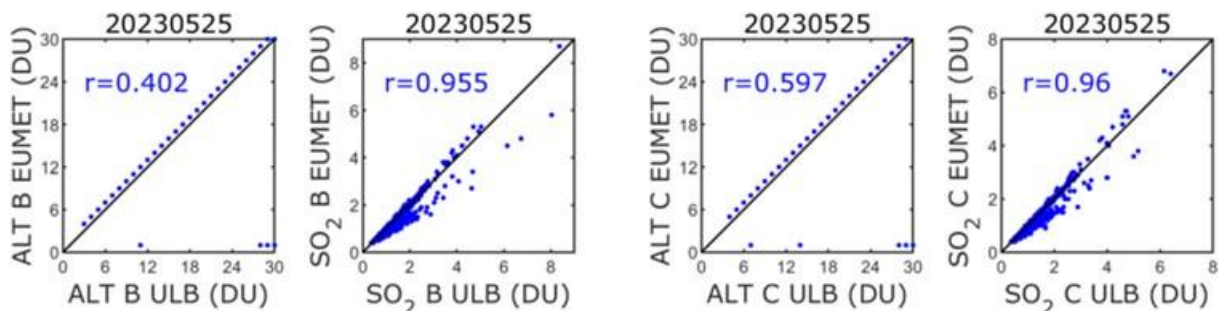**Figure 7.39. Same as Figure 7.36 but for 24/05/2023.**

Figure 7.40. Same as Figure 7.36 but for 25/05/2023.

IASI O3:

The IASI NRT O3 product (v6.5) has been released as operational product on 18 May 2022. Here we present statistical results when comparing the EUMETSAT product disseminated by EUMETCast in BUFR format (OZO) with the native product produced at ULB (FORLI-O3 v20191122) for 6 days representative of six months: January 15th, February 15th, March 15th, April 15th, May 15th and June 15th, 2023, for Metop-B and Metop-C. This allows monitoring if any discrepancy occurs between the two, EUMETSAT and native, products. The data have been filtered

following the recommendations of the Product User Manual. Furthermore, data associated with DOFS>2 have also been filtered out.

O3 total and 0 – 6 km column are investigated. Detailed statistics for total column between OZO data and FORLI-O3 data (v20191122) for each of the six days are presented in Table 7.22. No critical deviation was found for these dates.

The difference between individual pixels in native and BUFR format is due to the fact that the NRT EUMETSAT version is the v2015, and only 1/10 pixels are treated, this means clearly a lower number of observations due to the fact that FORLI is time consuming.

Table 7.22. Statistics for total column between OZO data and FORLI-O3 data for six days: January 15th, February 15th, March 15th, April 15th, May 15th and June 15th, 2023.

15 January 2023	IASI-C		IASI-B	
	Native	BUFR	Native	BUFR
Individual Pixels	404537	99100	398219	99244
Common Pixels	86938 (21.49%)		87173 (21.89%)	
Correlation	0.9993		0.9993	
Mean Total Column Differences (DU)	2.0819±2.1136		2.0866±2.2183	
Mean Total Column Relative Differences (%)	0.7522±0.7041		0.7509±0.7169	

15 February 2023	IASI-C		IASI-B	
	Native	BUFR	Native	BUFR
Individual Pixels	376422	97071	384144	95848
Common Pixels	84694 (22.50%)		84184 (21.91%)	
Correlation	0.9993		0.9993	
Mean Total Column Differences (DU)	1.9658±3.3940		1.9697±3.3438	
Mean Total Column Relative Differences (%)	0.7768±0.8779		0.7672±0.8584	

| 15 March 2023	IASI-C		IASI-B	
	Native	BUFR	Native	BUFR
Individual Pixels	380083	89407	380083	88594
Common Pixels	78528 (20.66%)		78081 (20.54%)	
Correlation	0.9997		0.9998	
Mean Total Column Differences (DU)	2.5589±1.6777		2.5257±1.6456	
Mean Total Column Relative Differences (%)	0.9065±0.5405		0.8926±0.5348	

15 April 2023	IASI-C		IASI-B	
	Native	BUFR	Native	BUFR
Individual Pixels	403306	94928	401594	94796
Common Pixels	83267 (20.65%)		83170 (20.71%)	
Correlation	0.9997		0.9997	
Mean Total Column Differences (DU)	2.7485±1.5886		2.6735±1.5872	
Mean Total Column Relative Differences (%)	0.8887±0.4720		0.8721±0.4766	

15 May 2023	IASI-C		IASI-B	
	Native	BUFR	Native	BUFR
Individual Pixels	377589	92249	375656	94165
Common Pixels	81663 (21.63%)		83251 (22.16%)	
Correlation	0.9997		0.9997	
Mean Total Column Differences (DU)	2.5607±1.3243		2.4803±1.4278	
Mean Total Column Relative Differences (%)	2.5607±1.3243		0.8278±0.4696	

15 June 2023	IASI-C		IASI-B	
	Native	BUFR	Native	BUFR
Individual Pixels	352125	83826	414621	99674
Common Pixels	73671 (20.92%)		87788 (21.17%)	
Correlation	0.9993		0.9992	
Mean Total Column Differences (DU)	2.1763±1.5359		2.1466±1.5939	
Mean Total Column Relative Differences (%)	0.7461±0.5323		0.7372±0.5463	

Figure 7.41 and Figure 7.42 show the correlation plots for total and 0 – 6 km columns, respectively, between OZO data and FORLI-O3 for each platform. Correlation coefficients (in blue) are ~1.

So far, the discrepancies are found within the numerical errors inherent to the use of different IT infrastructure.
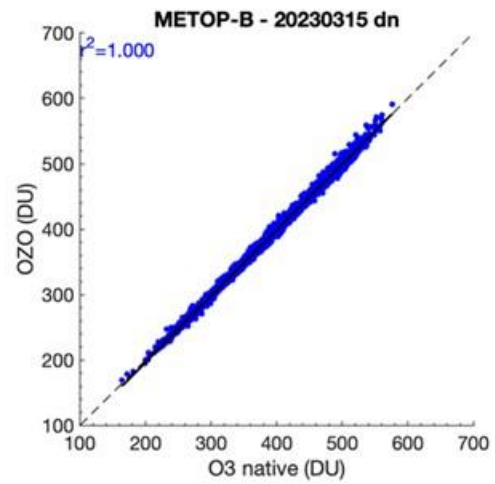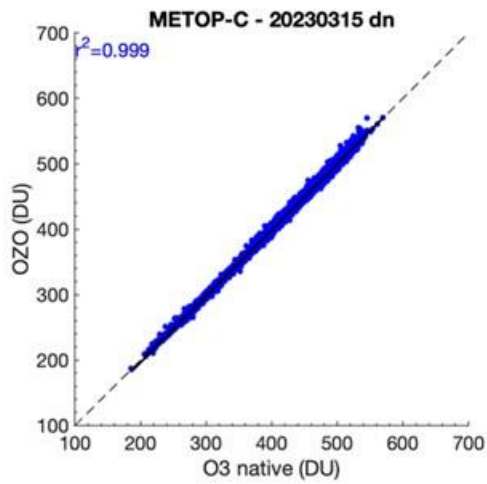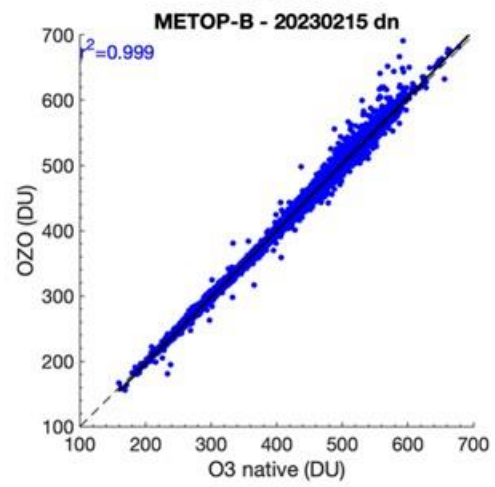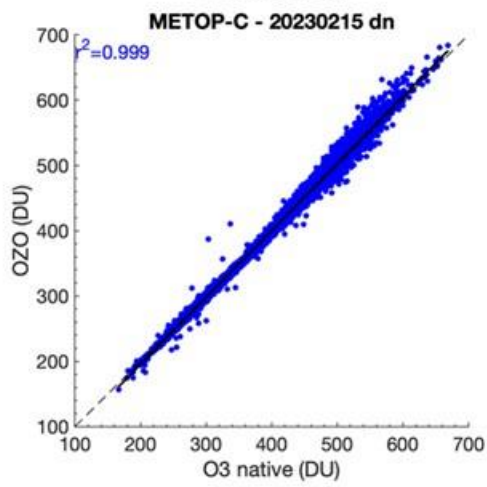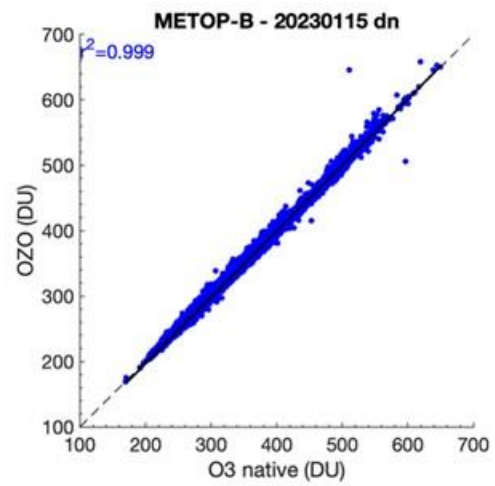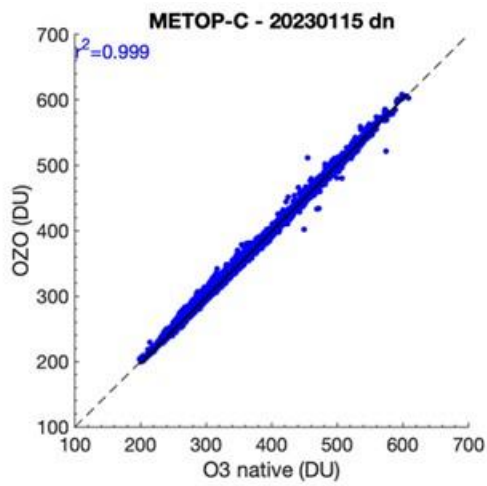
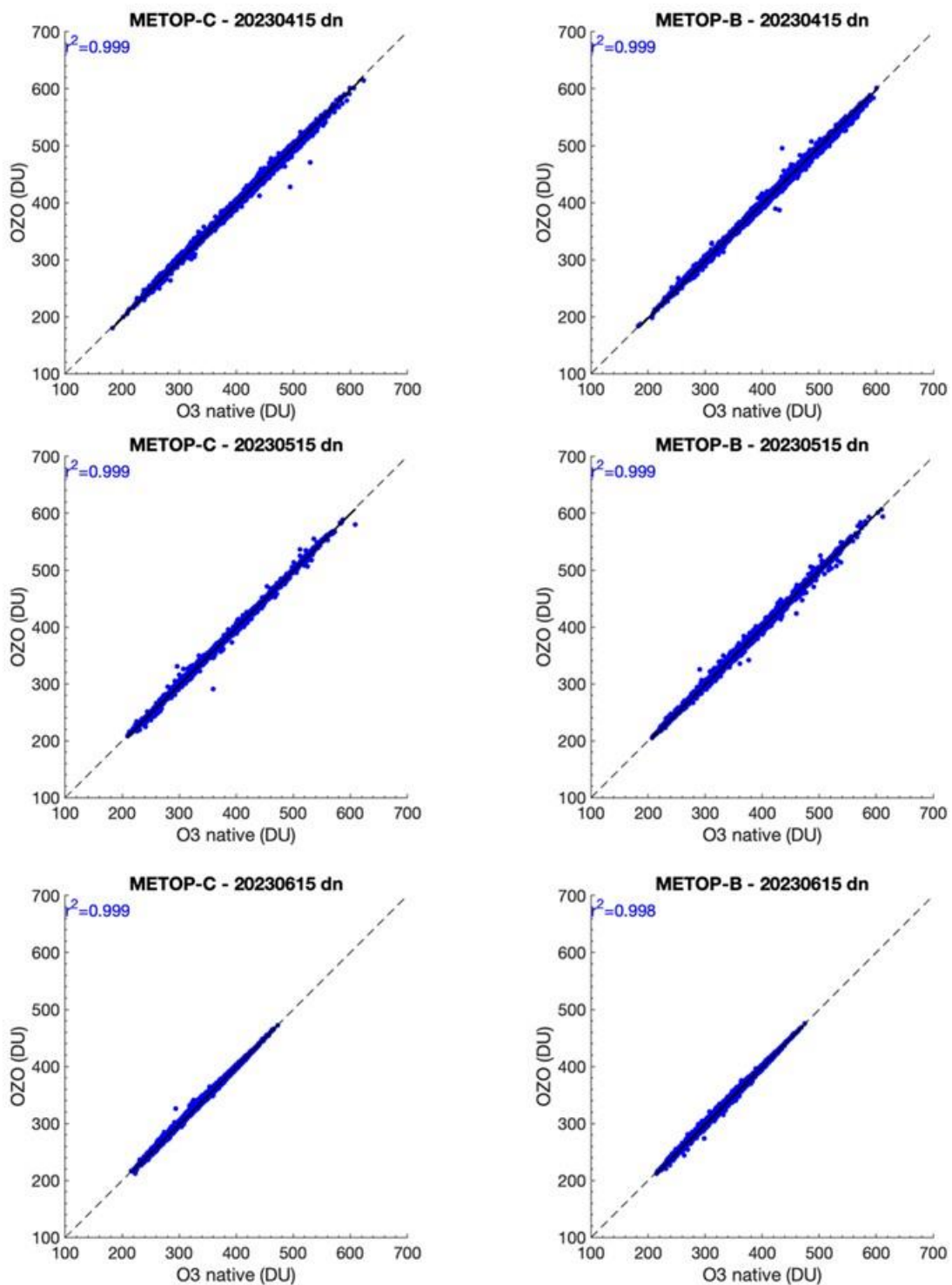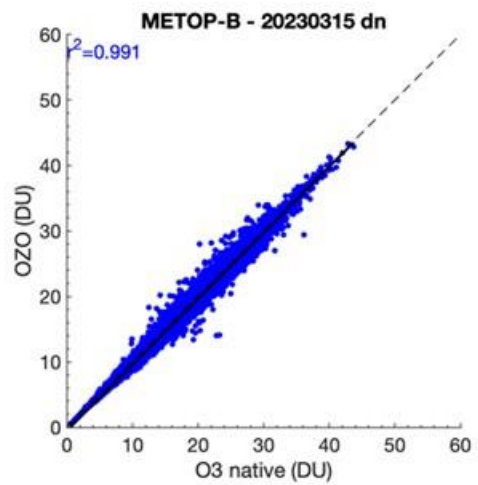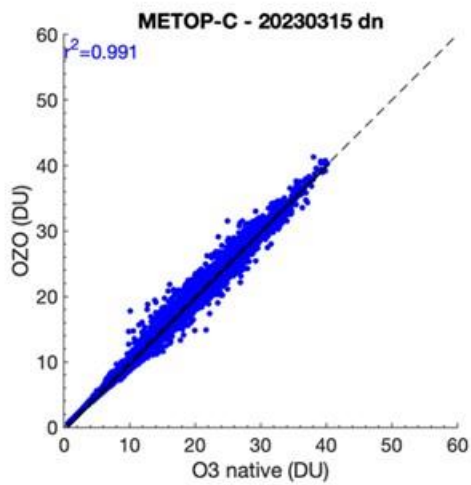**Figure 7.41. Correlation plots for total column between OZO and FORLI-O3 data for each platform for six days: January 15th, February 15th, March 15th, April 15th, May 15th and June 15th, 2023. X-axis corresponds to Native data (DU) and Y-axis corresponds to OZO data (DU).**
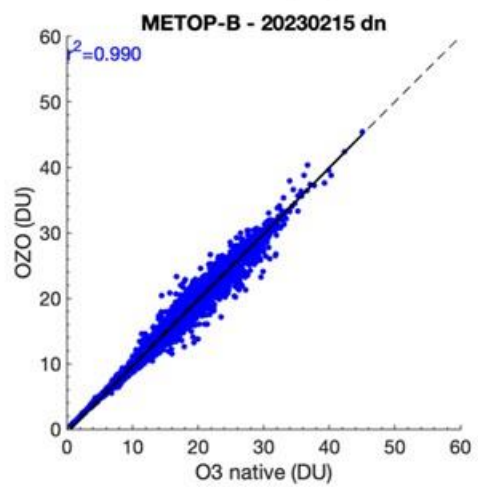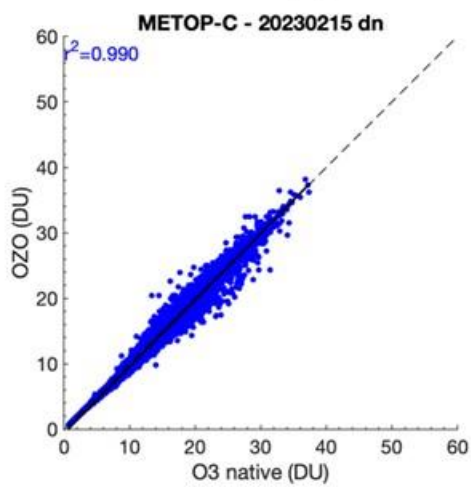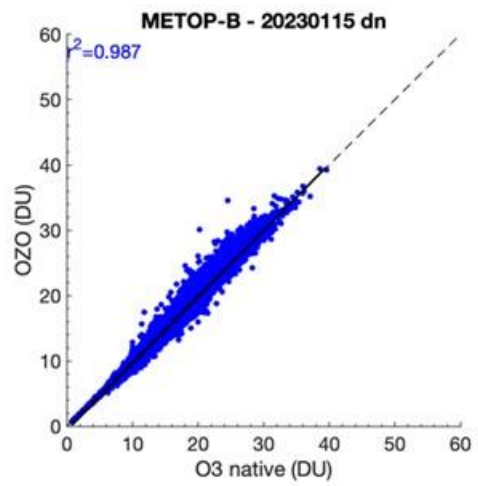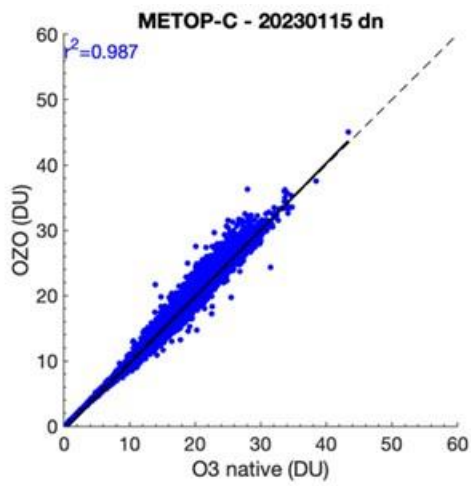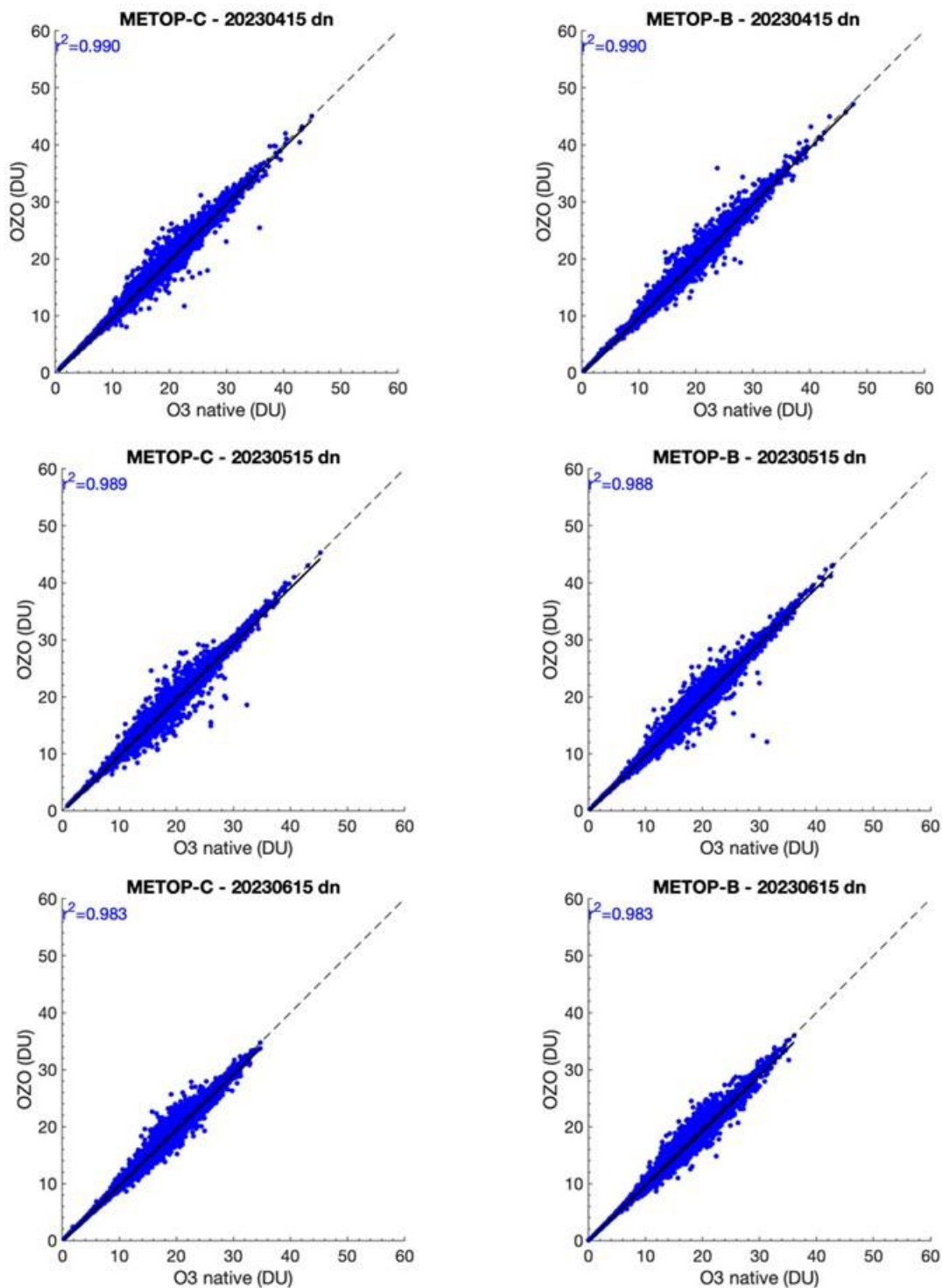
Figure 7.42. Correlation plots for 0-6km column between OZO and FORLI-O3 data for each platform for six days: January 15th, February 15th, March 15th, April 15th, May 15th and June 15th, 2023. X-axis corresponds to Native data (DU) and Y-axis corresponds to OZO data (DU).

IASI HNO3:

The IASI NRT HNO3 product (v6.5) has been released as operational product on 18 May 2022. Here we present statistical results when comparing the EUMETSAT product disseminated by EUMETCast in BUFR format (NAC) with the native product produced at ULB (FORLI-HNO3

v20191122) for six days representative of six months: January 15th, February 15th, March 15th, April 15th, May 15th and June 15th, 2023, for Metop-B and Metop-C. This allows monitoring if any discrepancy occurs between the two, EUMETSAT and native, products. The data have been filtered following the recommendations of the Product User Manual.

HNO3 total column is investigated. Detailed statistics for total column between NAC data and FORLI-HNO3 data (v20191122) for each of the six days are presented in Table 7.23. No critical deviation was found for these dates.

Table 7.23. Statistics for total column between NAC data and FORLI-HNO3 data for 6 days: July 15th, August 15th, September 15th, October 15th, November 15th and December 15th, 2022.

15 January 2023	IASI-C		IASI-B	
	Native	BUFR	Native	BUFR
Individual Pixels	274293	65068	268455	64214
Common Pixels	57325 (20.90%)		56519 (21.05%)	
Correlation	0.9998		0.9998	
Mean Total Column Differences (x10^{16} molec cm^{-2})	0.0053±0.0182		0.0053±0.0202	
Mean Total Column Relative Differences (%)	0.7247±1.3522		0.7207±1.4177	

15 February 2023	IASI-C		IASI-B	
	Native	BUFR	Native	BUFR
Individual Pixels	255172	61864	261817	61607
Common Pixels	53097 (20.81%)		52994 (20.24%)	
Correlation	0.9998		0.9998	
Mean Total Column Differences (x10^{16} molec cm^{-2})	0.0078±0.0158		0.0079±0.0177	
Mean Total Column Relative Differences (%)	0.8904±1.3586		0.8781±1.3822	

15 March 2023	IASI-C		IASI-B	
	Native	BUFR	Native	BUFR
Individual Pixels	328273	63857	328337	62523
Common Pixels	57458 (17.50%)		56358 (17.16%)	
Correlation	0.9998		0.9998	
Mean Total Column Differences (x10^{16} molec cm^{-2})	0.0062±0.0178		0.0066±0.0184	
Mean Total Column Relative Differences (%)	0.8026±1.3457		0.8207±1.3730	

15 April 2023	IASI-C		IASI-B	
	Native	BUFR	Native	BUFR
Individual Pixels	329198	65233	326602	64555
Common Pixels	58932 (17.90%)		58159 (17.81%)	
Correlation	0.9998		0.9998	
Mean Total Column Differences ($\times 10^{16}$ molec cm^{-2})	0.0066 ± 0.0172		0.0075 ± 0.0182	
Mean Total Column Relative Differences (%)	0.7277 ± 1.3431		0.7593 ± 1.3373	

15 May 2023	IASI-C		IASI-B	
	Native	BUFR	Native	BUFR
Individual Pixels	298269	67279	292685	68260
Common Pixels	60788 (20.38%)		61584 (21.04%)	
Correlation	0.9998		0.9998	
Mean Total Column Differences ($\times 10^{16}$ molec cm^{-2})	0.0062 ± 0.0173		0.0070 ± 0.0177	
Mean Total Column Relative Differences (%)	0.6470 ± 1.2648		0.6833 ± 1.2979	

15 June 2023	IASI-C		IASI-B	
	Native	BUFR	Native	BUFR
Individual Pixels	289851	64415	342076	76309
Common Pixels	57994 (20.01%)		68881 (20.14%)	
Correlation	0.9920		0.9996	
Mean Total Column Differences ($\times 10^{16}$ molec cm^{-2})	0.0058 ± 0.1125		0.0074 ± 0.0273	
Mean Total Column Relative Differences (%)	0.5085 ± 7.5012		0.6396 ± 1.6570	

Figure 7.43 shows the correlation plots for total column, respectively, between NAC data and FORLI-HNO3 for each platform. Correlation coefficients (in blue) are ~1.

So far, the discrepancies are found within the numerical errors inherent to the use of different IT infrastructure.
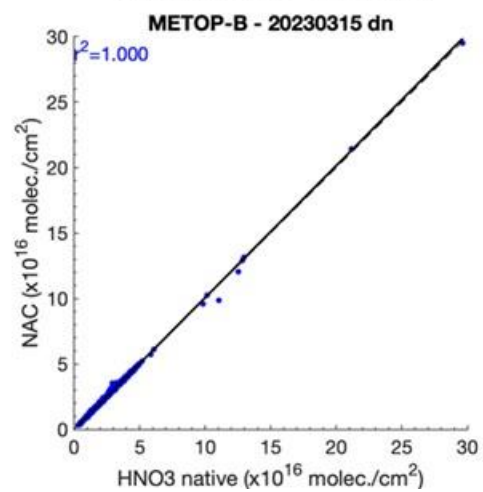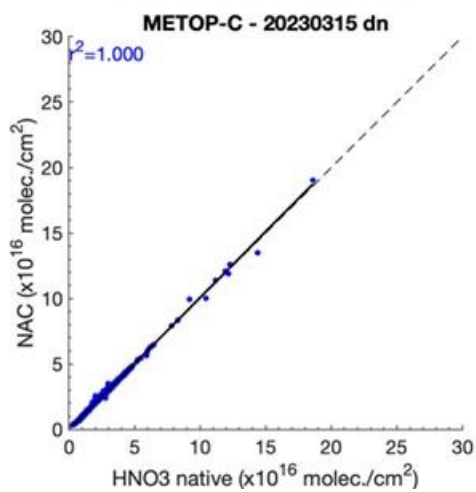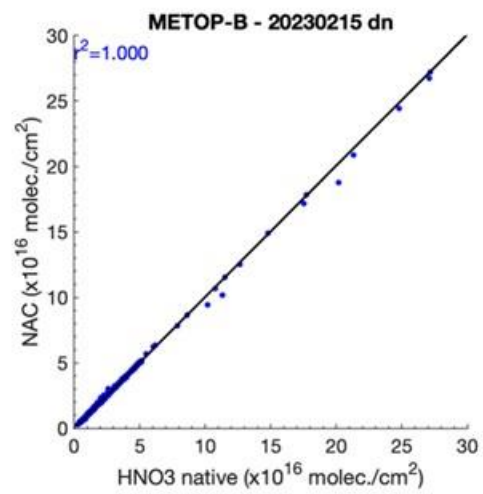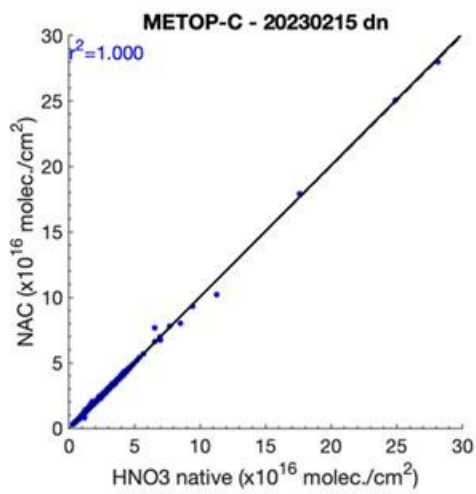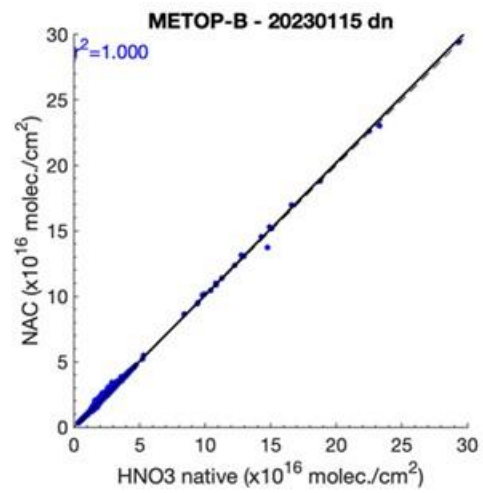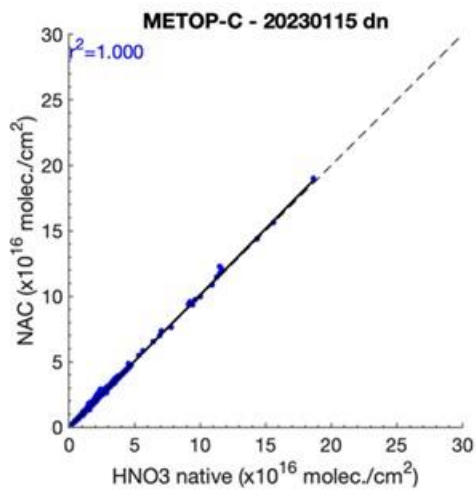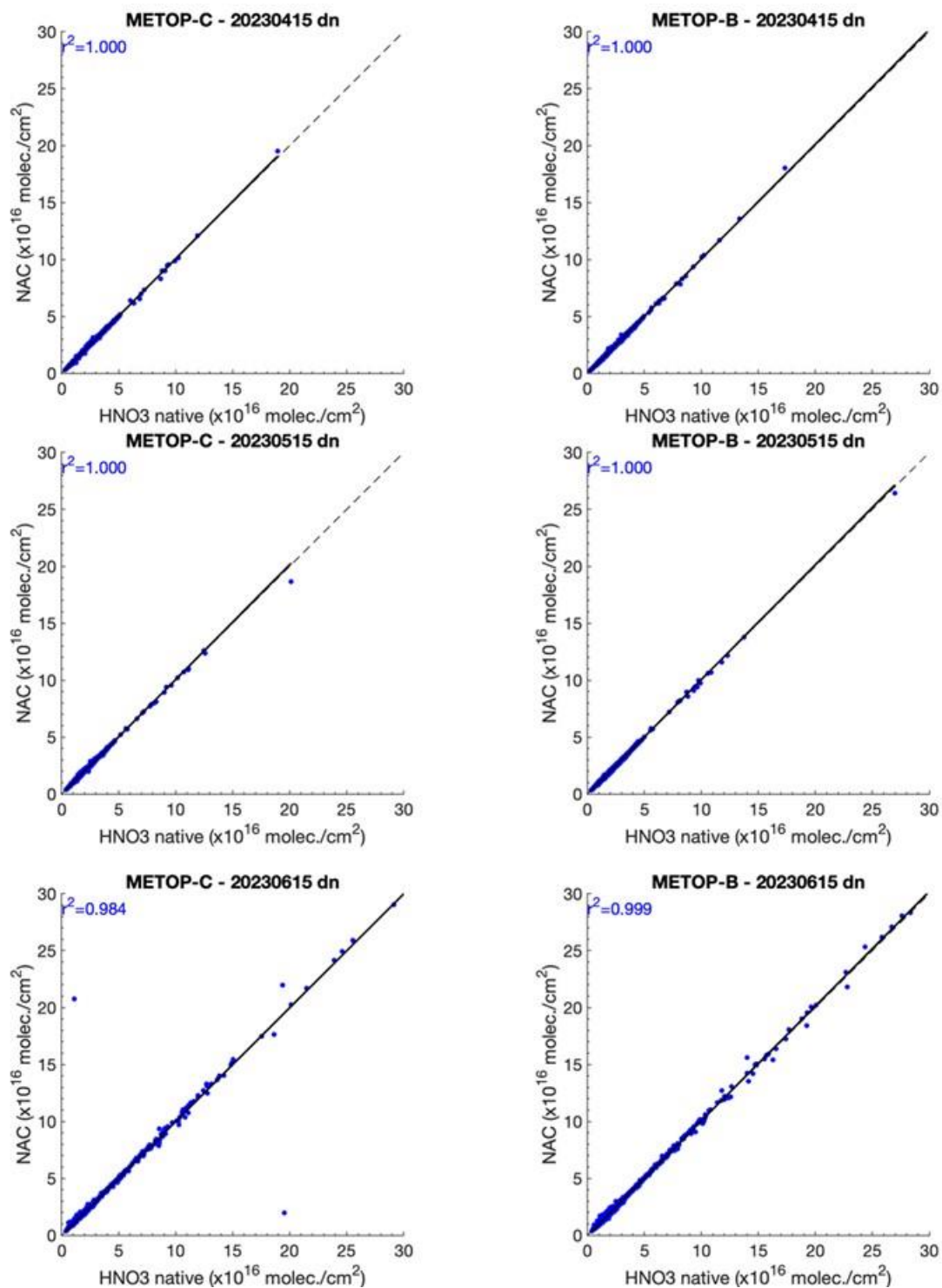
Figure 7.43. Correlation plots for total column between NAC and FORLI-HNO3 data for each platform for six days: January 15th, February 15th, March 15th, April 15th, May 15th and June 15th, 2023. X-axis corresponds to Native data (molec./cm²) and Y-axis corresponds to NAC data (molec./cm²).

Validation with CO FTIR ground-based data

This section presents the work of Bavo Langerock (BIRA-IASB) that compared the Metop-A/B/C IASI CO data against FTIR measurement data available from the NDACC (Network for the

Detection of Atmospheric Composition Change). The Copernicus Atmosphere Monitoring Service (CAMS) projects supports selected NDACC instruments and Pis for rapid delivery of quality measurements to the NDACC data host (contract CAMS27). Recent FTIR measurement data is now available for many more sites (in this study data from 23 sites is used).

These ground-based, remote-sensing instruments are sensitive to the CO abundance in the troposphere and lower stratosphere, i.e. between the surface and up to 20 km altitude. CO total columns are validated (from surface to 100 km). A description of the FTIR instruments and retrieval methodology can be found at https://nors.aeronomie.be. The typical uncertainty on the FTIR CO column is approximately 3 %, which is also used in the color scale in Figure 7.45.

In this comparison each FTIR measurement is co-located to all IASI measurements within a time difference of 3 hours and within a distance of 50 km to the effective location of the FTIR measurement (this effective location is calculated along the line of sight of the FTIR measurement). The IASI *a priori* is substituted in the FTIR retrieval and subsequently the FTIR retrieved profile with the IASI *a priori* is smoothed using the IASI averaging kernel, as described in Rodgers *et al.*, 2003. In the plots the relative differences are calculated using the latter FTIR columns (smoothed with the IASI averaging kernels). This validation methodology is described in more detail in Ronsmans *et al.*, 2016. All figures for the individual stations can be browsed on https://cdop.aeronomie.be.

Table 7.24. Statistics between IASI-B/C and FTIR CO smoothed total columns for the entire time period January 2017 – June 2023 (the column "std" is the standard deviation of the local FTIR columns relative to the standard deviation of the IASI columns)

	Metop-B					Metop-C				
	# meas.	Std.	R	rel. Diff.	Std. Rel. Diff.	# meas.	Std.	R	rel. Diff.	Std. Rel. Diff.
Eureka	928	0.7	0.87	18.2	16.3	0	-	-	-	-
Ny Ålesund	182	1.2	0.91	20.2	8.39	130	1.1	0.91	20.3	8.42
Thule	6083	0.8	0.84	5.33	11.3	3205	0.8	0.84	7.08	11.2
Kiruna	1176	1.1	0.82	-2.96	7.37	720	1.1	0.83	-2.61	6.96
Harestua	217	1.1	0.84	8.47	7.02	3	-	-	13.9	0.11
St. Petersburg	1155	0.9	0.87	8.13	6.97	485	0.9	0.84	9.32	6.41
Bremen	473	0.9	0.87	8.03	7.05	211	0.9	0.82	7.56	7.60
Garmisch	3028	0.9	0.86	2.35	7.44	1386	0.9	0.89	2.23	6.87
Zugspitze	3815	0.9	0.9	-1.16	6.44	2119	0.9	0.91	-1.36	6.10
Jungraujoch	1169	0.9	0.95	0.04	4.64	852	0.9	0.94	-0.40	4.74
Toronto	1666	0.7	0.79	22.2	14.6	1125	0.7	0.85	22.7	13.1
Rikubetsu	85	0.9	0.87	5.01	7.13	49	1.0	0.82	1.43	7.11
Boulder	4438	0.9	0.87	-1.56	8.00	3804	0.8	0.85	-1.35	9.85
Tsukuba	363	0.8	0.84	7.50	9.62	187	0.9	0.92	4.24	5.98
Izana	1137	1.0	0.95	-0.47	4.21	573	0.9	0.96	0.80	4.41
Mauna Loa	1526	1.1	0.99	-0.80	2.81	632	1.1	0.99	-0.71	2.76
Altzomoni	1579	1.1	0.96	4.38	4.30	1027	1.1	0.96	4.17	4.53
Paramaribo	119	0.9	0.92	9.00	4.57	0	-	-	-	-
Porto Velho	278	0.9	0.98	9.82	6.64	35	0.8	0.83	7.89	5.91
La Reunion Maido	2542	1.0	0.99	4.97	3.30	706	1.0	0.98	5.39	4.09
Wollongong	2386	0.8	0.93	7.08	7.51	1511	0.8	0.93	6.37	7.41

Lauder	3220	0.9	0.96	9.32	5.88	2142	0.9	0.96	8.97	5.67
Arrival Heights	514	0.9	0.95	16.7	7.50	382	0.9	0.93	16.0	7.77
Average for all sites		0.9	0.90	6.95	7.35		0.9	0.90	5.90	6.84

The correlation coefficients of the Taylor diagrams (Figure 7.44 and Table 7.24) are generally ranging from ~0.8 to nearly 1, showing a very good agreement between the IASI and FTIR data, for Metop-B and Metop-C. However, some sites are special:

1. Rikubetsu, Ny Ålesund and Harestua have only a few co-located measurements and are statistically less relevant

2. Toronto has a low correlation although the site has many co-locations. This may be due to some co-locations where the IASI concentration is much higher than observed by the FTIR and probably related to false co-locations during fire events. The FTIR time-series seems to suffer from outliers being too low.

3. At Kiruna, Thule and Eureka the satellite underestimates the CO columns by up to 30 % during the early spring weeks and is related to a reduced sensitivity of the IASI CO product during local spring.

The Taylor diagrams in Figure 7.44 and statistics in Table 7.24 also show that the standard deviations of the FTIR columns values are smaller compared the satellite standard deviation probably due to higher noise on the satellite time-series. Almost all site points are shifted left of the satellite reference, typically with a factor of 0.8 to 1 of the standard deviation of the satellite CO columns.

Figure 7.45 shows the time-series of bi-weekly mean relative differences for the time period January 2017 – June 2023. Red indicates a positive bias (IASI > NDACC) while blue indicates an underestimation of the satellite retrievals. The chosen color scale is based on the FTIR typical uncertainty. The IASI retrieval uncertainty should be added (typically around 4 %), so only biases above 5 % are to be considered significant. In the Northern Hemisphere a seasonal changing bias is observed: overestimation during summer and underestimation during winter months. A similar seasonal dependence but less pronounced is observed in the Southern Hemisphere. A longer time period is required to study this seasonal dependence in more detail.

We can conclude that for most of the 23 stations included in the comparison, mean relative differences, or biases, are less than 10 % (see the individual station plots at https://cdop.aeronomie.be under Validation Results). For the Eureka, Ny Ålesund and Arrival Heights stations, located at high latitudes, biases are larger. A similar bias is found by Buchholz *et al.* (2017) when comparing with MOPITT data. When looking at the stations between -60° and 60°, the Toronto station shows the largest biases (mean bias ±20 %) which seems to be due to outliers.

The IASI data are generally overestimating with the overall bias of approx 6.5 % being off the same order as the reported combined total uncertainty of 5 % (Table 7.24).
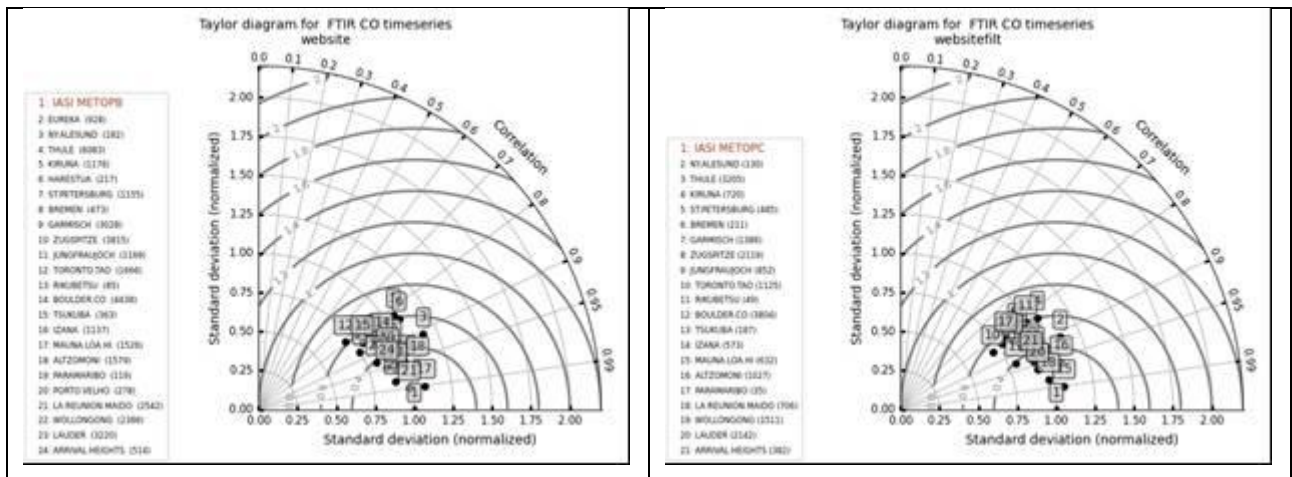
Figure 7.44. Correlation plots for IASI-B (left) and IASI-C (right) CO total columns against 23 NDACC FTIR sites. The stations are slightly shifted to the left, indicating that the satellite time-series has a higher standard deviation (more noisy).
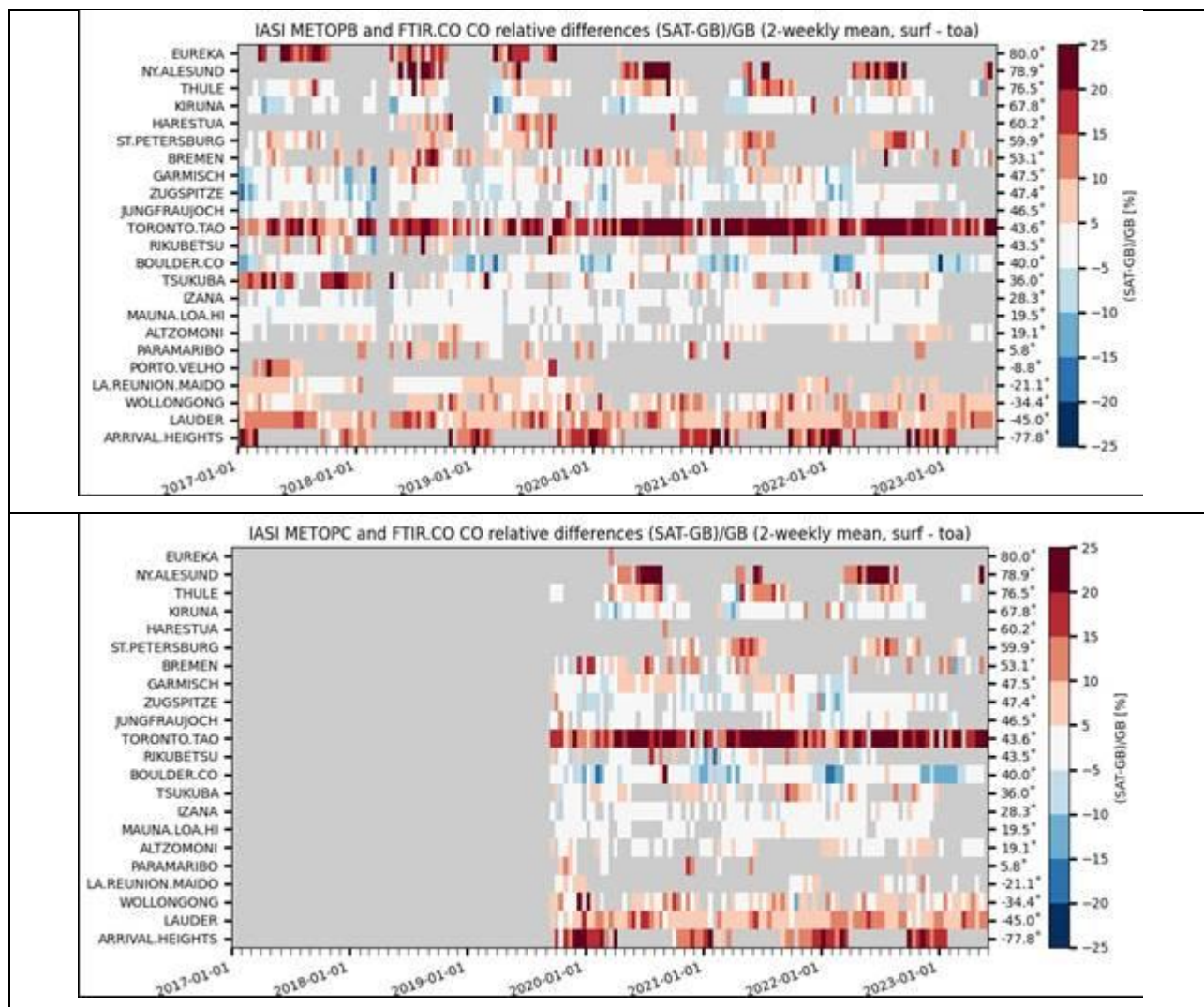
Figure 7.45. Time-series of bi-weekly relative difference for IASI-B (top) and IASI-C (bottom). The Metop-C relative bias time-series seems to correspond closely to the Metop-B time-series.

References:

Buchholz, R. R., Deeter, M. N., Worden, H. M., Gille, J., Edwards, D. P., Hannigan, J. W., Jones, N. B., Paton-Walsh, C., Griffith, D. W. T., Smale, D., Robinson, J., Strong, K., Conway, S., Sussmann, R., Hase, F., Blumenstock, T., Mahieu, E., and Langerock, B.: Validation of MOPITT carbon monoxide using ground-based Fourier transform infrared spectrometer data from NDACC, Atmos. Meas. Tech., 10, 1927-1956, 2017.
https://doi.org/10.5194/amt-10-1927-2017

Rodgers, C. D., and Connor, B. J.: Intercomparison of remote sounding instruments, J. Geophys. Res., 108, 4116-4129, 2003.
https://doi.org/10.1029/2002JD002299

Ronsmans, G., Langerock, B., Wespes, C., Hannigan, J. W., Hase, F., Kerzenmacher, T., Mahieu, E., Schneider, M., Smale, D., Hurtmans, D., De Mazière, M., Clerbaux, C., and Coheur, P.-F.: First characterization and validation of FORLI-HNO$_3$ vertical profiles retrieved from IASI/Metop, Atmos. Meas. Tech., 9, 4783-4801,2016.
https://doi.org/10.5194/amt-9-4783-2016

8. List of AC SAF users

The institutes of registered users of AC SAF products are listed below.

8.1. FMI archive

Europe:

Armenia:
- ICHD

Austria:
- Central Institute for Meteorology and Geodynamics
- Private individual
- Sistema GmbH
- University of Veterinary Medicine
- University of Vienna (2 users)

Belarus:
- National Academy of Sciences
- State University

Belgium:
- BIRA-IASB
- Flanders Marine Institute
- Ghent University (12 users)
- Karel de Grote University College
- KMI (4 users)
- KU Leuven
- ULB (3 users)

Bulgaria:
- Bulgarian Academy of Science
- Space Research and Technology Institute (2 users)

Croatia:
- J. J. Strossmayer University of Osijek

Czech Republic:
- Czech Hydrometeorological Institute (4 users)
- Global Change Research Institute

Denmark:
- Aarhus University (2 users)
- DMI (2 users)
- DTU Compute

Estonia:
- Estonian Environment Agency
- Intertrust

Finland:
- FMI (10 users)

- Häme University of Applied Sciences
- University of Helsinki (2 users)

France:
- AERIS/ICARE
- Aix-Marseille University
- CNRS (3 users)
- Grenoble Alpes University
- Laboratory of Atmospheric Optics
- Lasem
- LATMOS
- LISA (2 users)
- LISA-CNRS
- LSCE-IPSL-CNRS
- Météo France (5 users)
- Mines Paristech
- Open University
- Private Individual
- Reuniwatt
- Sistema
- Sorbonne University
- University of La Reunion
- University of Lille
- University of Paris Est Creteil

Germany:
- Brandenburg University of Technology
- Datiaperti
- DLR (3 users)
- DWD (4 users)
- EUMETSAT (19 users)
- Federal Office for Radiation Protection
- Forschungszentrum Jülich GmbH (4 users)
- Fraunhofer Institute
- Gymnasium Olching
- Oldenburg University
- Private individual
- Max Planck Institute for Chemistry (5 users)
- Sabrina Szeto Consulting
- Technical University of Munich
- University of Bremen (4 users)
- University of Cologne
- University of Hildesheim
- University of Konstanz
- University of Münster
- University of Potsdam

Greece:
- AUTH (4 users)
- Eratosthenes Centre of Excellence
- Hellenic Centre for Marine Research
- IESL/FORTH
- National and Kapodistrian University of Athens
- National Technical University of Athens (2 users)
- Private Individual
- University of Athens
- University of the Aegean
- University of Crete (2 users)

Hungary:
- Eötvös Loránd University (2 users)
- Hungarian Academy of Sciences
- Hungarian Meteorological Service (2 users)
- Individual
- University of Szeged

Ireland:
- Trinity College Dublin

Italy:
- ARPA Valle d'Aosta
- B-Open Solutions S.r.l. (2 users)
- CNR-ISAC
- European Space Agency
- fabbricadigitale
- IFAC-CNR (2 users)
- Julia Wagemann Consulting
- LaMMA Consortium (2 users)
- MEEO
- National Institute for Astrophysics
- Private Individual
- Regional Environmental Protection Agency Calabria
- University of Bologna (2 users)
- University of Milan
- University of Modena and Reggio Emilia
- University of Venice

Latvia:
- Latvian Environment, Geology and Meteorology Centre

Lithuania:
- Lithuanian National Meteorological Service
- Vilnius University

Malta:
- University of Malta

The Netherlands:
- BESSR
- ESA
- KNMI (6 users)
- S[&]T Corporation
- Wageningen University & Research (2 users)

Norway:
- Norwegian Institute for Air Research (2 users)
- UiT The Arctic University of Norway

Poland:
- CloudFerro
- IMGW
- Institute of Environmental Protection (2 users)
- Institute of Geodesy and Cartography
- Military University of Technology
- University of Warsaw

Portugal:
- Instituto Dom Luiz
- Instituto Português do Mar e da Atmosfera (4 users)
- University of Aveiro
- University of Lisbon
- University of Trás-os-Montes and Alto Douro (2 users)

Republic of North Macedonia:
- Hydrometeorological Service

Romania:
- Babes-Bolyai University (3 users)
- Global Top Systems
- INCAS
- INOE (2 users)
- National Meteorological Administration
- University of Galați (3 users)
- Politehnica University of Bucharest

Russia:
- Altai State University
- Daghestan Scientific Centre of Russian Academy of Sciences
- Federal Research Center Krasnoyarsk Scientific Center of the Siberian Branch of the RAS (2 users)
- Fedorov Institute of Applied Geophysics
- Institute of Atmospheric Physics
- Institute of Computational Modeling of the Siberian Branch of the RAS
- Institute of Global Climate and Ecology
- Irkutsk State Transport University
- Moscow State University
- Planeta (3 users)

- Research Center of Ecological Safety
- Roscosmos
- St. Petersburg State University
- Tomsk State University of Control Systems and Radioelectronics
- V.E. Zuev Institute of Atmospheric Optics

Serbia:
- Geographical institute "Jovan Cvijic", SASA

Slovakia:
- Private Individual

Slovenia:
- Bide-san, s.p.

Spain:
- Autonomous University of Barcelona
- Barcelona Supercomputing Center
- Basque Meteorology Agency
- CREAF-CSIC-UAB
- GREA
- I.E.S. Punta del Verde
- Modeliza
- Pablo de Olavide University
- Polytechnic University of Catalonia (2 users)
- University of Alicante
- University of Barcelona (3 users)
- University of the Basque Country
- University of Extremadura
- University of Granada (2 users)
- University of Málaga
- University of Valencia (3 users)
- University of Valladolid (2 users)

Sweden:
- NBI/Handelsakademin
- SMHI (5 users)

Turkey:
- Hacettepe University
- Istanbul University
- Middle East Technical University
- Turkish State Meteorological Service (2 users)
- Van Yüzüncü Yıl University

Ukraine:
- Batata LLC
- Scientific Centre for Aerospace Research of the Earth
- Taras Shevchenko National University of Kyiv
- UHMC

- Ukrainian Hydrometeorological Institute (2 users)

United Kingdom:
- ECMWF (2 users)
- ESA
- IDEMS International
- Office of National Statistics
- Private individual
- Rutherford Appleton Lab (2 users)
- Satavia Ltd.
- Satellite Applications Catapult
- Science and Technology Facilities Council (2 users)
- siHealth Ltd.
- University College London
- University of Edinburgh
- University of Hertfordshire
- University of Leeds
- University of Leicester
- University of Oxford
- University of York

Asia:

Bangladesh:
- Institute of Forestry and Environmental Sciences
- Stamford University
- University of Dhaka

China:
- Anhui Institute of Optics and Fine Mechanics
- Anhui Institute of Meteorological Sciences
- Anhui Normal University
- Beijing Municipal Environmental Monitoring Center
- Beijing Normal University (2 users)
- China Academy of Sciences (7 users)
- China Meteorological Administration
- China University of Mining and Technology (6 users)
- Chinese Academy of Meteorological Sciences (2 users)
- HTHJ
- Institute of Atmospheric Physics (2 users)
- Institute of Desert Meteorology
- Institute of Earthquake Forecasting
- Institute of Remote Sensing and Digital Earth (3 users)
- Jiangsu Meteorological Observatory
- Jiangsu Normal University (2 users)
- Jilin University
- Lanzhou University (2 users)
- Lanzhou Jiaotong University
- Nanjing University

- Nanjing University of Information Science & Technology (6 users)
- National Satellite Meteorological Center
- National University of Defense Technology
- Northeast Normal University
- Northwest Normal University
- Peking University (3 users)
- School
- Shandong University
- Shanghai University
- Shenzhen University
- Southern University of Science and Technology
- State Environmental Protection Key Lab of Satellite Remote Sensing
- Sun Yat-Sen University (2 users)
- The Chinese University of Hong Kong (2 users)
- The Institute of Atmospheric Physics (3 users)
- Tsinghua University (2 users)
- (unknown) (3 users)
- University of Science and Technology (3 users)
- Xiamen University
- Zhejiang University (2 users)

India:
- Anna University
- Aryabhatta Research Institute of Observational Sciences
- Banaras Hindu University
- Birla Institute of Technology
- Bose Institute
- Council of Scientific and Industrial Research
- CSIR-NIO
- CSIR-NPL
- Dibrugarh University
- "Education"
- IIT KGP
- Indian Institute of Technology Delhi
- Indian Institute of Technology Kharagpur (4 users)
- Indian Institute of Technology Roorkee (2 users)
- Indian Institute of Tropical Meteorology (3 users)
- Indian Space Research Organization (2 users)
- Jawaharlal Nehru Technological University, Kakinada
- Jawaharlal Nehru University
- Malaviya National Institute of Technology Jaipur
- Mangalore University
- MSRIT
- National Atmospheric Research Laboratory (2 users)
- National Centre for Medium Range Weather Forecasting
- National Institute of Technology
- National Remote Sensing Centre

- Savitribai Phule Pune University (2 users)
- School of Planning and Architecture, Bhobal
- SIG
- SRM Institute of Science and Technology
- University of Calcutta
- University of Hyderabad
- University of Kalyani
- Vikram Sarabhai Space Centre (2 users)
- Vindhyan Ecology and Natural History Foundation

Indonesia:
- Bandung Institute of Technology
- Meteorological, Climatological, and Geophysical Agency (3 users)
- National Institute for Aeronautics and Space
- Sumatera Institute of Technology

Japan:
- Chiba University
- Ibaraki University
- Japan Meteorological Agency
- Kyushu University
- National Institute for Environmental Studies
- Waseda University

Malaysia:
- Malaysian Space Agency
- National University of Malaysia (5 users)

Myanmar:
- Yangon Technological University

Nepal:
- International Centre for Integrated Mountain Development (2 users)
- Institute for Advanced Sustainability Studies
- Institute of Tibetan Plateau Research
- Institute of Engineering

Pakistan:
- University of the Punjab
- National University of Sciences & Technology

Philippines:
- Manila Observatory

Singapore:
- National University of Singapore (2 users)

South Korea:
- Chungnam National University (3 users)
- Gwangju Institute of Science and Technology (4 users)
- Hankuk University of Foreign Studies
- Korea Meteorological Administration (2 users)

- Korea Polar Research Institute
- National Institute of Environmental Research (2 users)
- National Meteorological Satellite Center (4 users)
- Pukyong National University
- Yonsei University (3 users)
- Kongju National University
- Seoul National University

Sri Lanka:
- Central Environmental Authority

Taiwan:
- Academia Sinica
- Garmin
- National Central University (2 users)
- National Taipei University
- Research Center for Environmental Changes

Thailand:
- Asian Institute of Technology
- King Mongkut's Institute of Technology Ladkrabang

Vietnam:
- University of Science (2 users)

Middle East:

Iran:
- Atmospheric Science & Meteorological Research Center
- Islamic Azad University
- Tabriz University
- "University"

Iraq:
- Al Iraqia University
- Mustansiriyah University

Israel:
- Israel Institute for Biological Research
- University of Tel Aviv (2 users)

Oman:
- Sultan Qaboos University

Saudi Arabia:
- King Abdullah University of Science and Technology (2 users)
- Private individual

United Arab Emirates:
- Khalifa University
- Uruk Engineering & Contracting

North America:

Canada:
- Canadian Space Agency
- Dalhousie University
- University of Saskatchewan

United States of America:
- Caltech
- Colorado State University
- EMDO Lab
- Florida State University
- Harvard-Smithsonian Center for Astrophysics
- Intertek
- Joint Center for Satellite Data Assimilation
- Michigan Technological University (5 users)
- Mote Marine Laboratory
- NASA (2 users)
- Naval Research Laboratory
- NOAA
- Northeastern University
- Princeton University
- Private Individual
- SpaceKnow Inc.
- Texas A&M University
- The Aerospace Corporation
- Trinity Consultants Inc.
- University of Alabama in Huntsville
- University of Alaska (2 users)
- University of California (2 users)
- University of Central Florida
- University of Colorado Boulder
- University of Kansas
- University of Maryland
- University of Washington
- Unknown
- USGS
- U.S. Environmental Protection Agency

South America:

Argentina:
- Universidad Nacional de Córdoba
- Universidad Nacional de Rosario

Brazil:
- APAC
- Federal University of Western Pará
- LAPIS

- Universidade Federal de Alagoas

Chile:
- University of the Americas

Colombia:
- Universidad EAFIT

Ecuador:
- Universidad San Francisco de Quito (2 users)

Guatemala:
- ASEFOR
- INSIVUMEH

Mexico:
- Ibero Puebla
- Instituto Politecnico Nacional

Paraguay:
- Universidad San Carlos

Peru:
- Servicio Nacional de Meteorología e Hidrología del Perú

Uruguay:
- Universidad de la República

Australia / New Zealand:

- Bureau of Meteorology
- University of Canterbury (3 users)
- University of Melbourne (2 users)
- University of Southern Queensland (2 users)
- University of Sydney

Africa:

Algeria:
- Meteo Algeria

Cameroon:
- African Institute for Mathematical Sciences

Egypt:
- Egyptian Meteorological Authority (2 users)
- National Research Institute of Astronomy and Geophysics

Eritrea:
- Department of Environment

Ethiopia:
- Addis Ababa University

Ghana:
- Ghana Meteorological Agency
- University of Energy and Natural Resources

Morocco:
- Abdelmalek Essaadi University
- EM5D
- Maroc Météo
- University of Hassan II Casablanca

Nigeria:
- Abdou Moumouni University
- Federal University Lafia

South Africa:
- National Chemical Emergency Centre
- South African Weather Service (2 users)
- Stellenbosch University
- University of KwaZulu-Natal
- University of Pretoria
- University of the Witwatersrand

Registered users: **600**

8.2. DLR archive

Europe:

Austria:
- University of Veterinary Medicine
- University of Vienna

Belarus:
- National Academy of Sciences

Belgium:
- Antea Group
- BIRA-IASB (5 users)
- Flanders Marine Institute
- Ghent University (8 users)
- KMI (3 users)
- ULB (4 users)

Bulgaria:
- Space Research and Technology Institute (2 users)

Czech Republic:
- Charles University
- Czech Hydrometeorological Institute (5 users)
- Global Change Research Institute

Denmark:
- Aarhus University (2 users)
- DTU Compute

Estonia:
- Estonian Environment Agency
- Intertrust

Finland:
- FMI (9 users)
- Häme University of Applied Sciences

France:
- AERIS/ICARE
- Aix-Marseille University
- CNRS (3 users)
- Grenoble Alpes University
- Institute of Environmental Geosciences
- Laboratory of Atmospheric Optics
- Lasem
- LATMOS (3 users)
- LISA
- LISA-CNRS
- LSCE-IPSL-CNRS
- Météo France (4 users)
- Mines Paristech
- Open University
- Reuniwatt
- Sistema
- Sorbonne University
- University of La Reunion

Germany:
- Brandenburg University of Technology
- Datiaperti
- DLR (4 users)
- DWD (2 users)
- EUMETSAT (18 users)
- Forschungszentrum Jülich GmbH (2 users)
- Fraunhofer Institute
- Gymnasium Olching
- Heidelberg University
- Karlsruhe Institute of Technology
- Max Planck Institute for Chemistry (4 users)
- Private individual
- Sabrina Szeto Consulting
- Technical University of Munich
- University of Bremen (7 users)
- University of Cologne (2 users)
- University of Hildesheim
- University of Münster

Greece:
- AUTH (4 users)
- Eratosthenes Centre of Excellence
- Hellenic Centre for Marine Research
- IESL/FORTH
- National and Kapodistrian University of Athens
- National Technical University of Athens (2 users)
- Private Individual
- University of Athens
- University of Crete (2 users)

Hungary:
- Hungarian Meteorological Service (3 users)
- Individual
- University of Szeged

Ireland:
- Trinity College Dublin

Italy:
- B-open Solutions S.r.l. (2 users)
- CNR-ISAC
- fabbricadigitale
- IFAC-CNR
- Italian National Research Council
- Julia Wagemann Consulting
- LaMMA Consortium
- MEEO
- National Institute of Geophysics and Volcanology
- Private Individual
- Regional Environmental Protection Agency Calabria
- University of Bologna
- University of Modena and Reggio Emilia
- University of Venice

Latvia:
- Latvian Environment, Geology and Meteorology Centre

Lithuania:
- Lithuanian National Meteorological Service

Malta:
- University of Malta

The Netherlands:
- BESSR
- KNMI (7 users)
- S[&]T Corporation
- Wageningen University & Research (2 users)

Norway:
- UiT The Arctic University of Norway

Poland:
- CloudFerro
- Institute of Environmental Protection (2 users)
- Institute of Geodesy and Cartography
- Institute of Meteorology and Water Management-NRI
- Military University of Technology
- University of Warsaw

Portugal:
- Instituto Dom Luiz (2 users)
- Instituto Português do Mar e da Atmosfera (3 users)
- University of Tras-os-Montes and Alto Douro

Romania:
- Babes-Bolyai University (3 users)
- Global Top Systems
- INOE (3 users)
- University of Galați (3 users)
- Politehnica University of Bucharest

Russia:
- Altai State University
- Institute of Computational Modeling of the Siberian Branch of the RAS
- Institute of Global Climate and Ecology
- Irkutsk State Transport University
- Planeta

Serbia:
- Geographical institute "Jovan Cvijic", SASA

Slovakia:
- Private Individual

Slovenia:
- Bide-san, s.p.

Spain:
- Autonomous University of Barcelona
- GREA
- Modeliza
- Pablo de Olavide University
- Polytechnic University of Catalonia (2 users)
- Universitat Politècnica de València
- University of Alicante
- University of Barcelona (3 users)
- University of Granada (3 users)
- University of Extremadura (2 users)
- University of Oviedo

- University of Valencia (3 users)
- University of Valladolid

Sweden:
- SMHI (4 users)
- The Swedish Defence Research Agency (2 users)

Turkey:
- Hacettepe University
- Kastamony University
- Middle East Technical University
- Turkish State Meteorological Service (2 users)
- Van Yüzüncü Yıl University

Ukraine:
- Batata LLC
- Scientific Centre for Aerospace Research of the Earth
- UHMC
- Ukrainian Hydrometeorological Institute

UK:
- ECMWF (4 users)
- ESA
- IDEMS International
- Hibarcus
- Private individual
- Rutherford Appleton Lab
- Satavia Ltd.
- Satellite Applications Catapult
- Science and Technology Facilities Council (2 users)
- siHealth Ltd.
- University of Hertfordshire
- University of Leeds
- University of Leicester (2 users)
- University of York (2 users)

Asia:

Bangladesh:
- Institute of Forestry and Environmental Sciences
- University of Dhaka

China:
- Anhui Normal University
- Anhui Institute of Meteorological Sciences University of Dhaka
- Anhui Institute of Optics and Fine Mechanics (2 users)
- Anhui University (3 users)
- Beijing Municipal Environmental Monitoring Center
- Beijing Normal University
- Chinese Academy of Meteorological Sciences

- China Academy of Sciences (7 users)
- China Meteorological Administration
- China University of Mining and Technology (6 users)
- HTHJ
- Institute of Atmospheric Physics
- Institute of Geographic Sciences and Natural Resources Research, China Academy of Sciences
- Institute of Remote Sensing and Digital Earth
- Jiangsu Meteorological Observatory
- Jiangsu Normal University (2 users)
- Jinan University
- Lanzhou University
- Nanjing University (3 users)
- Nanjing University of Information Science & Technology (4 users)
- National Satellite Meteorological Center
- Northeast Normal University
- Northwest Normal University
- Peking University (4 users)
- PIE
- Piesat Information Technology Co. ,Ltd.
- School
- Shandong University (2 users)
- Shanghai University
- Shenzhen University
- South China Agricultural University
- Southern University of Science and Technology
- State Environmental Protection Key Lab of Satellite Remote Sensing
- The Chinese University of Hong Kong (2 users)
- The Institute of Atmospheric Physics (2 users)
- Tsinghua University (2 users)
- University of Science and Technology (4 users)
- (unknown) (4 users)
- Wuhan University
- Wuhan University of Technology
- Zhejiang Academy of Agricultural Sciences
- Zhejiang University

India:
- Anna University
- Aryabhatta Research Institute of Observational Sciences
- Banaras Hindu University
- Birla Institute of Technology
- Bose Institute
- Central University of Hyderabad
- Central University of Rajasthan
- CSIR-NIO
- Dibrugarh University (2 users)
- "Education"

- IIT KGP
- Indian Institute of Technology Delhi
- Indian Institute of Technology Kharagpur (3 users)
- Indian Institute of Technology Roorkee (2 users)
- Indian Institute of Tropical Meteorology (3 users)
- Indian Space Research Organization (2 users)
- Jawaharlal Nehru University
- Malaviya National Institute of Technology Jaipur
- MSRIT
- National Atmospheric Research Laboratory
- National Centre for Medium Range Weather Forecasting
- National Institute of Technology
- Savitribai Phule Pune University (2 users)
- School of Planning and Architecture, Bhobal
- SIG
- SRM Institute of Science and Technology
- University of Calcutta
- University of Hyderabad
- University of Kalyani
- Vikram Sarabhai Space Centre

Indonesia:
- Bandung Institute of Technology
- Meteorological, Climatological, and Geophysical Agency (3 users)
- National Institute for Aeronautics and Space
- Sumatera Institute of Technology

Japan:
- Chiba University
- Fukuoka University
- Ibaraki University
- Japan Meteorological Agency
- Kyushu University (2 users)
- Nagoya University
- National Institute for Environmental Studies
- Remote Sensing Technology Center of Japan
- Waseda University

Malaysia:
- Malaysian Space Agency
- National University of Malaysia (4 users)

Myanmar:
- Yangon Technological University

Nepal:
- Institute for Advanced Sustainability Studies
- Institute of Engineering
- International Centre for Integrated Mountain Development (2 users)

Pakistan:
- National University of Sciences and Technology
- University of the Punjab

Singapore:
- National University of Singapore (2 users)

South Korea:
- Chungnam National University (3 users)
- Gwangju Institute of Science and Technology (4 users)
- Korea Meteorological Administration
- Korea Polar Research Institute
- National Institute of Environmental Research (2 users)
- National Meteorological Satellite Center (3 users)
- Seoul National University (4 users)
- Ulsan National Institute of Science and Technology
- University of Suwon
- Yonsei University (6 users)

Sri Lanka:
- Central Environmental Authority

Taiwan:
- National Central University

Thailand:
- King Mongkut's Institute of Technology Ladkrabang

Vietnam:
- University of Science (2 users)

Middle East:

Iran:
- Khavaran Institute of Higher Education
- Tabriz University
- "University"
- University of Tehran

Iraq:
- Al Iraqia University
- Mustansiriyah University

Saudi Arabia:
- King Abdulaziz City for Science and Technology
- King Abdullah University of Science and Technology
- Private individual

United Arab Emirates:
- Khalifa University
- Uruk Engineering & Contracting

North America:

Canada:
- Environment and Climate Change Canada (4 users)
- University of Saskatchewan

USA:
- Arizona State University
- Caltech (2 users)
- Colorado State University
- Florida State University
- Johns Hopkins University
- Harvard University (3 users)
- Intertek
- Joint Center for Satellite Data Assimilation
- Michigan Technological University (3 users)
- NASA (5 users)
- NOAA (3 users)
- Princeton University
- Private Individual
- Smithsonian Astrophysical Observatory
- SpaceKnow Inc.
- Texas A&M University
- Trinity Consultants Inc.
- University of Alabama in Huntsville
- University of Alaska (2 users)
- University of California (3 users)
- University of Central Florida
- University of Colorado Boulder
- University of Houston
- University of Illinois
- University of Maryland (3 users)
- University of North Carolina at Chapel Hill
- University of Washington (2 users)
- University of Wisconsin-Madison
- Unknown
- USGS
- U.S. Environmental Protection Agency
- Utah State University

South America:

Argentina:
- Argentine Air Force
- Universidad Nacional de Rosario

Brazil:
- APAC
- LAPIS

- Universidade Federal de Alagoas
- University of São Paulo

Chile:
- University of the Americas

Colombia:
- Universidad EAFIT

Ecuador:
- Universidad San Francisco de Quito

Guatemala:
- INSIVUMEH

Mexico:
- Ibero Puebla
- Instituto Politecnico Nacional

Paraguay:
- Universidad San Carlos

Peru:
- Servicio Nacional de Meteorología e Hidrología del Perú

Uruguay:
- Universidad de la República

Australia / New Zealand:

- Environmental Systems & Services
- University of Canterbury (2 users)
- University of Melbourne (2 users)
- University of Southern Queensland

Africa:

Algeria:
- Meteo Algeria

Cameroon:
- African Institute for Mathematical Sciences

Egypt:
- Egyptian Meteorological Authority (2 users)
- National Research Institute of Astronomy and Geophysics

Eritrea:
- Department of Environment

Ghana:
- Ghana Meteorological Agency

Morocco:
- Abdelmalek Essaadi University
- EM5D
- Maroc Météo

- National Center for Meteorological Research
- University of Hassan II Casablanca

Nigeria:
- Federal University Lafia

South Africa:
- South African Weather Service
- Stellenbosch University
- University of Pretoria
- University of the Witwatersrand
- Ware Jacob Enterprises

Registered users: **542**

8.3. DMI (NUV product via FTP)

- Meteorological Institute of Romania
  $\Rightarrow$ Several commercial companies obtain the data from MIR
- Danish Meteorological Institute, Denmark
- TrygFonden, Denmark
- Department for Health, Greenland Homerule
- The Danish Cancer Society, Denmark
- Libraries of Hjørring Community
- SunSense AS, Norway
- Richard McKenzie, New Zealand
- Elian Wolfram, Laser Research Center and Applications, Argentina
- KMI, Belgium
- By & Havn I/S, Denmark

Registered users: **11**

8.4. KNMI (unofficial NRT AAI via FTP)

- FMI, Finland
- William B. Hanson Center for Space Science, USA
- University of Leicester, UK

Registered users: **3**

8.5. Known international projects that use EUMETCast or WMO/GTS

- MACC project
- SACS service
- Temis WWW service
- ESA GlobVapour
- ESA CCI Ozone project

8.6. EUMETCast

Albania	4	Iceland	1	Portugal	5
Algeria	4	India	1	Qatar	3
Angola	1	Iran, Islamic Republic of	32	Reunion	1
Armenia	1	Iraq	2	Romania	10
Austria	19	Ireland	7	Russian Federation	7
Azerbaijan	3	Israel	4	Rwanda	2
Belgium	10	Italy	281	San Marino	1
Benin	1	Jordan	1	Saudi Arabia	3
Bosnia and Herzegovina	1	Kazakhstan	6	Senegal	5
Botswana	4	Kenya	6	Serbia	2
Brazil	3	Kuwait	2	Seychelles	1
Bulgaria	6	Kyrgyzstan	1	Slovakia	6
Burkina Faso	1	Latvia	1	Slovenia	1
Cameroon	2	Lebanon	4	South Africa	5
Canada	1	Lesotho	2	South Sudan	1
China	4	Liberia	1	Spain	43
Congo	1	Libya	1	Sudan	1
Congo, Democratic Republic of	1	Lithuania	2	Sweden	5
Croatia	1	Luxembourg	1	Switzerland	15
Cyprus	1	Madagascar	3	Syrian Arab Republic	1
Czech Republic	20	Malawi	2	Tajikistan	1
Denmark	5	Mali	1	Tanzania, United Republic of	3
Egypt	3	Malta	2	Togo	1
Estonia	3	Mauritania	3	Tunisia	3
Eswatini	2	Mauritius	2	Turkey	7
Ethiopia	5	Moldova, Republic of	1	Turkmenistan	1
Finland	5	Morocco	5	Uganda	2
France	56	Mozambique	2	Ukraine	3
Gabon	1	Namibia	1	United Arab Emirates	3
Georgia	1	The Netherlands	21	United Kingdom	112
Germany	104	Niger	2	United States	1
Ghana	5	Nigeria	6	Uzbekistan	1
Greece	18	Norway	4	Vietnam	1
Guinea-Bissau	2	Oman	2	Yemen	1
Hong Kong	1	Pakistan	1	Zambia	3
Hungary	10	Poland	12	Zimbabwe	2
TOTAL (January 2022)	**999**				

9. Updates during the reporting period

Listed below are the major configuration updates concerning operational data processing and archiving. If new versions of relevant AC SAF documents are released during the reporting period, they should be listed here also.

9.1. Software updates

17 April   KNMI: OPERA update (version 2.20)

9.2. Hardware updates

Nothing to report.

9.3. Documentation updates

26 January   DLR: Combined Algorithm Theoretical Basis Document and Product User Manual for the offline daily averaged L3 trace gas column products (issue 1/D)

26 January   DLR: Combined Algorithm Theoretical Basis Document and Product User Manual for the offline monthly averaged L3 trace gas column products (issue 1/D)

30 January   DLR: Validation Report for the offline daily/monthly averaged L3 trace gas column products (issue 1/2023)

8 March   FMI: AC SAF Configuration Management Plan (issue 4.0)

28 March   KNMI: OPERA Software Release Note (version 2.20)

29 March   FMI: AC AF Product Requirements Document (issue 2.1)

12 April   FMI: System Version Document (issue 1.14)

27 April   FMI: AC SAF Operations Report 2/2022 (revision 1)

10. Changes and usage statistics of the web portal

Listed below are the major changes in the appearance and content on the [AC SAF main web pages](#). Additionally some web page usage statistics gathered by Google Analytics are listed.

10.1. Changes in appearance and content

Table 10.1. Changes in appearance and content of the main AC SAF web pages during the reporting period

Date	Description
3 April	*datarecord_access.php*: Locations of CHOCHO, Trop_BrO and L3 H2O/NO2 data records updated
21 April	*products/gome-2_level-3_daily.php* created *products/gome-2_level-3_monthly.php* created *offline_access.php* updated to include the products mentioned above (L2 and L3 products separated)
27 June	DLER data record page *datarecords/ler_demo.php* created, *datarecord_access.php* updated to include demonstrational DLER

In addition to updates above, following routine updates are conducted whenever necessary:

- The links to public AC SAF user documents are updated whenever new documents or new versions of existing documents become available
- The "top story" on the front page is updated
- News list on the front page is updated

APPENDIX 1

Table A.1 presents the overall summary of orders from AC SAF archive at FMI, sorted by product types, during the reporting period

Table A.2 presents a detailed summary of product orders from AC SAF archive at FMI during the reporting period.

Table A.1. Overall summary of product orders, by product type, during the reporting period

Product type	Number of orders	Number of users	Number of products	Total size
OOP-A	1	1	414	20.0 GB
OOP-B	-	-	-	-
OHP-A	11	4	3954	887 GB
OHP-B	16	3	28367	7.09 TB
OHP-C	4	3	4	1.00 GB
ARS-A	-	-	-	-
ARS-B	9	1	3840	3.96 GB
ARS-C	10	2	3864	3.98 GB
ARP-A	1	1	85	529 MB
ARP-B	15	7	1472	10.5 GB
ARP-C	15	7	1398	10.0 GB
OUV-A	38	3	75512	10.9 GB
OUV-B	38	3	38152	5.60 GB
OUV-AB	40	3	62984	10.4 GB
OUV-BC	44	7	42204	8.48 GB
LER-MSC-AB	4	3	4	7.99 GB
LER-PMD-AB	4	3	4	7.99 GB

Table A.2. More detailed summary of product orders during the reporting period

JANUARY			
Product type	Number of products	Order size	Institute / company
ARS-B ARS-C	424 424	872 MB	AUTH, Greece
ARS-B ARS-C	435 439	899 MB	AUTH, Greece
OHP-A	4	1.49 GB	RMI, Belgium
OUV-BC	Time series for 333 days Selected subset: UVADD, UVBDD Location: 18.07E 59.32N (24.2 kB in total)		FMI, Finland

OUV-BC	Time series for 60 days Selected subset: UVBDD Location: 20.00E 60.00N (4.17 kB in total)		FMI, Finland
OHP-C	1	251 MB	Servicio Nacional de Meteorología e Hidrología del Perú
OHP-A	99	24.3 GB	University of the Basque Country, Spain
OUV-A OUV-AB OUV-B OUV-BC	Time series for 5654 days Selected subset: UVADD, UVBDD, UVADR, UVBDR Location: 0.88W 41.65N (526 kB in total)		University of Barcelona, Spain
OUV-A OUV-AB OUV-B OUV-BC	Time series for 5654 days Selected subset: UVADD, UVBDD, UVADR, UVBDR Location: 0.38W 39.47N (526 kB in total)		University of Barcelona, Spain
OUV-A OUV-AB OUV-B OUV-BC	Time series for 5654 days Selected subset: UVADD, UVBDD, UVADR, UVBDR Location: 6.37W 39.48N (526 kB in total)		University of Barcelona, Spain
OUV-A OUV-AB OUV-B OUV-BC	Time series for 5654 days Selected subset: UVADD, UVBDD, UVADR, UVBDR Location: 4.42W 36.72N (526 kB in total)		University of Barcelona, Spain
OUV-A OUV-AB OUV-B OUV-BC	Time series for 5654 days Selected subset: UVADD, UVBDD, UVADR, UVBDR Location: 2.93W 43.26N (526 kB in total)		University of Barcelona, Spain
OUV-A OUV-AB OUV-B OUV-BC	Time series for 5654 days Selected subset: ERYDD, DNADD, VITDD, UVADD, UVBDD Location: 0.88W 41.65N (589 kB in total)		University of Barcelona, Spain
OUV-A OUV-AB OUV-B OUV-BC	Time series for 5654 days Selected subset: ERYDR, DNADR, VITDR, UVADR, UVBDR Location: 0.88W 41.65N (589 kB in total)		University of Barcelona, Spain
OUV-A OUV-AB OUV-B OUV-BC	Time series for 5654 days Selected subset: ERYDR, DNADR, VITDR, UVADR, UVBDR Location: 2.93W 43.26N (589 kB in total)		University of Barcelona, Spain

OUV-A OUV-AB OUV-B OUV-BC	Time series for 5654 days Selected subset: ERYDR, DNADR, VITDR, UVADR, UVBDR Location: 4.42W 36.72N (589 kB in total)	University of Barcelona, Spain
OUV-A OUV-AB OUV-B OUV-BC	Time series for 5654 days Selected subset: ERYDR, DNADR, VITDR, UVADR, UVBDR Location: 6.37W 39.48N (589 kB in total)	University of Barcelona, Spain
OUV-A OUV-AB OUV-B OUV-BC	Time series for 5654 days Selected subset: ERYDR, DNADR, VITDR, UVADR, UVBDR Location: 0.38W 39.47N (589 kB in total)	University of Barcelona, Spain
OUV-A OUV-AB OUV-B OUV-BC	Time series for 5654 days Selected subset: ERYDD, DNADD, VITDD, UVADD, UVBDD Location: 0.88W 41.65N (589 kB in total)	University of Barcelona, Spain
OUV-A OUV-AB OUV-B OUV-BC	Time series for 5654 days Selected subset: ERYDD, DNADD, VITDD, UVADD, UVBDD Location: 0.38W 39.47N (589 kB in total)	University of Barcelona, Spain
OUV-A OUV-AB OUV-B OUV-BC	Time series for 5654 days Selected subset: ERYDD, DNADD, VITDD, UVADD, UVBDD Location: 4.42W 36.72N (589 kB in total)	University of Barcelona, Spain
OUV-A OUV-AB OUV-B OUV-BC	Time series for 5654 days Selected subset: ERYDD, DNADD, VITDD, UVADD, UVBDD Location: 6.37W 39.48N (589 kB in total)	University of Barcelona, Spain
OUV-A OUV-AB OUV-B OUV-BC	Time series for 5654 days Selected subset: ERYDD, DNADD, VITDD, UVADD, UVBDD Location: 2.93W 43.26N (589 kB in total)	University of Barcelona, Spain

FEBRUARY			
Product type	**Number of products**	**Order size**	**Institute / company**
LER-MSC-AB LER-PMD-AB	1 1	3.99 GB	IESL/FORTH, Greece
ARP-B ARP-C	22 21	310 MB	FMI, Finland

Product type	Number of products	Order size	Institute / company
ARP-B ARP-C	818 821	11.7 GB	AUTH, Greece
ARS-B ARS-C	424 424	872 MB	AUTH, Greece
ARS-B ARS-C	439 437	901 MB	AUTH, Greece
ARS-B ARS-C	435 439	899 MB	AUTH, Greece
ARP-B ARP-C	57 56	811 MB	FMI, Finland
ARP-B ARP-C	247 247	3.54 GB	AUTH, Greece
OUV-A OUV-AB OUV-B OUV-BC	5701 Selected subset: ERYDD, UVADD, UVBDD, ERYDR, UVADR, UVBDR Region: 10.0W-15.0E, 25.0-50.0N (470 MB in total)		University of Barcelona, Spain
OUV-A OUV-AB OUV-B OUV-BC	5701 Selected subset: ERYDD, UVADD, UVBDD, ERYDR, UVADR, UVBDR Region: 20.0W-5.0E, 25.0-50.0N (470 MB in total)		University of Barcelona, Spain
OUV-A OUV-AB OUV-B OUV-BC	5701 Selected subset: ERYDD, UVADD, UVBDD, ERYDR, UVADR, UVBDR Region: 10.0W-15.0E, 25.0-50.0N (470 MB in total)		University of Barcelona, Spain
OUV-A OUV-AB OUV-B OUV-BC	5701 Selected subset: ERYDD, UVADD, UVBDD, ERYDR, UVADR, UVBDR Region: 20.0W-5.0E, 25.0-50.0N (470 MB in total)		University of Barcelona, Spain
MARCH			
Product type	**Number of products**	**Order size**	**Institute / company**
OUV-BC	69 Selected subset: UVADD, UVBDD, UVI Region: 18.0-29.0E, 53.0-61.0N (1.95 MB in total)		LVGMC, Latvia

ARS-B ARS-C	397 398	817 MB	AUTH, Greece
ARP-B	5	36.2 MB	EMDO Lab, USA
OUV-A OUV-AB OUV-B OUV-BC	5713 Selected subset: ERYDD, UVADD, UVBDD, ERYDR, UVADR, UVBDR Region: global (19.6 GB in total)		University of Barcelona, Spain
OUV-BC	717 Selected subset: ERYDD, UVADD, UVBDD, ERYDR, UVADR, UVBDR Region: global (2.46 GB in total)		University of Barcelona, Spain
OUV-A OUV-AB OUV-B OUV-BC	5721 Selected subset: ERYDD, UVADD, UVBDD, ERYDR, UVADR, UVBDR Region: 60.0W-60.0E, 0.0-90.0N (3.62 GB in total)		University of Barcelona, Spain
ARP-B ARP-C	43 43	617 MB	FMI, Finland
APRIL			
Product type	**Number of products**	**Order size**	**Institute / company**
OHP-C	1	249 MB	University of Science and Technology, China
OHP-B	2166	543 GB	University of Science and Technology, China
ARP-A ARP-B	85 85	1.06 GB	FMI, Finland
OHP-A	5	1.81 GB	Jilin University, China
OUV-A OUV-AB OUV-B OUV-BC	Time series for 5766 days Selected subset: ERYDD, DNADD, VITDD, UVADD, UVBDD, ERYDR, DNADR, VITDR, UVADR, UVBDR Location: 2.15E 41.39N (918 kB in total)		University of Barcelona, Spain
OUV-A OUV-AB OUV-B OUV-BC	Time series for 5766 days Selected subset: ERYDD, DNADD, VITDD, UVADD, UVBDD, ERYDR, DNADR, VITDR, UVADR, UVBDR Location: 3.70W 40.42N (918 kB in total)		University of Barcelona, Spain

OUV-A OUV-AB OUV-B OUV-BC	Time series for 5766 days Selected subset: ERYDD, DNADD, VITDD, UVADD, UVBDD, ERYDR, DNADR, VITDR, UVADR, UVBDR Location: 1.55W 47.22N (918 kB in total)	University of Barcelona, Spain
OUV-A OUV-AB OUV-B OUV-BC	Time series for 5768 days Selected subset: ERYDR, DNADR, VITDR, UVADR, UVBDR Location: 6.06E 33.11N (601 kB in total)	University of Barcelona, Spain
OUV-A OUV-AB OUV-B OUV-BC	Time series for 5768 days Selected subset: ERYDD, DNADD, VITDD, UVADD, UVBDD Location: 5.80W 35.77N (601 kB in total)	University of Barcelona, Spain
OUV-A OUV-AB OUV-B OUV-BC	Time series for 5768 days Selected subset: ERYDD, DNADD, VITDD, UVADD, UVBDD Location: 9.13W 38.72N (601 kB in total)	University of Barcelona, Spain
OUV-A OUV-AB OUV-B OUV-BC	Time series for 5768 days Selected subset: ERYDR, DNADR, VITDR, UVADR, UVBDR Location: 2.93W 43.26N (601 kB in total)	University of Barcelona, Spain
OUV-A OUV-AB OUV-B OUV-BC	Time series for 5768 days Selected subset: ERYDR, DNADR, VITDR, UVADR, UVBDR Location: 9.13W 38.72N (601 kB in total)	University of Barcelona, Spain
OUV-A OUV-AB OUV-B OUV-BC	Time series for 5768 days Selected subset: ERYDR, DNADR, VITDR, UVADR, UVBDR Location: 5.80W 35.77N (601 kB in total)	University of Barcelona, Spain
OUV-A OUV-AB OUV-B OUV-BC	Time series for 5768 days Selected subset: ERYDD, DNADD, VITDD, UVADD, UVBDD Location: 2.93W 43.26N (601 kB in total)	University of Barcelona, Spain
OUV-A OUV-AB OUV-B OUV-BC	Time series for 5768 days Selected subset: ERYDD, DNADD, VITDD, UVADD, UVBDD Location: 2.15E 41.39N (601 kB in total)	University of Barcelona, Spain

OUV-A OUV-AB OUV-B OUV-BC	Time series for 5768 days Selected subset: ERYDR, DNADR, VITDR, UVADR, UVBDR Location: 2.15W 41.39N (601 kB in total)		University of Barcelona, Spain
OUV-A OUV-AB OUV-B OUV-BC	Time series for 5768 days Selected subset: ERYDD, DNADD, VITDD, UVADD, UVBDD Location: 6.06E 33.11N (601 kB in total)		University of Barcelona, Spain
OHP-C	1	251 MB	V.E. Zuev Institute of Atmospheric Optics, Russia
OHP-B	1	251 MB	V.E. Zuev Institute of Atmospheric Optics, Russia
OHP-C	1	250 MB	V.E. Zuev Institute of Atmospheric Optics, Russia
OHP-B	1	251 MB	V.E. Zuev Institute of Atmospheric Optics, Russia

MAY			
Product type	**Number of products**	**Order size**	**Institute / company**
ARP-B ARP-C	37 36	520 MB	FMI, Finland
OUV-BC	1 Selected subset: ERYDD, DNADD, PLADD, VITDD, UVADD, UVBDD, ERYDR, DNADR, PLADR, VITDR, UVADR, UVBDR, JO1D, JNO2, UVI Region: global (17.5 MB in total)		CNU, South Korea
ARP-B ARP-C	18 16	243 MB	FMI, Finland
OHP-A	836	122 GB	Ibaraki University, Japan
ARP-B ARP-C	18 20	271 MB	FMI, Finland
LER-MSC-AB LER-PMD-AB	1 1	3.99 GB	Université de la Reunion, France
OOP-A	414	20 GB	Ghent University, Belgium
OUV-A OUV-AB OUV-B OUV-BC	Time series for 5768 days Selected subset: ERYDR, DNADR, VITDR, UVADR, UVBDR Location: 4.83E 45.70N (601 kB in total)		University of Barcelona, Spain
OHP-A	438	108 GB	Ibaraki University, Japan
ARP-B ARP-C	11 11	161 MB	FMI, Finland

JUNE			
Product type	**Number of products**	**Order size**	**Institute / company**
ARS-B ARS-C	437 438	900 MB	AUTH, Greece
ARS-B ARS-C	424 425	878 MB	AUTH, Greece
ARS-B ARS-C	425 425	882 MB	AUTH, Greece
LER-MSC-AB LER-PMD-AB	1 1	3.99 GB	University of Chinese Academy of Sciences
OHP-B	2562	639 GB	University of Science and Technology, China
OHP-B	2577	642 GB	University of Science and Technology, China
OHP-B	2603	650 GB	University of Science and Technology, China
OHP-B	2604	651 GB	University of Science and Technology, China
OHP-B	859	216 GB	University of Science and Technology, China
OHP-B	2128	532 GB	University of Science and Technology, China
OHP-B	2607	654 GB	University of Science and Technology, China
OHP-B	2560	637 GB	University of Science and Technology, China
LER-MSC-AB LER-PMD-AB	1 1	3.99 GB	Federal University of Western Pará, Brazil
OUV-BC	31 Selected subset: UVI Region: 18.0-29.0E, 53.0-61.0N (658 kB in total)		Latvian Environment, Geology and Meteorology Centre
OHP-B	2136	535 GB	University of Science and Technology, China
OHP-A	425	104 GB	Ibaraki University, Japan
OUV-AB	2 Selected subset: JO1D, JNO2 Region: global (2.52 MB in total)		National Remote Sensing Centre, India
OUV-AB	1004 Selected subset: JO1D, JNO2 Region: global (1.27 GB in total)		National Remote Sensing Centre, India
OUV-A OUV-AB OUV-B OUV-BC	5478 Selected subset: JO1D, JNO2 Region: global (6.48 GB in total)		National Remote Sensing Centre, India
OHP-B	2562	639 GB	University of Science and Technology, China
OHP-B	2560	637 GB	University of Science and Technology, China
OHP-A	437	107 GB	Ibaraki University, Japan
OHP-A	438	108 GB	Ibaraki University, Japan

OHP-B	1	250 MB	Ibaraki University, Japan
OHP-A	426	104 GB	Ibaraki University, Japan
OHP-A	421	103 GB	Ibaraki University, Japan
OHP-B	440	110 GB	Ibaraki University, Japan
ARP-B ARP-C	11 10	154 MB	FMI, Finland
ARP-B ARP-C	11 11	161 MB	FMI, Finland
ARP-C	15	109 MB	S[&]T, Netherlands
ARS-C	15	15.6 MB	S[&]T, Netherlands
OUV-A OUV-AB OUV-B OUV-BC	Time series for 5709 days Selected subset: ERYDD, DNADD, VITDD, UVADD, UVBDD Location: 4.85E 45.75N (594 kB in total)		University of Barcelona, Spain
ARP-B ARP-C	48 51	716 MB	FMI, Finland
ARP-C	1	7.4 MB	ASEFOR, Guatemala
OHP-A	425	104 GB	Ibaraki University, Japan
ARP-B ARP-C	41 39	583 MB	FMI, Finland

APPENDIX 2

Table A.3 presents a detailed summary of failed product orders from AC SAF archive at FMI during the reporting period. The middle column indicates whether the failure was related to problems with AC SAF archive and/or ordering system or was the problem on the user's side.

Table A.3. Summary of failed product orders during the reporting period

Date	Error type	Failure description and details
7 June	Internal	Order ID: 2186 User institute: University of Science and Technology, China Order contents: 2560 x OHP Ordering log error message: 'Zip package could not be uploaded to the ordering server' Failure description: Due to several large orders already uploaded to the ordering server, the disk space of 4 TB had run out. Corrective action: After the preceding large orders had been automatically deleted after one week, this order was manually processed and uploaded to the ordering server. Final outcome: The user was notified about the upload by email 20 June. User made no further contact.
12 June	Internal	Order IDs: 2187, 2188, 2189 User institute: Federal University of Western Pará, Brazil Order contents: 1 x LER-MSC-AB, 1 x LER-PMD-AB Ordering log error message: 'Zip package could not be uploaded to the ordering server' Failure description: Due to several large orders already uploaded to the ordering server, the disk space of 4 TB had run out. Corrective action: After the preceding large orders had been automatically deleted after one week, one of these similar failed orders (2187) was manually processed and uploaded to the ordering server. Final outcome: The user was notified about the upload by email 20 June. User made no further contact.

Date	Error type	Failure description and details
15 June	Internal	Order ID: 2195 User institute: National Remote Sensing Centre, India Order contents: 5478 x OUV Ordering log error message: 'Zip package could not be uploaded to the ordering server' Failure description: Due to several large orders already uploaded to the ordering server, the disk space of 4 TB had run out. Corrective action: After the preceding large orders had been automatically deleted after one week, this order was manually processed and uploaded to the ordering server. Final outcome: The user was notified about the upload by email 20 June. User sent a 'thank you' email on the same day.